UNIVERSITÀ DEGLI STUDI DI PARMA

FACOLTÀ DI SCIENZE MATEMATICHE, FISICHE E NATURALI

Dipartimento di Fisica M. Melloni

Models in Statistical Physics on Infinite Graphs

Dottorato di Ricerca in Fisica

XXIII Ciclo

Supervisore:
Prof. **Davide Cassi**

Dottorando:
Riccardo Campari

Contents

Introduction

Physicists and mathematicians love regularity, mainly for the reason that it makes things simple, clear and, primely, computable; nature, on the other hand, has its own way of deciding what's the right way to behave, and although it presents the attentive observer with beautifully ordered crystals, impressive fractals and perfectly spherical soap bubbles, the vast majority of matter we interact with every day has no definite structural order: wood, plastic, cloth, all are microscopically complex structures which do not enjoy neither translational nor scale invariance, nor any other form of symmetry.

However, even when the spatial disposition of the constituents of matter is highly irregular, what determines the physical properties of the system are not so much the details of the distribution, as the topological structure of their interactions, which can usually be safely reduced to nearest neighbour or next-nearest neighbour relations.

As a consequence, both regular and complex matter are well described by means of graphs, which represent in a compact form the interactions among their constituents.

When paired with an underlying mathematical model, a graph is able to describe many physical systems in an approximate yet effective way. Furthermore, a graph can equally well model a network of interacting agents, as one often finds in economic literature, or computers - the Internet is the prime example - or abstract data structures in IT, or a deluge of other possibilities.

A formal introduction to graphs, as well as some of their many peculiar characteristics, is given in **Chapter** 1.

Given their broad applicability, it is not surprising that a great wealth of scientific literature in many fields regards physical and mathematical models defined on graphs. In particular, during my doctoral period I focused on two different general purpose models, which enjoy a wide diffusion: discrete random walks and the Ising model.

Random Walks

Regarding random walks, my current research focuses on the statistics of multiple agents simultaneously travelling on an infinite graph, and their collective properties.

Several degrees of technical difficulty accompany this endeavour, associated with keeping track of multiple positions, on the one hand, and with the non-linearity of collective properties, on the other. A simplifying picture can be sometimes achieved by means of the distance graph, each vertex of which corresponds to a relative position of the particles, so that, for example, simultaneous encounters of all the particles correspond to a return to the origin in the distance graph.

Constructing the distance graph proves however impossible in general, so that case specific methods need to be used to calculate the same quantities.

While further work is in progress, the results I obtained up to date regard three particles moving on an infinite line: owing to the homogeneity of the structure, a distance graph exists, which corresponds to the triangular 2-d lattice, so that the probability of finding the particles at given relative distances can be straightforwardly calculated by means of a standard Fourier transform and saddle point approximation.

As a further step, we computed the probability that the minimum and maximum distances among the particles are lower than some constant d, and found that asymptotically they scale as a function of d^2/t, implying that the surfaces of fixed probability undergo a regular diffusion.

The results have been submitted for publication [1].

Chapter 2 contains an introduction to random walks on infinite graphs. **Chapter** 3 presents some results about regular and more general graphs, which highlight fairly recent results in the field. **Chapter** 4, finally, describes the results I obtained in the field of multiple random walks and future perspectives.

The Ising Model

The second area of research I investigated revolves around the magnetization properties of the ferromagnetic Ising model on arbitrary graphs. More specifically, my aim was to find a relationship between the long range topology of a graph and its spontaneous magnetization.

Several results are present in literature for regular lattices, fractals and a few more general graphs, and an extension of the Mermin-Wagner theorem states that transient on the average graphs show indeed spontaneous magnetization; however, a very wide set of graphs was still uncovered, and no sufficiently general criterion for assessing the existence of long range correlation existed.

The approximate direction of exploration was clear since the beginning: on the one side, the number of different paths present in a graph is a first measure of the quality of the correlation between far away points; in turn, the transmission of information from one vertex to another is strongly inhibited when all the paths connecting them must cross just a small number of edges of the graph.

These considerations formed the basis from which we proceeded to the construction of two theorems: a necessary condition for the presence of spontaneous magnetization, in zero external field and no boundary conditions, and a sufficient condition for its absence. These two theorems represent the most encompassing criteria to date for what regards the magnetizability of graphs: all the known structures enter the hypothesis of either of the theorems, even though no sufficient and necessary condition is known.

The gap left between the hypotheses of the two theorems regards a very small class of pathological graphs whose existence is not even acknowledged.

The two theorems have been published in [2] and [3].

A part of my study was cast into an analysis of the different ways in which spontaneous magnetization can be defined, as either a spin expectation value or a long range order, for a single spin or averaged over the graph, under an external field or boundary conditions or neither. A chapter has been devoted to a thorough discussion of the matter.

In **Chapter** 5 the basics of the ferromagnetic Ising model are presented, together with the the most important results the scientific literature presents regarding the magnetization of complex structures. In **Chapter** 6 the sufficient condition for the absence of spontaneous magnetization is discussed in depth, as is the sufficient condition for the presence of spontaneous magnetization found in **Chapter** 7. Finally, **Chapter** 8 deals with the different definitions of spontaneous magnetization and their relations.

1 Graphs

1.1 Definition of Graphs and their Embeddings. Subgraphs

An **undirected graph** (from now on simply **graph**) $\mathcal{G}$ is a pair $(\mathcal{P}, \mathcal{L})$, where $\mathcal{P}$ is a countable collection of vertices and $\mathcal{L} \subset \mathcal{P} \times \mathcal{P}$ is a set of unoriented arcs (or bonds or edges) between points.

The structure of a graph can be described algebraically, thus allowing for easier mathematical computations, by means of the **adjacency matrix** A_{ij}, defined as

$$A_{ij} = \begin{cases} 1 & if \quad (i,j) \in \mathcal{L} \\ 0 & if \quad (i,j) \notin \mathcal{L}. \end{cases} \tag{1.1.1}$$

An **embedding** of a graph $\mathcal{G}$ into a space $\mathcal{S}$ is a structure in $\mathcal{S}$ which replicates the vertices (to each vertex in $\mathcal{P}$ corresponds a point in $\mathcal{S}$) and the edges (for each arc of $\mathcal{L}$ a line exists in $\mathcal{S}$ between the corresponding points, with the peculiarity that two separate lines never intersect) of $\mathcal{G}$. Of course a graph needs not be embeddable in any given space (e.g. an infinite 3-d regular lattice can not be embedded into a plane), and there are examples of graphs which can not be embedded in a separable way into any finite-dimension space.

Definition. A graph which can be embedded on a plane is called a **planar graph**.

> A set of n points linked in all the possible ways is called a **complete graphs** and denoted by K_n. For $n \leq 4$, K_n is planar, otherwise it is not (see Fig.1.1).

The graphs as mathematical objects have no awareness of any Euclidean space they may be embedded into: if we draw a graph on a sheet of paper we choose one of infinite equivalent ways of representing it, and all the details, e.g. the length of the bonds or the position of vertices, have no significance at all. All in all, the graph is essentially a topological structure, which is equivalent to the class of all

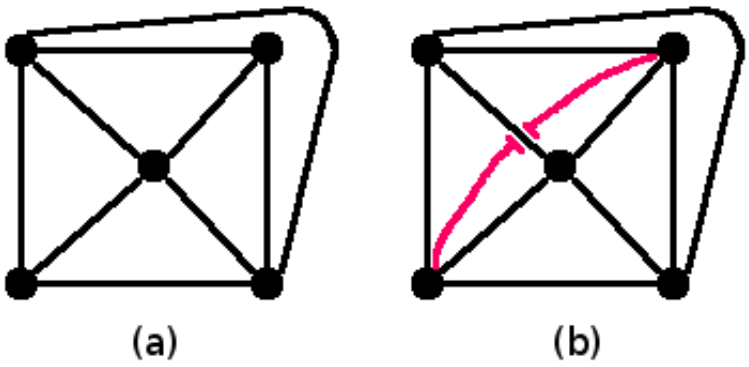

Figure 1.1: (a) The planar graph K_4, and (b) the non-planar graph K_5.

its possible embeddings.

Definition. Any pair $\mathcal{G}' = (\mathcal{P}', \mathcal{L}')$, such that

- $\mathcal{P}' \subset \mathcal{P}$,
- $\mathcal{L}' \subset \mathcal{L}$, and
- $\mathcal{L}'$ contains only links between elements of $\mathcal{P}'$,

is called a **subgraph**, and it's denoted $\mathcal{G}' \subset \mathcal{G}$.

Since dealing with actually infinite graphs is difficult, we will usually employ the subgraphs as their growing approximation: one calculates observables on a set $\{\mathcal{G}_N\}$ of finite subgraphs, each including its predecessor, then takes the $N \to \infty$ limit.

The **vertex boundary** $\partial\mathcal{G}'$ of a **subgraph** $\mathcal{G}'$ is defined as the set of points of $\mathcal{P}'$ that share a bond with at least one point of the set $\mathcal{P} \setminus \mathcal{P}'$:

$$\partial\mathcal{G}' = \{i \in \mathcal{P}' : (i,k) \in \mathcal{L} \text{ for some } k \in \mathcal{P} \setminus \mathcal{P}'\}\,.$$

The ratio of the size of the boundary to the size of the bulk of a subgraph, in the thermodynamic limit, is an important quantity in a great deal of applications, as it enters the hypotheses of a number of theorems in physics and mathematics.

As an example, in solid state physics one can consider periodic boundary conditions when studying the Schrödinger equation of a crystal, in order to make the calculations easier: since the ratio is asymptotically $1/R$ as the linear size R of the system grows, it tends to zero for large size crystals, and one is guaranteed to obtain essentially the same results as with non periodic boundary conditions.

Most notably, when the ratio doesn't tend to zero as the size of the subgraph grows, as in the case of the Cayley tree (also known as Bethe lattice), the effect of the border on the overall behaviour of the system is overwhelming, and what happens there determines the bulk behaviour of the structure.

1.2 Chemical Distance and the Intrinsic Metric

Definition. As we are next going to introduce random walks on graphs, we define a **path** γ_{ij}, between two points i and j, as a collection of consecutive bonds of $\mathcal{L}$, where consecutive means that each pair shares a vertex with the next one:

$$\gamma = \{(i, l_1), (l_1, l_2), \ldots, (l_{D-1}, j)\}\,.$$

A path is **self-avoiding** if no edge appears in it more than once.

A closed self-avoiding path γ_{ii}, i.e. a path whose starting point is also its ending point, is called a **loop**.

The existence of a loop implies that there are $2(\#\gamma_{ii})$ different loops sharing the same or reverse ordering of edges, but with different starting points. We call the equivalence class of all such loops a **cycle**.

We write the set of all possible paths between two points i and j as Γ_{ij}.

Definition. Directly associated to the concept of path, the **chemical distance** d_{ij} between two points i and j is defined as the length of the shortest path connecting them.

$$d_{ij} = \min_{\gamma_{ij} \in \Gamma_{ij}} \#\gamma_{ij} \tag{1.2.1}$$

Any minimum distance path is called a **geodetic**.
We can now define an important property of graphs:

Definition. A graph $\mathcal{G}$ is **connected** when for any pair $(i, j) \in \mathcal{P}$ a path exists having them as extremes.

As disconnected graphs are essentially a set of independent connected graphs, in the following we will only consider connected graphs.

Definition. We have introduced vertex boundaries in the previous section; a slightly different kind of boundary is the **bond boundary**: let L be a collection of links $L = \{l_i\}$; if removing L divides the graph into two connected subgraphs $\mathcal{S}_1$ and $\mathcal{S}_2$, i.e.

- all the paths γ_{ij} on $\mathcal{G}$ from a point $i \in \mathcal{S}_1$ to a point $j \in \mathcal{S}_2$ must cross one link of L,
- a path exists between any pair of points both belonging to $\mathcal{S}_1$ or to $\mathcal{S}_1$

we call L a **bond boundary**.

The *chemical distance* straightforwardly induces the so-called **intrinsic metric of the graph**: it is in fact trivial to prove that

- $d_{ij} \geq 0$,
- $d_{ij} = 0$ iff $i = j$,
- $d_{ik} + d_{kj} \geq d_{ij}$, $\forall k \in \mathcal{P}$.

The intrinsic metric of the graph is the most immediate and natural metric which can be defined on a graph, but it is not the most useful nor powerful: when considering physical and mathematical models on a graph, a number of fundamental quantities don't depend on chemical distances, but on other distances - slight modifications of euclidean distance, in the case of models on regular lattices - which therefore appear more apt to describe the corresponding physics.

Definition. The **coordination number** of a vertex $i \in \mathcal{P}$ is defined as the number of arcs which have i as an extreme:

$$z_i = \#\{l \in \mathcal{L} : i \in l\} = \sum_j A_{ij},$$

where A_{ij} is the adjacency matrix which we have defined at the beginning of this chapter.

In the following we will mostly be concerned with graphs whose z_i are *uniformly limited*, i.e. an integer z_{Max} exists such that

- $z_i \leq z_{Max} \forall i \in \mathcal{P}$,
- a point $j \in \mathcal{P}$ exists for which $z_j = z_{Max}$.

One of the reasons why the condition $z_i \leq z_{Max}$ is important is that many inequalities and theorems can be proved as long as it holds. Another point is that the thermodynamic limit will probably be ill-defined if points arbitrarily far from the origin are allowed to have more and more first neighbours.

1.3 Infinite Graphs, Van Hove Spheres, Intrinsic Fractal Dimension and All That

As in this thesis we will be dealing essentially with infinite graphs, it is convenient to introduce now some concepts which will be used later on.

An essential tool for analytical calculations on infinite graphs is a generalization of the continuous Euclidean sphere, called **Van Hove sphere** [4]. The **Van Hove sphere** $S_{i,r}$, of centre i and radius r, is the subgraph of $\mathcal{G}$ given by the set of vertices $P_{i,r} = \{j \in \mathcal{P} : d_{ij} \leq r\}$ and by the set of links $\mathcal{L}_{i,r} = \{(j,k) \in \mathcal{L} : i, j \in P_{i,r}\}$.

Let now N_r be the maximum number of vertices included in any Van Hove sphere of radius r:

$$N_r = \sup_{i \in \mathcal{G}} \# S_{i,r}.$$

It should be noted that the case of infinite N_r corresponds to unbounded z_i: if $z_i \leq z_{Max}$ then

$$N_r \leq z_{Max} \left(z_{Max} - 1 \right)^{r-1}.$$

Definition. The **intrinsic fractal dimension** d_{frac} is defined as

$$d_{frac} = \min \left\{ d : N_r \leq C r^d + E \right\}, \tag{1.3.1}$$

for some constants C and E.

It differs from the continuous *fractal dimension* in that it refers to the topological nature of the graph (i.e. to its natural - chemical - distance), and not on the metric structure of the space into which the graph is embedded. The limiting case $d_{frac} = \infty$ corresponds to an exponential or faster-than-exponential growth of N_r.

A d-dimensional **Euclidean lattice** is just the pair $\left(\mathbb{Z}^d, \mathcal{L} \right)$ with $\mathcal{L}$ consisting of all the edges between first neighbours, as seen in the natural embedding of $\mathbb{Z}^d$ in R^d.
A Van Hove sphere of radius R for such a graph is the set of points inside a structure S, formed by the juxtaposition of the 2^d standard simplices of edge R having as normal vectors $(\pm 1, \ldots, \pm 1)$, or equivalently the set of points $\vec{x}$ satisfying

$$\begin{cases} a_1^i x_1 + a_2^i x_2 + \cdots + a_d^i x_d \leq R \\ a_i \in \{+1, -1\} \text{ for } i = 1, 2, \ldots, d \end{cases}.$$

The volume of each simplex, and thus of S, is $\sim R^d$, and so $d_{frac} = d$ for Euclidean lattices.

As a last tool, we now introduce the **measure** of an infinite subset in the thermodynamic limit: let $\{S_N\}$ be a sequence of sets satisfying

$$S_1 \subset S_2 \subset \cdots \subset S_k \subset \ldots,$$

whose size $\# S_N$ tends to infinity with N, and let $\{R_N\}$ be a sequence of subsets verifying

$$\begin{cases} R_1 \subset R_2 \subset \cdots \subset R_k \subset \ldots \\ R_N \subset S_N \end{cases}.$$

We call *measure* of the subset $R = \lim_{N \to \infty} R_N$ with respect to the set $S = \lim_{N \to \infty} S_N$ the quantity

$$\mu(R) = \lim_{N \to \infty} \frac{\# R_N}{\# S_N}.$$

We will always implicitly think of S as the whole vertex set of a graph $\mathcal{G} = (\mathcal{P}, \mathcal{L})$, and furthermore we will use

$$\mu(R) = \lim_{N\to\infty} \frac{\#\mathcal{G}'_N}{\#\mathcal{G}_N}$$

as an improper notation for

$$\mu(R) = \lim_{N\to\infty} \frac{\#R_N}{\#S_N},$$

whenever $\mathcal{G}'_N \subset \mathcal{G}_N$ for all N.

1.4 Bipartite Graphs

A **bipartite graph** is defined as having the following property: its vertex set can be divided into two subsets $\mathcal{P}_1$ and $\mathcal{P}_2$, so that the elements in $\mathcal{P}_1$ only share edges with elements in $\mathcal{P}_2$, and *vice versa*.

> Any regular Euclidean lattice is bipartite: since the chemical distance of a point from the origin is just $d_{0x} = \sum_{i=1,\dots,d} x_i$, vertices having an even d_{0x} are only linked to vertices having odd distance from the origin.

Proposition. Every path between two points, $i, j \in \mathcal{P}_1$ in a bipartite graph is even.

Proof. It is obvious that a path of length l ending in j has its first element k in $\mathcal{P}_1$ after two steps; iterating this proposition, it follows that any path lands in $\mathcal{P}_1$ only after an even number of steps, while all the odd-numbered steps end up in $\mathcal{P}_2$.

Theorem. A graph is bipartite if and only if all of its closed paths $\gamma_{i\to i}$ are even.

> $\Rightarrow$ if a graph is bipartite, then all of its loops are even, as they are path where both the starting and the ending point lie in $\mathcal{P}_1$;
> $\Leftarrow$ the inverse implication can be proved as follows: set $i \in V$, and let $\mathcal{C}_1 \subset \mathcal{P}$ be the subset set of vertices at even distance from i, and let $\mathcal{C}_2 = \mathcal{P} \setminus \mathcal{C}_1$; suppose now that an edge exists between two points j and k in C_1, and take a geodetic from j to i, and a geodetic from i to k: since they are both of even length, it is possible to connect j to k with an odd path, which contradicts the hypothesis, so no edge between elements of $\mathcal{C}_1$ exists. Analogously, no edge (j, k) between elements of $\mathcal{C}_2$ can exist, otherwise it would be possible to create an odd loop, through i and k, for j.

When each of the elements of $\mathcal{P}_1$ is connected to all of the elements of $\mathcal{P}_2$, we call $\mathcal{G}$ a **complete bipartite graph**. This definition is fully equivalent to the one obtained by reversing the roles of $\mathcal{P}_1$ and $\mathcal{P}_2$.
It is common to write $K_{l,m}$ for the complete bipartite graph where $\#\mathcal{P}_1 = l$ and

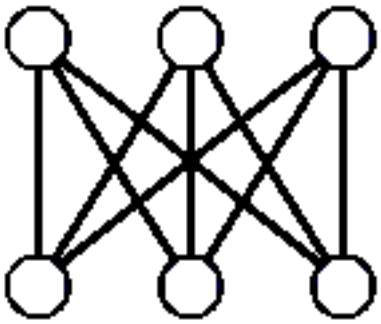

Figure 1.2: The complete bipartite graph $K_{3,3}$.

$\#\mathcal{P}_2 = m$.

An important example of complete bipartite graph is $K_{3,3}$ (see Fig.1.2): its most prominent feature is that of being the simplest non-planar bipartite graph which can be constructed. The reader has probably encountered a (quite sadistic) puzzle game, where you are given two sets of three points each and are asked to connect each elements of the first set to all the elements of the second set without intersecting lines. We will prove elsewhere that this is indeed impossible.

1.5 Trees

A **tree** is a connected graph $\mathcal{G}$ which contains no cycles.

Theorem. A graph $\mathcal{G}$ is a tree if and only if $\mathcal{G}$ has no cycles and if adding any new edge between non adjacent vertices creates exactly one cycle.

From the definition of tree it immediately follows that if we add a new edge (i, j) to a tree, exactly one cycle is created, which can be obtained by taking the only self-avoiding path connecting i to j on $\mathcal{G}$ and adding to it the new edge.
To prove the converse, i.e. that $\mathcal{G}$ is connected, we need to prove that a path exists between $i, j \in \mathcal{P}$. If they are adjacent, there is nothing to prove. If they aren't, add the edge $(i.j)$ to the graph: by virtue of the hypothesis exactly one cycle is created; in particular, a self avoiding loop exists whose last step is on the edge (i, j),

$$\{(j, k), \ldots, (z, i), (i, j)\}.$$

If we remove the last edge from the loop, we obtain a path from j to i whose edges are all in $\mathcal{G}$, which proves the thesis.

Given an arbitrary graph, a **spanning tree** is a tree $\mathcal{S} = \{\mathcal{P}', \mathcal{L}'\}$ whose vertex

set is the same as $\mathcal{P}$, and $\mathcal{L}' \subset \mathcal{L}$. We call a **chord** of the spanning tree any edge in $\mathcal{L} \setminus \mathcal{L}'$; the graphs obtained by adding any one chord to $\mathcal{S}$ have exactly one cycle.

A cycle which spans all the vertices of a graph is called a **spanning cycle**.

1.6 Independent Cycles and Cocycles

The presence of cycles is a fundamental property of graphs even for non mathematicians, as it determines the strength of correlation between distant vertices in a given physical model. In the case of electric networks, the circuits built on the independent cycles (in a sense which we will specify below) are enough to solve the whole network, and in the Ising model the quantity of long range cycles is a key component in determining whether the system magnetizes.

Following Harary [5], we introduce a technique to formally cope with cycles: first consider the sum operation over the field $\{0, 1\}$, where $1 + 1 = 0$. When applied to sums of vertices, it yields $i + i = 0i = 0$, and when applied to sums of edges $(l, m) + (l, m) = 0(l, m) = 0$.
A $0 - chain$ is a collection P of vertices, $P \subset \mathcal{P}$, while a $1 - chain$ is a collection of edges, $L \subset \mathcal{L}$.

We define the **boundary operator** ∂ as a linear operator sending $1 - chains$ to $0 - chains$, such that

$$\partial l = i + j$$

whenever $l = (i, j)$.

Analogously, the **coboundary operator** δ is linear and sends $0 - chains$ to $1 - chains$ according to the rule

$$\delta i = \sum_{k=1}^{z_i} (i, j_k),$$

where j_k is a first neighbour of i.

According to the $1 + 1 = 0$ rule of the field, the ∂ operator does what one would expect given its name, at least in simple cases: if we take a path $\gamma_{i \to j}$, $\partial \gamma_{i \to j}$ yields its extrema:

$$\partial \gamma_{i \to j} = \{i, j\},$$

while the boundary of a loop is the empty set.

The coboundary operator has a simple effect if we consider a connected set $I \subset \mathcal{P}$: δI is the set of links one must cut in order to disconnect I from the rest of the graph.

Cycle Basis

A $1 - chain$ with empty boundary is a collection of cycles that do not share edges; we call it a **cycle vector**. Since the sum of cycles, according to the $1 + 1 = 0$

rule, is a cycle, the cycle vectors form a vector space on the field $\{0, 1\}$. As usual, a basis of this space is a maximal collection of independent vectors $\{v_i\}$, where independent means that

$$0 = \sum_{i=1}^{N} \alpha_i v_i$$

only for $\alpha_i = 0$ for all $i = 1, \ldots, N$.

The set of cycles $\{v_i\}$, which one obtains by adding one link to a given spanning tree, is actually a basis of the cycle space:

- they are independent, as each of them contains an edge that no other v_j has;
- they generate the vector space, as a sum of such cycles is enough to produce every possible cycle [5].

1.7 Eulerian Graphs

A well known problem in graph theory, which is traditionally tied to the very birth of this branch of mathematics, is the Königsberg Bridge Problem: in the town of Königsberg, once capital of East Prussia, now Kaliningrad, Russia, two rivers join forming an island; at the time when the problem was first formulated, seven bridges existed which joined the different regions formed by the rivers (see Fig.1.3). Is it possible to walk all the bridges without crossing any bridge twice ?

The negative answer to the problem was first given by Euler in 1735. He used a graph to describe the topological structure of the problem and abstract all the superfluous details. The bottom line of his reasoning is that one needs an edge to get to, and an edge to get away from, every vertex, the only possible exceptions being the vertex from which the walk starts and the vertex where the walk ends. Therefore at most two vertices can have an odd coordination number, and the Königsberg Bridge problem admits no solution.

While this condition is necessary to be able to transverse all the edges in a graph exactly once, we have not proved it to be sufficient. In order to do so, we define an **Eulerian graph** as a graph such that it is possible to find a path which traverses each edge exactly once, goes through all vertices and ends at the starting point. We call such path an **Eulerian cycle**. While it is clear that an Eulerian graph needs to be connected, the following theorem [5] needs a proof.

Theorem. The following statements are equivalent for a graph $\mathcal{G}$ which is finite, connected and non-trivial (i.e.: there are no points with coordination number 1):

1. $\mathcal{G}$ is Eulerian;
2. every vertex of $\mathcal{G}$ has even coordination number;
3. the set of lines of $\mathcal{G}$ can be partitioned into cycles.

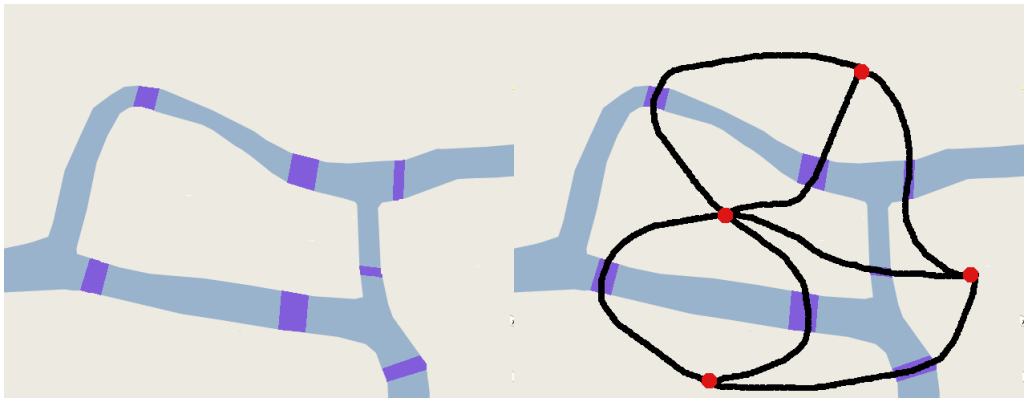

Figure 1.3: The island at Königsberg (now Kaliningrad, Russia) and its graph representation.

Proof. $1 \Rightarrow 2$
Given any Eulerian path γ - i.e. any cycle which contains all vertices and all edges - each point appears in γ an even number of times, as for each ingoing step there is an outgoing step.

$2 \Rightarrow 3$
Since the coordination number is at least 2 and the graph is finite, any path which never steps back will sooner or later visit a vertex which it has already visited. Let C_1 be a cycle thus determined, and call $\mathcal{G}_1$ the graph obtained by removing the edges of C from $\mathcal{G}$. $\mathcal{G}_1$ now has even coordination number (possibly 0) at every vertex: if it contains no lines, then the implications is proved; otherwise, one can find a cycle C_2 in $\mathcal{G}_1$ starting from any vertex with coordination number at least 2, and obtain the corresponding graph $\mathcal{G}_2$. Since the graph is finite, this process will exhaust all possible edges, so that the set of lines in $\mathcal{G}$ can actually be partitioned into cycles.

$3 \Rightarrow 1$
Take any partition into cycles $\{C_i\}$ of $\mathcal{G}$: since $\mathcal{G}$ is connected, a cycle C_j must exist which has at least a vertex v_j in common with C_1, and the union of C_1 and C_j is itself a cycle. One can iterate the previous operation until the cycles are exhausted, and the final cycle will span all the edges in $\mathcal{G}$, which proves the implication and the thesis is thus demonstrated.

□

It is now straightforward to prove the result by Euler.

Corollary. A graph $\mathcal{G}$ with exactly two vertices of odd coordination number can be traversed by a path which crosses all its edges.

Let i and j be the vertices with odd coordination number. Add an edge (i, j) to the graph, so that it now has even an coordination number at every vertex. Then an Eulerian cycle γ exists for the new graph, and we can choose the starting point so that (i, j) is the last traversed edge. Then $\gamma \setminus \{(i, j)\}$ is a path which starts from j, ends in i and visits all the edges of $\mathcal{G}$.

A slightly more general result is the following.

Corollary. A graph $\mathcal{G}$ with exactly $2n$ vertices ($n \geq 1$) of odd coordination number can be partitioned into n self-avoiding paths.

Arbitrarily divide the $2n$ of odd coordination number vertices into n pairs, and add the corresponding edges to the graph. The graph obtained is Eulerian, and can thus be partitioned into cycles. For each cycle γ that contains $l \geq 1$ pairs among the n we have chosen, fix the starting point so that the last edge visited is one of the l edges: then remove all l pairs from γ, so that it can be divided into l paths, each beginning and ending in one of the $2l$ vertices. Since each pair is present exactly in one cycle, it is possible to divide $\mathcal{G}$ into exactly n paths starting from and ending at the vertices of odd coordination number.

1.8 Hamiltonian Graphs

A further characterization of finite graphs regards the possibility of visiting all its points (not its edges) exactly once with a self-avoiding path, which we then call **Hamiltonian path**. If a **Hamiltonian cycle** - a Hamiltonian path which returns to the starting point on the last step - exists, the graph is called a **Hamiltonian graph**.

A graph is called k**-connected** if it can be disconnected by removing k vertices.

Proposition. Any Hamiltonian graph is at least 2-connected.

Since the graph is Hamiltonian, a cycle C exists which spans all the points, so the graph is connected, and $k \geq 1$. Suppose now that $k = 1$: in that case a point i exists such that by removing it $\mathcal{G}$ is divided into two non-empty disconnected subgraphs $\mathcal{A}$ and $\mathcal{B}$. Choose i as the starting point in i: C will first visit either $\mathcal{A}$ or $\mathcal{B}$, so that before visiting the other subgraph it will have to step on i again, and a third time on the final step of the cycle, which is absurd. Thus $k \geq 2$.

Graphs that are not Hamiltonian all share a **theta graph**, which is made of two non-adjacent vertices of coordination number 3, while all other vertices have coordination number 2 (see Fig.1.4). In fact the following holds.

Theorem. A 2-connected non-Hamiltonian graph contains a *theta subgraph*.

Several theorems exist stating sufficient and necessary conditions for a graph to be Hamiltonian, but no results as encompassing as those for Eulerian graphs exist. A summary, with no proof, of such results follows.

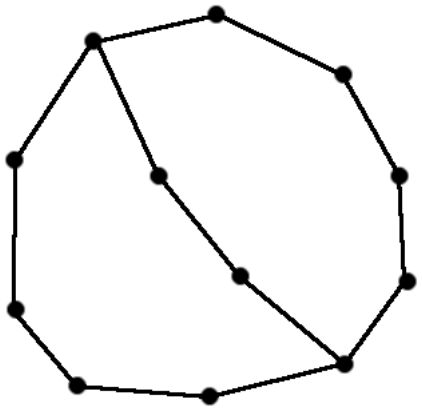

Figure 1.4: An example of *theta graph*.

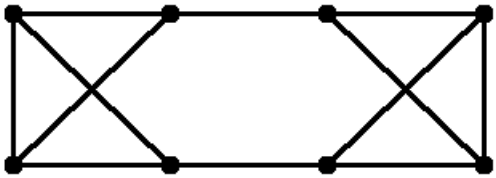

Figure 1.5: A Hamiltonian graph for which there are 8 vertices of coordination number 3.

Theorem. A graph $\mathcal{G}$ has $p \geq 3$ points. If

- for all n such that $1 \leq n < (p-1)/2$ the number of points of coordination number lower than or equal to n is less than n,
- in the case of odd p the number of points of coordination number exactly $(p-1)/2$ does not exceed $(p-1)/2$,

then $\mathcal{G}$ is Hamiltonian.

The previous theorem is by no way necessary: the graph in Fig.1.5 is an immediate counterexample, as the graph is clearly Hamiltonian, while the number of points of coordination number 3 is 8, thus breaking the hypothesis of the previous theorem.

It also comprises two classical results which are simpler to state.

Corollary. Let a graph $\mathcal{G}$ have $p \geq 3$ vertices; if for every pair (i, j) of non-adjacent points $z_i + z_j \geq p$, then $\mathcal{G}$ is Hamiltonian.

Corollary. Let $\mathcal{G}$ be a graph made of $p \geq 3$ vertices. If, for all vertices i, $z_i \geq p/2$,

then $\mathcal{G}$ is Hamiltonian.

2

Random Walks on Graphs

Random walks have been the focus of a wide area of research for over a hundred years. The most striking fact about them is their impressive area of applicability, which ranges from finance - with particular regard to the market fluctuations - to genetics, from psychology to neurophysiology, from statistics to physics.

Since their many incarnations are completely outside the scope of this thesis, it will suffice to recall the most meaningful example for a physicist: the Brownian motion, that's to say the effect of the thermal agitation of water on minuscule particles laying on its surface, resulting in their movement.

The Brownian motion was arguably observed for the first time in 1785 by Jan Ingenhousz, a Dutch scholar best known for discovering photosynthesis, and is named after Robert Brown, a Scottish botanist, which analysed the phenomenon in 1827.

It was initially modelled as a physical process by Einstein [6] and Smoluchowsky [7], in two seminal papers at the beginning of the XX Century; the former scientist predicted a diffusion coefficient for the particles, by means of continuous time random walk, and the latter was able to experimentally verify the prediction.

Since, however, we are interested in the study of graphs, which are discrete structures, we will have to yield the continuum space, and as a matter of choice we will consider almost exclusively discrete time, although the technology of continuum time will be discussed in some detail later on.

2.1 Definition of Discrete Time Random Walks

Time-Independent Discrete Time Random Walk

In a **time-independent discrete time random walk** (RW from now on), an abstract walker moves at discrete time intervals around the vertices of a graph $\mathcal{G}$ in a haphazard fashion. More precisely, if the walker is at vertex i at time t, it will be at a site j at time $(t+1)$ with probability p_{ij}.

The time-independent part means that the p_{ij} doesn't depend explicitly on time, and it is understood that the transition probability doesn't depend on the history of the RW; the latter case is usually referred to as self-interacting RW, and is considerably more difficult to tackle.

The probability p_{ij} needs to satisfy some obvious assumptions

- $p_{ij} \geq 0$;
- $p_{ij} = 0$ iff $(i, j) \in \mathcal{L}$, so as to respect the structure of the graph.

While it may seem mandatory that $\sum_j p_{ij} = 1$, it is not really the case, as a RW can contain traps - where the walker is destroyed - or sources - where new walkers spring into existence. As a matter of fact, in the following we'll be mostly concerned with the case of **conservative RWs** so, unless otherwise stated, we assume that $\sum_j p_{ij} = 1$.

The fundamental quantity to be computed in a RW is $P_{ij}(t)$, which is the probability that a walker starting at vertex i ends up at j after t steps. $P_{ij}(t)$ can be computed as the sum, over all the paths γ of length t connecting i to j, of the weights $P_\gamma = \prod_{(l,m)\in\gamma} p_{l,m}$; since this definition is frankly encumbering, a more straightforward algebraic formula is used, which reduces the sum to a matrix product:

$$P_{ij}(t) = \sum_{l_1} \cdots \sum_{l_{(t-1)}} p_{il_1} \dots p_{l_{(t-1)}j} = (p^t)_{ij}, \tag{2.1.1}$$

where p is the matrix of elements p_{ij}. Obviously $P_{ij}(0) = \delta_{ij}$.

Another important quantity is the **probability of first visit** $F_{ij}(t)$: to compute it one needs to sum over all the different paths which tread on the vertex j for the first time after t steps.

While this may be close to impossible to compute directly, F_{ij} can be easily linked to P_{ij}: in order to be at vertex j at time t, a walker either arrives for the first time in j at t, or it has trodden on j for the first time at some $\tau < t$, and then wandered about, hitting j again after $(t-\tau)$ more steps; since the first arrival times τ are mutually exclusive, it is licit to write

$$P_{ij}(t) = \sum_{\tau=0}^{t} F_{ij}(\tau) P_{jj}(t-\tau) + \delta_{ij}\delta_{t0}, \tag{2.1.2}$$

where last term keeps track of the initial position. The latter equation allows one, in principle, to compute the numbers $F_{ij}(t)$ once the transition probabilities are known. As a matter of fact, a simpler approach, exploiting generating functions is the more viable solution, as we will see below.

Yet another meaningful quantity is $F_{ij}^{(r)}(t)$, the probability that the random walker

arrives at j for the r-th time after t steps. It satisfies the recurrence equation

$$F_{ij}^{(r)}(t) = \sum_{\tau} F_{ij}^{(r-1)}(t-\tau)F_{jj}(\tau). \tag{2.1.3}$$

As they are convolutions of the probabilities of first return, all the $F_{ij}^{r}(t)$ can be computed in principle once the $F_{ij}(t)$ are known. Once again, there is an alternative way of computing such quantities, employing generating functions, which is much easier. We'll see it later.

Simple Random Walks

A specific widely used type of RW is the **simple random walk**, in which the single-step transition probabilities are defined as

$$p_{ij} = \frac{1}{z_i}. \tag{2.1.4}$$

A *simple RW* is evidently conservative, and a simple correlation exists between $P_{ij}(t)$ and $P_{ji}(t)$ on the one hand, $F_{ij}(t)$ and $F_{ji}(t)$ on the other one:

$$z_i P_{ij} = z_j P_{ji}, \tag{2.1.5}$$

$$z_i F_{ij} = z_j F_{ji}; \tag{2.1.6}$$

this result can be immediately proven by noting that any path γ of weight P_γ connecting i to j can be walked *vice versa*, with the resulting weight being $\frac{z_i}{z_j}P_\gamma$.

2.2 Generating Functions

Employing **generating functions** is a very powerful way of dealing with sequences of numbers. A *generating function* is a power series whose coefficients are the numbers in our sequence. Letting A_n be such numbers, we define $\tilde{A}(\lambda)$ as

$$\tilde{A}(\lambda) = \sum_{n=0}^{\infty} A_n \lambda^n. \tag{2.2.1}$$

Generating functions are a discrete version of the Laplace transform, and they have several advantages over manipulating directly the numbers A_n, as we are next going to describe.

Deconvolution

Given two sequences A_n and B_n, with $A_n = B_n = 0$ for $n < 0$, their **convolution** is defined as $C_n = \sum_p A_p B_{n-p}$. The corresponding generating functions are simply related by the following:

$$\tilde{C}(\lambda) = \tilde{A}(\lambda)\tilde{B}(\lambda); \tag{2.2.2}$$

in fact

$$\begin{aligned}\tilde{C}(\lambda) &= \sum_n \lambda^n \left(\sum_p A(p)B(n-p) \right) = \sum_n \lambda^n \left(\sum_p A(p) \sum_q B(q)\delta(p+q-n) \right) \\ &= \sum_p \sum_q A(p)B(q)\lambda^{p+q} = \tilde{A}(\lambda)\tilde{B}(\lambda).\end{aligned}$$

In the specific case of RWs, we combine Eqs.(2.1.2) and (2.2.2) and obtain

$$\tilde{P}_{ij}(\lambda) = \tilde{F}_{ij}(\lambda)\tilde{P}_{jj}(\lambda) + \delta_{ij}. \tag{2.2.3}$$

A new path to computing $F_{ij}(t)$ is thus open, which can be a valid alternative to the brute force computation we hinted at above.

The deconvolution properties of generating functions yield a straightforward formula for $F_{ij}^{(r)}(t)$, the probability that a walker arrives at j for the r-th time after t steps, as of Eq.(2.1.3):

$$\tilde{F}_{ij}^{(r)}(\lambda) = \tilde{F}_{ij}^{(r-1)}(\lambda)\tilde{F}_{jj}(\lambda) = \left[\tilde{F}_{ij}(\lambda)\right]^{r-1} \tilde{F}_{jj}(\lambda). \tag{2.2.4}$$

Recurrence Relations

The main tools for computing generating functions analytically are **recurrence relations** of the form

$$A_n = f(A_{(n-1)}, \ldots, A_{n-k}) : \tag{2.2.5}$$

in some cases it is indeed possible to obtain closed form expressions for generating functions by multiplying the n-th term by λ^n and then summing over n; the generating function is then completely determined once the first k terms of the sequence have been calculated.

The Fibonacci numbers ϕ_n are defined by

$$\phi_n = \phi_{n-1} + \phi_{n-2}, \tag{2.2.6}$$

with $\phi_0 = 0$ and $\phi_1 = 1$. Multiplying Eq.(2.2.6) by λ^n and summing over $n = 2, 3, \ldots$ one obtains

$$\tilde{\phi}(\lambda) - \lambda\phi_1 - \phi_0 = \lambda \left[\tilde{\phi}(\lambda) - \phi_0\right] + \lambda^2\tilde{\phi}(\lambda),$$

and finally

$$\tilde{\phi}(\lambda) = \frac{\lambda}{(1 - \lambda - \lambda^2)}. \tag{2.2.7}$$

Asymptotic Expansion

Having a generating function $\tilde{A}(\lambda)$ in closed form is by no means enough to get an analytic form for the coefficients A_n, as this often proves an impossible feat to accomplish. It is nevertheless possible to obtain the asymptotic behaviour of A_n as $n \to \infty$ by a variety of techniques.

We follow here an elementary approach as in a paper by Montroll and Weiss [8], many more details can be found in references [9, 10] Let $\lambda = e^{-y}$, and take for granted that

- $\tilde{A}\left(\lambda(y)\right)$ converges as $y \to 0^+$,
- $A_n > 0 \ \forall n$,

Hypothesize now that

$$\tilde{A}(\lambda) \sim f(y^{-1}),$$

where $f(l) = l^\sigma L(l)$, with

- L(l) monotonically increases for $l > l_0$,
- $\lim_{l\to\infty} L(l) = +\infty$,
- $\sigma > 0$,
- $L(cl) \sim L(l)$ as $l \to \infty$.

Under these assumptions

$$A_1 + A_2 + \cdots + A_n \sim \frac{f(n)}{\Gamma(\sigma+1)}. \tag{2.2.8}$$

Computing A_n is then a matter of algebra:

$$A_n \sim \frac{f(n) - f(n-1)}{\Gamma(\sigma+1)}.$$

2.3 Paths Counting

When a simple random walk occurs on a **homogeneous** graph (e.g. a regular lattice), a simple connection is found between $P_{ij}(t)$ and $N_{ij}(t)$, the number of different paths of t steps connecting i to j: keeping into account that each path has a weight z^{-t} attached to it,

$$\begin{aligned} P_{ij}(t) &= z^{-t} N_{ij}(t), \\ \tilde{P}_{ij}(\lambda) &= \tilde{N}_{ij}(\lambda/z). \end{aligned} \tag{2.3.1}$$

Analogously, $M_{ij}(t)$, the number of paths which arrive in j for the first time after t steps, is closely related to $F_{ij}(t)$:

$$\begin{aligned} F_{ij}(t) &= z^{-t} M_{ij}(t), \\ \tilde{F}_{ij}(\lambda) &= \tilde{M}_{ij}(\lambda/z). \end{aligned} \tag{2.3.2}$$

2.4 Number of Points Visited

It is possible to compute the average number of distinct points visited in a t-step RW by employing the quantities we studied earlier. Let $S(t)$ be this probability, then

$$S_i(t) = 1 + \sum_{j \neq i} \left[F_{ij}(1) + F_{ij}(2) + \cdots + F_{ij}(t) \right]; \tag{2.4.1}$$

the heading one on the right-hand side is the starting point i, and the sum over time of each $F_{ij}(t)$ is the probability that site j has been visited at least once in the first t steps. In the general case, $S_i(t)$ depends on the starting site, while in homogeneous graphs the index i can be dropped.
To compute the generating function for $S_i(t)$, we first introduce the average number of new sites visited at time t, i.e.

$$\Delta_i(t) = S_i(t) - S_i(t-1) = \sum_{j \neq i} F_{ij}(t),$$

for all $t = 1, 2, \ldots$.
Its generating function is

$$\tilde{\Delta}_i(\lambda) = \sum_{t=1}^{\infty} \lambda^t \Delta(t) = \sum_j \tilde{F}_{ij}(\lambda) - \tilde{F}_{ii}(\lambda).$$

Inverting Eq.(2.2.3), one can write

$$\tilde{\Delta}_i(\lambda) = \sum_j \left[\frac{\tilde{P}_{ij}(\lambda) - \delta_{ij}}{\tilde{P}_{ii}(\lambda)} \right] - \left[1 - \frac{1}{\tilde{P}_{ii}(\lambda)} \right] = \sum_j \frac{\tilde{P}_{ij}(\lambda)}{\tilde{P}_{ii}(\lambda)} - 1.$$

Since $\sum_j P_{ij}(t) = 1$, the following holds:

$$\sum_j \tilde{P}_{ij}(\lambda) = \sum_t \lambda^t \sum_j P_{ij}(t) = \frac{1}{1-\lambda},$$

which entails

$$\tilde{\Delta}_i = \left[(1-\lambda)\, \tilde{P}_{ii}(\lambda) \right]^{-1}.$$

Returning now to $S_i(t)$, we notice that

$$S_i(t) = 1 + \Delta_i(1) + \cdots + \Delta_i(t),$$

so that its generating functions satisfies

$$\begin{aligned} \tilde{S}_i(\lambda) &= 1 + \lambda\,(1 + \Delta_i(1)) + \lambda^2\,(1 + \Delta_i(1) + \Delta_i(2)) + \ldots \\ &= \left(1 + \lambda + \lambda^2 + \ldots\right) + \lambda\left(1 + \lambda + \lambda^2 + \ldots\right)\Delta_i(1) + \ldots \\ &= (1-\lambda)^{-1}\left[1 + \lambda\Delta_i(1) + \lambda^2\Delta_i(2) + \ldots\right] \\ &= (1-\lambda)^{-2}\,\tilde{P}_{ii}(\lambda)^{-1}. \end{aligned} \tag{2.4.2}$$

So the knowledge of the probabilities of return on a graph is enough to determine the behaviour of $S_i(t)$. As before, the dependence of $S_i(t)$ on i is not trivial in a general graph, while the index can be dropped for homogeneous graphs.

2.5 Transience and Recurrence

Definition. A RW on a graph is said to be **recurrent** if the probability of ever returning to the starting point is 1, that is to say

$$\sum_t F_{ii}(t) = 1. \tag{2.5.1}$$

Equivalently, a RW on a graph is recurrent when the average number of visits of the starting point is infinite, i.e. when

$$\sum_t P_{ij}(t) = +\infty.$$

That the two definitions are indeed the same can be easily proven: when $i = j$, Eq.(2.2.3) reads

$$\tilde{P}_{ii}(\lambda) = \Big(1 - \tilde{F}_{ii}(\lambda)\Big)^{-1},$$

so that

$$\lim_{\lambda\to 1} \tilde{F}_{ii}(\lambda) = \sum_t \tilde{F}_{ii}(t) \Rightarrow \lim_{\lambda\to 1} \tilde{P}_{ii}(\lambda) = +\infty.$$

On the other hand,

$$\tilde{F}_{ii}(\lambda) = 1 - \frac{1}{\tilde{P}_{ii}(\lambda)}$$

implies the converse relation.

It is essential to notice that, on a connected graph, if the RW is recurrent at j, it is recurrent starting from any other vertex.

A way to prove it is as follows: it is obvious that, for any i,

$$P_{jj}(t) > \sum_{\tau_1}\sum_{\tau_2} F_{ji}(\tau_1)P_{ii}(t-\tau_1-\tau_2)F_{ij}(\tau_2).$$

Now multiply by λ^t and sum over t: after a little math it results that

$$\tilde{P}_{jj}(\lambda) > \tilde{F}_{ji}(\lambda)\tilde{P}_{ii}(\lambda)\tilde{F}_{ij}(\lambda);$$

so that $\tilde{P}_{ii}(1) = +\infty$, implies $\tilde{P}_{jj}(1) = +\infty$ for all j.

Definition. When $\sum_t F_{ii}(t)$ is less than 1, the RW is called **transient**, and there

is a finite chance for a walker never to return to the starting point.

Any **finite** graph $\mathcal{G}$, that's to say a graph such that

$$\#\mathcal{P} < \infty,$$

is recurrent.

The problem of transience/recurrence is thus only meaningful in the case of infinite size graphs, which are usually obtained as the limit of a sequence of growing finite graphs.

2.6 Traps in a Random Walk

A useful generalization of the RW is obtained by introducing traps. The transition probabilities then satisfy

$$\sum_j p_{ij} = 1 - d_i, \tag{2.6.1}$$

where $d_i > 0$ is the **probability of death** of the walker. Traps then determine the possibility that after a step the RW goes nowhere, which is the same as saying that it's been destroyed.
If traps are everywhere on the graph, we expect the walker to die relatively soon. To give a quantitative meaning to this affirmation, take the case of a graph with all vertices satisfying $d_i = d$. Now let $D(t)$ be the probability that the walker is dead after t steps, and let $A(t) = 1 - D(t)$. An immediate recursion rule is the following:

$$A(t) = A(t-1)(1-d),$$

which can be iterated to obtain

$$A(t) = (1-d)^t,$$

and finally

$$D(t) = 1 - (1-d)^t. \tag{2.6.2}$$

The probability of death can be considered an effective cut-off on the length of the RW, of size $1/\log(1-d)$. Actually, this is exactly what happens in generating functions for $\lambda < 1$: paths of length greater than $\log(\lambda^{-1})$ are exponentially suppressed since

$$\tilde{P}_{ij}(t) = \sum_t \lambda^t P_{ij}(t).$$

As seen from another point of view, the $\lambda \to 1$ limit of generating functions can be seen as a regulator for divergent quantities (e.g. expected number of returns in a recurrent graph) or for the thermodynamic limit, as they allow for the exploration of just a finite part of the graph.

2.7 Spectral Dimension

In this section we mainly follow ref. [11].

Local Spectral Dimension

Quantities like $F_{ii}(t)$ and $P_{ii}(t)$ usually show a well-defined behaviour as $t \to \infty$, which in most cases is a power law [11]. The **local spectral dimension**, provided that it exists, is defined as $\tilde{d}$ in the following asymptotic expression for $t \to \infty$:

$$P_{ii}(t) \sim t^{-\tilde{d}/2}. \tag{2.7.1}$$

The local spectral dimension can be proved in effect to be site independent [11], more precisely the previous equation implies

$$P_{hk}(t) \sim t^{-\tilde{d}/2},$$

for all h, k. In a more general, albeit less intuitive, fashion, the local spectral dimension can be defined as

$$\tilde{d} = -2 \lim_{t\to\infty} \frac{\log P_{ii}(t)}{\log t}, \tag{2.7.2}$$

which has the advantage of including both the limiting case $\tilde{d} = \infty$, for decays faster than any power law, and possible logarithmic corrections to the $P_{ii}(t)$, which are indeed frequent.

Introducing traps in a random walk can substantially change the asymptotic behaviour of the graph. In particular, a finite number of traps shifts the fractal dimension from $\tilde{d}$ to $(\tilde{d}+1)$ whenever $\tilde{d} < 2$ (as the walk is recurrent, even a single trap has a sizeable effect on the behaviour of the RW), while it does not affect transient random walks, i.e. $\tilde{d} > 2$. The case of $\tilde{d} = 2$ depends on the sub-leading behaviour in t, so it can not be fully examined based on $\tilde{d}$ alone, as the spectral dimension by definition conceals such details.

The case for an infinite amount of traps is more complex, as its effect depend on the details of the distribution. We will not discuss it here.

The local spectral dimension $\tilde{d}$ is a separate entity from the intrinsic fractal dimension d_{frac}, which we defined in Eq.(1.3.1) as a measure of the growth of the number of points inside a Van Hove sphere.

Average Spectral Dimension

While the local spectral dimension is the same on each point of the graph, the average behaviour of the probabilities of return on the graph vertices is not guaranteed to yield the same asymptotics. As long as the cardinality of the graph is finite, or the graph is homogeneous, the average behaviour will give the same spectral dimension; when a graph is inhomogeneous, though, things get murkier.

To introduce the problem, let us define graph averages of quantities defined on each vertex:

$$\langle A_j \rangle = \lim_{R\to\infty} \frac{1}{\#S_{0,R}} \sum_{i\in S_{0,R}} A_i, \tag{2.7.3}$$

where $i \in S_{0,R}$ is a short-hand notation implying that the sum runs over the vertices of the Van Hove sphere $S_{0,R}$, of radius R and centred in 0 (more properly, $i \in S_{0,R}$ should read $i \in P_{0,R}$, and $\#S_{0,R}$ should read $\#P_{0,R}$, where $P_{0,R}$ is the set of vertices of the Van Hove sphere $S_{0,R}$) (See Sec.1.2).

As long as the graph $\mathcal{G}$ is embeddable in a finite dimensional space, i.e. $\mathcal{G}$ has finite fractal dimension, the average does not depend on what point we choose as the origin.
We can now define the average probabilities of return and of first return:

$$\begin{aligned} P(t) &= \langle P_{ii}(t) \rangle, \\ F(t) &= \langle F_{ii}(t) \rangle. \end{aligned}$$

The averaged expectation values of the number of returns on the graph and the average probability of ever returning to the origin can then be found as a limit of the respective generating function:

$$\begin{aligned} \sum_t P(t) &= \lim_{\lambda\to 1^-} \tilde{P}(\lambda), \\ \sum_t F(t) &= \lim_{\lambda\to 1^-} \tilde{F}(\lambda). \end{aligned}$$

Definition. A graph on which

$$\lim_{\lambda\to 1^-} \tilde{F}(\lambda) = 1$$

is said **recurrent on average**, while if the limit is less than one the graph is said **transient on average**.

The corresponding asymptotic behaviour then defines the average spectral dimension

$$\bar{d} = -2 \lim_{t\to\infty} \frac{\log P(t)}{\log t}. \tag{2.7.4}$$

The main property of $\bar{d}$ is its invariance under a large class of transformations, which make the average spectral dimension a robust measure of the fundamental structure of the graph. More in detail, transformations that leave $\bar{d}$ unchanged are

- the addition (or subtraction) of a finite number of traps: only a finite amount of points, in the thermodynamic limit, will be closer than a given R to the traps, and thus will be able to perceive its presence (it should be noted, however, that each local probability function will be affected by the presence of even a single trap, and so will its asymptotic behaviour);

- a bounded rescaling of the probabilities, i.e. $p_{ij} \mapsto p'_{ij}$, with

$$0 < p_{min} \leq p'_{ij} < p_{Max}$$

  whenever $p_{ij} > 0$ (and of course $\sum_j p'_{ij} \leq 1$ for all i);

- adding links between vertices not farther away than an arbitrary but finite chemical distance;

- topological rescaling, i.e. first partitioning the graph $\mathcal{G}$ into an infinite family of connected subgraphs $\{\mathcal{G}_\alpha\}$, with $\#\mathcal{G}_\alpha \leq D < \infty$; then substituting each $\mathcal{G}_\alpha$ with $\mathcal{G}'_\alpha$, connecting each pair $(\mathcal{G}'_\alpha, \mathcal{G}'_\beta)$ with links if and only if $(\mathcal{G}_\alpha, \mathcal{G}_\beta)$ were connected.

Using these spectral dimension-preserving transformations can reduce a complex graph to a simpler version, allowing for an otherwise difficult computation of $\bar{d}$. Conversely, it is possible to transform a known simple graph into a very involved and highly inhomogeneous version of itself, while preserving the asymptotic behaviour of the average probability of return.

The average spectral dimension and the local spectral dimension are the same on all regular lattices and exactly decimable fractals, and in fact it wasn't until fairly recently [12–15] that concrete examples of graphs exhibiting different $\bar{d}$ and $\tilde{d}$ emerged.

It is indeed possible that macroscopic inhomogeneity of the graph entails different asymptotic behaviours when considering its homogeneous subgraphs; in this case one speaks of **spectral classes**, each characterized by a given spectral dimension. We will see examples of such behaviour in chapter 3.

2.8 Continuous Time Random Walks

A variation of the RWs on graphs we discussed until now is obtained by letting the random displacements occur at random continuous times instead of at fixed discrete steps.

Following Montroll and Weiss [8], let $t_1, t_2, \ldots$ be the times at which the steps occur; the quantities

$$T_1 = t_1, \;\; T_2 = t_2 - t_1, \;\; \ldots, \;\; T_n = t_n - t_{n-1}, \;\; \ldots$$

are independent random variables with a common probability distribution $\psi(t)$, i.e. $\psi(t)$ is the probability density that the particle jumps after loitering for a time t. $\psi(t)$ of course satisfies

$$\int_0^{+\infty} dt \; \psi(t) = 1.$$

A set of useful accessory probability functions is the class $\psi_n(t)$, giving the probability that the n-th step occurs at time t. For consistency reasons, it is convenient

to set $\psi_0(t) = \delta(t)$; the other ψ_n satisfy a simple recursion relation: in order for the n-th step to occur at time t, the $(n-1)-th$ step must have occurred at time $t' < t$, so that

$$\psi_n(t) = \int_0^t d\tau\ \psi(\tau)\psi_{n-1}(t-\tau). \tag{2.8.1}$$

While with discrete random walks we used the generating functions technique, here the most appropriate tool for the computation is the Laplace transform, which for $\psi(t)$ reads

$$\tilde{\psi}(y) = \int_0^{+\infty} dt\ e^{-yt}\psi(t). \tag{2.8.2}$$

Taking into account that $\tilde{\psi}_0(y) = 1$, the deconvolution properties of the Laplace transform yield as an immediate result

$$\tilde{\psi}_n(y) = \tilde{\psi}(y)\tilde{\psi}_{n-1}(y) = \left[\tilde{\psi}(y)\right]^n. \tag{2.8.3}$$

The probabilities $\bar{P}_{ij}(t)$ and $\bar{F}_{ij}(t)$ are the continuous-time equivalent of $P_{ij}(t)$ and $F_{ij}(t)$. We have to be more careful now, and explicitly notice that $\bar{P}_{ij}(t)$ is the probability functions that the walker has arrived at j at some time $t' \leq t$ and hasn't moved ever since, while $\bar{F}_{ij}(t)$ is the probability that the walker has arrived for the first time in j exactly at time t.
Since the transition probabilities for each step are still given by p_{ij}, a strong connection exists between the probability functions for discrete and continuous time RWs.
In the case of $\bar{F}_{ij}(t)$ we can write

$$\bar{F}_{ij}(t) = \sum_{n=0}^{\infty} F_{ij}(n)\psi_n(t); \tag{2.8.4}$$

once again the Laplace transform proves useful, as

$$\tilde{\bar{F}}_{ij}(y) = \sum_{n=0}^{\infty} F_{ij}(n)\left[\tilde{\psi}(y)\right]^n = \tilde{F}_{ij}\left(\tilde{\psi}(y)\right). \tag{2.8.5}$$

The case for $\bar{P}_{ij}(t)$ is a little more complex. Let $\bar{A}_{ij}(t)$ be the probability of arriving at j exactly at time t; then a reasoning analogous to the previous one entails

$$\begin{aligned} \bar{A}_{ij}(t) &= \textstyle\sum_{n=0}^{\infty} P_{ij}(n)\psi_n(t), \\ \tilde{\bar{A}}_{ij}(y) &= \tilde{P}_{ij}\left(\tilde{\psi}(y)\right). \end{aligned} \tag{2.8.6}$$

As we have already discussed, the walker arrived in j at some time $t' \leq t$ and then stopped; the probability of this happening is

$$\bar{P}_{ij}(t) = \int_0^t d\tau\ \bar{A}_{ij}(\tau)\left(1 - \int_0^{t-\tau} d\chi\ \psi(\chi)\right). \tag{2.8.7}$$

Compute now its Laplace transform:

$$\tilde{\bar{P}}_{ij}(y) = \tilde{\bar{A}}_{ij}(y) \cdot \int_0^\infty dt\; e^{-yt} \left(1 - \int_0^t d\chi\; \psi(\chi)\right);$$

the integral on the right side can be tackled as follows:

$$\int_0^\infty dt\; e^{-yt} \left(1 - \int_0^t d\chi\; \psi(\chi)\right) = \frac{1}{y} - \int_0^{+\infty} d\chi\; \psi(\chi) \int_\chi^{+\infty} dt\; e^{-yt}$$
$$\frac{1}{y} - \int_0^{+\infty} d\chi\; \psi(\chi) \frac{1}{y} e^{-y\chi} = \frac{1}{y}\left(1 - \tilde{\psi}(y)\right),$$

which entails

$$\tilde{\bar{P}}_{ij}(y) = \tilde{P}_{ij}\left(\tilde{\psi}(y)\right) \frac{1}{y}\left(1 - \tilde{\psi}(y)\right). \tag{2.8.8}$$

As a consequence, the continuous time RW is solved by the joint knowledge of the discrete time generating functions and the probability distribution for the jumps.

2.9 Vibrational Dynamics and Random Walks

It is possible to link the continuous-time RW (CTRW) to the vibrational dynamics of masses and springs on a graph for a simple random walk.

CTRW and the Spectrum of the Laplace Operator

To obtain this analogy, we first analyse the master equation for the probability $\bar{P}_{ij}(t)$. Let $w\; dt$ be the probability that a jump occurs in a time interval dt; the probability $\bar{P}_{(nj)}(t)$ that no jump occurs between 0 and t satisfies

$$\bar{P}_{(nj)}(t + dt) = \bar{P}_{(nj)}(t) \cdot (1 - w\; dt),$$

or

$$\frac{d\bar{P}_{(nj)}(t)}{dt} = -w\bar{P}_{(nj)}(t),$$

which entails

$$\bar{P}_{(nj)}(t) = Ae^{-wt},$$

for some constant A.
Since $\psi(t)\; dt = \bar{P}_{(nj)}(t)\; wdt$,

$$\psi(t) = w\bar{P}_{(nj)}(t) = wAe^{-wt}.$$

The constant A is then given by

$$1 = \int_0^\infty wAe^{-wt} = A.$$

The master equation for $\bar{P}_{ij}(t)$ reads

$$\bar{P}_{ij}(t+dt) \;=\; \bar{P}_{ij}(t)\cdot(1-w\;dt)+\sum_k A_{kj}\bar{P}_{ik}(t)\cdot\left(\frac{w}{z_k}dt\right),$$

or

$$\frac{d\bar{P}_{ij}(t)}{dt}=w\left(-\bar{P}_{ij}(t)+\frac{1}{z_k}\sum_k A_{kj}\bar{P}_{ik}(t)\right)=w\sum_k A_{kj}\left(\frac{\bar{P}_{ik}(t)}{z_k}-\frac{\bar{P}_{ij}}{z_i}(t)\right). \tag{2.9.1}$$

A formal solution can be written [16] as

$$\bar{P}_{ij}(t)=\exp\left[tw\left(\mathbf{A}\mathbf{Z}^{-1}-\mathbf{I}\right)\right]_{ji}, \tag{2.9.2}$$

where $\mathbf{A}_{lm}=A_{lm}$, $\mathbf{Z}_{lm}=z_l\delta_{lm}$ and $\mathbf{I}$ is the identity matrix. It is easy to see that the previous equation is indeed a solution: expanding the exponential function one obtains

$$\begin{aligned}\frac{d\bar{P}_{ij}(t)}{dt} &= \left(\sum_{n=1}^{\infty}\frac{nt^{n-1}w^n\left(\mathbf{A}\mathbf{Z}^{-1}-\mathbf{I}\right)^n_{ji}}{n!}\right)\\ &= \left(\sum_{n=1}^{\infty}\sum_s\left(\mathbf{A}\mathbf{Z}^{-1}-\mathbf{I}\right)_{js}\frac{(tw)^{n-1}\left(\mathbf{A}\mathbf{Z}^{-1}-\mathbf{I}\right)^{n-1}_{si}}{n!}\right)\\ &= w\sum_s\left(\mathbf{A}\mathbf{Z}^{-1}-\mathbf{I}\right)_{js}\bar{P}_{is}(t)=w\sum_s A_{js}\left[\frac{\bar{P}_{is}(t)}{z_s}-\frac{\bar{P}_{ij}(t)}{z_j}\right],\end{aligned}$$

which is indeed Eq.(2.9.1).
A continuous-time analogous of the averaging procedure we saw in Sec.2.7 defines the average return probability $\bar{P}(t)$:

$$\bar{P}(t)=\lim_{R\to\infty}\sum_{i\in S_{0,R}}\frac{\bar{P}_{ii}(t)}{\#S_{0,R}}=\lim_{R\to\infty}\frac{1}{\#S_{0,R}}\;Tr\exp\left[tw\left(\mathbf{A}_{S_{0,R}}\mathbf{Z}^{-1}_{S_{0,R}}-\mathbf{I}_{S_{0,R}}\right)\right]. \tag{2.9.3}$$

Under the same conditions as for the discrete-time RWs, or in the case that the graph is homogeneous, the average is independent of the choice of the origin 0.
Suppose now that $\mathbf{Z}=z\mathbf{I}$.
The right-hand part of the previous equation, when expressed in terms of the eigenvalues, yields an integral over the spectral density of the operator $(z^{-1}\mathbf{A}-\mathbf{I})$. As it is customary to consider the Laplace operator $\mathcal{L}=(\mathbf{z}-\mathbf{A})$, we will call $\rho_{\mathcal{L}}(\lambda)$ its spectral density, so that

$$\bar{P}(t)=\int_0^{\infty}d\lambda\;\rho_{\mathcal{L}}(\lambda)\exp\left(-tw\lambda/z\right).$$

Vibrational Dynamics of Masses and Springs

Consider the same graph $\mathcal{G}$ on which the CTRW happens with two modifications: on each site sits a mass m, and to each link corresponds a spring of elastic constant k. The mass is free to move, relative to the equilibrium position, in a fictitious space of dimension D, its position being labelled as $\vec{\phi}_i$.
Since there is no coupling among different components of the vector $\vec{\phi}_i$, the equations of motion for the springs can be written for a single component ϕ_i:

$$m\frac{d^2\phi_i}{dt^2} = k\sum_j A_{ij}\left(\phi_i - \phi_j\right).$$

It is straightforward to find solutions of the form

$$\phi_i(t) = e^{i\omega t}\phi_i(0),$$

as the equations of motion are then transformed into a system of algebraic equations:

$$\begin{cases} -m\omega^2\phi_i(0) = k\sum_j A_{ij}\left[\phi_j(0) - \phi_i(0)\right] = k\sum_j \left[A_{ij} - z\delta_{ij}\right]\phi_j(0) \\ i = 1, 2, \ldots \end{cases}.$$

In matrix form, the same equations read

$$k\left(z\mathbf{I} - \mathbf{A}\right)\phi(0) = k\mathcal{L}\phi(0) = m\omega^2\phi(0); \tag{2.9.4}$$

this formula links the possible values of ω to the eigenvalues of $\mathcal{L}$:

$$\omega_i^2 = \frac{k\lambda_i}{m}. \tag{2.9.5}$$

Since the eigenvalues are in a one-to-one correspondence, for an infinite graph the spectral distributions satisfy

$$\rho_{\mathcal{L}}(\lambda)d\lambda = \rho(\omega)d\omega,$$

and the averaging procedure reads

$$\bar{P}(t) = \int_0^\infty d\omega\ \rho(\omega)\exp\left(-tmw\omega^2/kz\right), \tag{2.9.6}$$

thus completing the relationship between a classical system of masses and springs and RWs.

The last equation links indissolubly the distribution of the normal modes of oscillation of the system to the behaviour of the average RW on the corresponding graph. This analogy goes further, linking the average spectral dimension $\bar{d}$ to the low frequency behaviour of $\rho(\omega)$.

3

Random Walks on General Graphs

3.1 Random Walks on d-Dimensional Regular Lattices

A most powerful technique which can be employed in the study of RWs is the Fourier transform. Its applicability wholly depends on two conditions: the periodicity of the graph (which therefore needs to be a regular lattice) and the homogeneity of its points. In this chapter we introduce the technique, including some technical details, and apply it to the simplest lattices.

Among the simplest types of graphs are regular d-dimensional cubic lattices with periodic boundary conditions, which can be computed using Fourier techniques [8]. A point on the lattice is written as $\mathbf{x} = (x_1, \ldots, x_d)$. The periodic boundary conditions read

$$(x_1 + n_1 N, \ldots, x_d + n_d N) = (x_1, \ldots, x_d) \tag{3.1.1}$$

where N is the edge of the cubic lattice. Let now $P_{\mathbf{x}}(t)$ be the probability that a random walker starting at some given point - which we call the origin - arrives at $\mathbf{x}$ at time t, while the one-step transition probabilities are given by $p_{\mathbf{x}}$, which satisfy $\sum_{\mathbf{x}} p_{\mathbf{x}} = 1$, as **we suppose that the number of walkers is conserved**. In general the $p_{\mathbf{x}}$ can have non-zero transition probabilities for points which aren't nearest-neighbours.
Since the one-step transition probabilities are given by $p_{\mathbf{x}}$, the following recurrence relation holds:

$$P_{\mathbf{x}}(t+1) = \sum_{\mathbf{y}} p_{(\mathbf{x}-\mathbf{y})} P_{\mathbf{y}}(t). \tag{3.1.2}$$

The two previous equations immediately entail $\sum_{\mathbf{x}} P_{\mathbf{x}}(t) = 1$.
The choice of the origin is unimportant, as the lattice is homogeneous.
From the previous equation it immediately follows that

$$P_{(x_1+n_1N,\ldots,x_d+n_dN)}(t) = P_{(x_1,\ldots,x_d)}(t). \tag{3.1.3}$$

Transition probabilities can be Fourier expanded as

$$\tilde{p}_{(2\pi\mathbf{x}/N)} = \sum_{\mathbf{y}} p_{\mathbf{y}} \ \exp\left(2\pi i \mathbf{x}\cdot\mathbf{y}/N\right);$$

they satisfy $\tilde{p}_{\mathbf{0}} = 1$ and $0 < \tilde{p}_{\mathbf{x}}(\lambda) \leq 1$ when $0 < \lambda \leq 1$.

3.2 Generating Functions for Regular Lattices

To proceed in the calculations we introduce the generating function

$$\tilde{P}_{\mathbf{x}}(\lambda) = \sum_{t=0}^{\infty} \lambda^t P_{\mathbf{x}}(t), \tag{3.2.1}$$

which satisfies $\sum_{\mathbf{x}} \tilde{P}_{\mathbf{x}}(\lambda) = (1-\lambda)$.

Eq.(3.1.2), together with the initial condition $P_{\mathbf{0}}(0) = 1$, yields

$$\tilde{P}_{\mathbf{x}}(\lambda) - \delta_{\mathbf{x},\mathbf{0}} = \lambda \sum_{\mathbf{y}} p_{(\mathbf{x}-\mathbf{y})} \tilde{P}_{\mathbf{y}}(\lambda).$$

In order to take advantage of the translational invariance, we introduce the Fourier expansion of the generating function:

$$u_{2\pi\mathbf{x}/N}(\lambda) = \sum_{\mathbf{y}} P_{\mathbf{y}}(\lambda) \exp\left(2\pi i \mathbf{x}\cdot\mathbf{y}\right). \tag{3.2.2}$$

It allows one to straightforwardly solve Eq.(3.1.2):

$$u_{2\pi\mathbf{x}/N}(\lambda) = \left[1 - \lambda\tilde{p}_{(2\pi\mathbf{x}/N)}\right]^{-1},$$

and by inverting the Fourier expansion we finally obtain

$$\begin{aligned}
\tilde{P}_{\mathbf{x}}(\lambda) &= N^{-d} \sum_{\mathbf{y}} \frac{\exp\left(-2\pi i \mathbf{x}\cdot\mathbf{y}/N\right)}{1 - \lambda\tilde{p}_{2\pi\mathbf{y}/N}} \\
&= \sum_{t} \lambda^t \left[N^{-d} \sum_{\mathbf{y}} \exp\left(-2\pi i \mathbf{x}\cdot\mathbf{y}\right) \left(\tilde{p}_{2\pi\mathbf{y}/N}\right)^t \right] \\
&= \sum_{t} \lambda^t P_{\mathbf{x}}(t).
\end{aligned}$$

3.3 Recurrent and Transient Random Walks on Regular Lattices

It is useful to divide $\tilde{P}_{\mathbf{x}}(\lambda)$ into two parts: one singular and one non-singular in the limit $\lambda \to 1$:

$$\tilde{P}_{\mathbf{x}}(\lambda) = (1-\lambda)^{-1} N^{-d} + \phi_{\mathbf{x}}(\lambda),$$

with

$$\phi_{\mathbf{x}}(\lambda) = N^{-d} \sum_{\mathbf{y}}{}' \frac{\exp(2\pi i \mathbf{x}\cdot \mathbf{y}/N)}{1 - \lambda \tilde{p}_{(2\pi \mathbf{x}/N)}}. \tag{3.3.1}$$

In the non-singular part $\phi_{\mathbf{x}}(\lambda)$, the primed sum runs over $\mathbf{y} \neq (0, \ldots, 0)$.
Since $\tilde{P}_{\mathbf{x}}(\lambda = 1)$ corresponds to the expected number of visits of $\mathbf{x}$ starting from the origin, $\sum_t P_{\mathbf{x}}(t) = \infty$ and the RW is trivially recurrent whatever the value of N, as long as N is finite.

In the limit $N \to \infty$ some two things happen:

- the singular part $(1 - \lambda)^{-1} N^{-d}$ gets killed,
- the sum over lattice points becomes an integral in $\theta = \lim_{N\to\infty} 2\pi \mathbf{y}/N$:

$$\tilde{P}_{\mathbf{x}}(\lambda) = \frac{1}{(2\pi)^d} \int_{-\pi}^{+\pi} \ldots \int_{-\pi}^{+\pi} d^d\theta \, \frac{\exp\left(-i\mathbf{x}\cdot\theta\right)}{1 - \lambda \tilde{p}_{\theta}}. \tag{3.3.2}$$

A new singularity at $\lambda = 1$ can of course emerge from the integral: to see how this happens, consider that, at fixed $p_{\mathbf{x}}$ and large but finite N, $\tilde{p}(\lambda = 1)$ satisfies

$$\tilde{p}(\lambda = 1) \sim 1 - \frac{c}{N},$$

with c a constant; this entails

$$\phi_{\mathbf{0}}(\lambda = 1) \sim N^{-d} \cdot N \cdot \sum_{\mathbf{x}}{}' 1 = N^{2-d}.$$

Therefore, for RWs on regular lattices of $d = 1, 2$ the number of returns to the origin is infinite (for $d = 2$ logarithmic corrections enter the game), and the RW is **recurrent**, while when $d \geq 3$ the RW is **transient**.

3.4 The Bethe Lattice

The Bethe lattice, also known as Cayley tree, is a tree with constant coordination number z. The pathological cases $z = 1$, corresponding to a pair of vertices, and $z = 2$, corresponding to the infinite line, will be ignored, and we will focus on the case $z \geq 3$. Because of the homogeneity of the Bethe lattices, propreties such as the probabilities of return, or of transition, do not depend on the choice of the origin.

The Bethe lattice has several interesting characteristic, essentially tied to the fact that the border of any sphere of Van Hove scales with the volume of the sphere itself. In fact S_R, the number of points at distance $R > 1$ from a point chosen as the origin is simply computed as

$$S_R = (z - 1) S_{R-1};$$

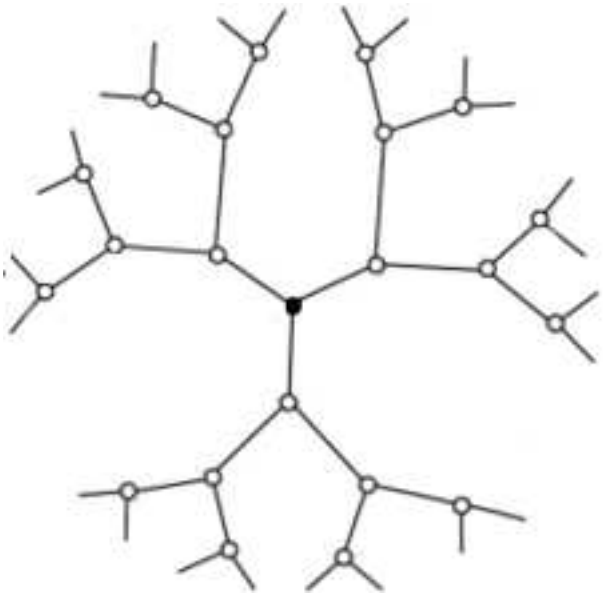

Figure 3.1: A Bethe lattice for $z = 3$.

since $S_0 = 1$ and $S_1 = z$, S_R satisfies

$$S_R = z(z-1)^{R-1} \tag{3.4.1}$$

for all $R \geq 1$. The number of points in a Van Hove sphere of radius R can be calculated as a sum over the S_R:

$$\begin{aligned} N_R &= \sum_{l=0}^{R} S_l = 1 + \sum_{l=1}^{R} z(z-1)^{l-1} = 1 + z\sum_{t=0}^{R-1}(z-1)^t \\ &= 1 + z\frac{(z-1)^R - 1}{(z-1)-1} = \frac{1}{z-2}\left((z-2) + z(z-1)^R - z\right) \\ &= \frac{z(z-1)^R - 2}{z-2}. \end{aligned} \tag{3.4.2}$$

It is easy to prove that N_R is in effect an integer number, in fact

$$\begin{aligned} z(z-1)^R - 2 &= (z-2)(z-1)^R + 2(z-1)^R - 2 \\ &= (z-2)(z-1)^R + 2\left[(z-1)^R - 1\right]; \end{aligned}$$

since the second term too can be divided by $(z-2)$, as

$$(z-1)^R - 1 = [(z-2)+1]^R - 1 = \sum_{l=0}^{R}\binom{R}{l}(z-2)^l - 1 = \sum_{l=1}^{R}\binom{R}{l}(z-2)^l,$$

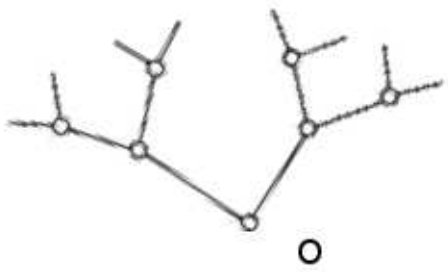

Figure 3.2: The subgraph $\mathcal{B}_1$ for $z = 3$ and its origin O.

N_R is indeed an integer.
The fractal dimension for the Bethe Lattice is infinity, since

$$\lim_{R\to\infty} \frac{\log N_R}{\log R} = +\infty,$$

or more properly there is no number d_{frac} such that

$$N_R \leq CR^{d_{frac}} + E$$

for some constants C and E.

It is now straightforward to prove that the ratio between surface and volume of any given sphere of Van Hove tends to a constant:

$$\lim_{R\to\infty} \frac{S_R}{N_R} = \frac{(z-2)}{(z-1)}.$$

Simple RW and Return Probabilities

Consider now a simple RW on the Bethe lattice. Because of its translational invariance, we drop the index of the starting point; since all the points at distance R are equivalent, instead of $P_{ij}(t)$ we write $P_R(t)$. The simplest way to proceed is by calculating the first return probabilities, as they make the best use of the tree nature of the lattice: each path returning to the origin for the first time at t makes a first step with probability 1, then performs a RW on the subgraph $\mathcal{B}_1$, returning to O - the origin of $\mathcal{B}_1$ - after $(t-2)$ steps, and finally steps back to the origin with probability $(z-1)/z$.

$$F_0(t) = P_0^{\mathcal{B}_1}(t-2)\frac{1}{z} \tag{3.4.3}$$

The subgraph $\mathcal{B}_1$ is one of the z equivalent subtrees obtained by severing the z links at the origin of the RW. The RW on $\mathcal{B}_1$ ceases to be both simple, as there is a trap in O of weight $(z-1)/z$, and homogeneous, while it retains its isotropy (its subtrees are equivalent).

Instead of trying to compute $P_0^{\mathcal{B}_1}(t)$, we consider the corresponding first return probabilities $F_0^{\mathcal{B}_1}(t)$, and then pass to generating functions; each path contributing to $F_0^{\mathcal{B}_1}(t)$ steps first - with probability $(z-1)/z$ - into one of the subtrees of $\mathcal{B}_1$, then it performs a RW on said subtree, which is once again $\mathcal{B}_1$, and finally steps back to O with probability $1/z$. It has then to satisfy

$$\begin{cases} F_0^{\mathcal{B}_1}(t) = \frac{z-1}{z} P_0^{\mathcal{B}_1}(t-2)\frac{1}{z} = \frac{z-1}{z^2} P_0^{\mathcal{B}_1}(t-2) \\ \\ \tilde{F}_0^{\mathcal{B}_1}(\lambda) = \frac{z-1}{z^2}\lambda^2 \tilde{P}_0^{\mathcal{B}_1}(\lambda) \end{cases} . \tag{3.4.4}$$

The usual relation between the generating functions, Eq.(2.2.3), holds, so we have

$$\frac{z-1}{z^2}\lambda^2 \left[\tilde{P}_0^{\mathcal{B}_1}(\lambda)\right]^2 - \tilde{P}_0^{\mathcal{B}_1}(\lambda) + 1 = 0,$$

which entails

$$\tilde{P}_0^{\mathcal{B}_1}(\lambda) = \frac{z^2}{2(z-1)\lambda^2}\left(1 - \sqrt{1 - 4\frac{z-1}{z^2}\lambda^2}\right) = \frac{z^2}{(z-1)\lambda^2}\alpha(\lambda/z); \tag{3.4.5}$$

we put

$$\alpha(\eta) = \frac{1}{2}\left(1 - \sqrt{1 - 4(z-1)\eta^2}\right).$$

The minus sign in front of the square root has been chosen so that

$$\lim_{\lambda \to 1} \tilde{P}_0^{\mathcal{B}_1}(\lambda) = P_0^{\mathcal{B}_1}(t=0) = 1.$$

Eq.(3.4.3) yields

$$\begin{aligned} \tilde{F}_0(\lambda) &= \frac{\lambda^2}{z}\tilde{P}_0^{\mathcal{B}_1}(\lambda) = \frac{z}{2(z-1)}\left(1 - \sqrt{1 - 4\frac{z-1}{z^2}\lambda^2}\right) \\ &= \frac{z}{z-1}\alpha(\lambda/z), \end{aligned} \tag{3.4.6}$$

and

$$\tilde{P}_0(\lambda) = \frac{1}{1 - \frac{z}{z-1}\alpha(\lambda/z)}. \tag{3.4.7}$$

To calculate $F_i(t)$, observe that all the paths linking the origin to i have to tread a common set of links, which is the only self-avoiding path connecting the two vertices. Then each of the points on the self-avoiding path will be visited for the

first time sooner or later, while at all previous times the RW will be on a subgraph of the Bethe lattice, which is - unsurprisingly - $\mathcal{B}_1$. Let t_j be the number of steps before first visiting the j-th vertex on the self-avoiding path: since the events are independent $P_i(t)$ satisfies

$$F_i(t) = \left(\frac{1}{z}\right)^d \sum_{t_0} \cdots \sum_{t_{d-1}} P_0^{\mathcal{B}_1}(t_0) \dots P_0^{\mathcal{B}_1}(t_{d-1}) \delta_{\left(d+\sum_k t_k - t\right)},$$

where d is the chemical distance between the origin and i; evidently $P_i(t)$ only depends on d. Passing to generating functions allows one to obtain an explicit expression:

$$\tilde{F}_i(\lambda) = \left(\frac{\lambda}{z}\right)^d \left[\tilde{P}_0^{\mathcal{B}_1}(\lambda)\right]^d = \left[\frac{z\alpha(\lambda/z)}{(z-1)\lambda}\right]^d, \tag{3.4.8}$$

and

$$\tilde{P}_i(\lambda) = \tilde{P}_0(\lambda)\tilde{F}_i(\lambda) = \left[\frac{z\alpha(\lambda/z)}{(z-1)\lambda}\right]^d \frac{1}{1-\frac{z}{z-1}\alpha(\lambda/z)}. \tag{3.4.9}$$

By expanding $\tilde{P}_0(\lambda)$ in power series, it is possible to obtain the asymptotic behaviour of $P_0(t)$ as $t \to \infty$ [17]:

$$P_0(t) \sim \frac{2^{3/2} z(z-1)}{\sqrt{\pi}\,(z-2)^2} t^{-3/2} \exp\left[-t \log\left(\frac{z}{2\sqrt{z-1}}\right)\right]. \tag{3.4.10}$$

The exponential law that one obtains on the Bethe lattice is easily understood as a consequence of the high probability of increasing the distance from the origin at each step.

3.5 Vibrational Spectrum and Specific Heat of the Bethe Lattice

Following a paper by Cassi [16], we now exploit Eq.(2.9.6) to obtain meaningful thermodynamic quantities on the Bethe lattice, namely the vibrational modes density for low ω and the vibrational specific heat.
The asymptotic behaviour of the average CTRW return times $\bar{P}(t)$, Eq.(2.9.6), can be obtained from Eq.(3.4.9) and Eq.(2.8.8):

$$\bar{P}(t) \sim \frac{z(z-1)}{\sqrt{4\pi}\,(z-2)^2} \left(\frac{tw\sqrt{z-1}}{z}\right)^{-3/2} \times \exp\left[-\frac{tw\left(z-2\sqrt{z-1}\right)}{z}\right].$$

Applying standard theorems for asymptotic expansions and Laplace transforms, one obtains the small ω behaviour of the spectral density ρ_ω, which displays a gap between $\omega = 0$ and the eigenvalue

$$\omega = \omega_c = \sqrt{\frac{k\left(z-2\sqrt{z-1}\,\right)}{mz}}.$$

Explicitly

$$\rho_\omega = \begin{cases} 0 & \omega < \omega_c \\ \omega\sqrt{\omega^2-\omega_c^2}\frac{z(z-1)^{-1/4}}{2\pi(z-2)^2\left(\frac{k}{m}\right)^{3/2}} & \omega \geq \omega_c \end{cases} . \tag{3.5.1}$$

The presence of the gap is essentially due to the exponential decay of the return probabilities, and it entails other important consequences, which we now explore.

Eq.(3.5.1) is a result valid for low frequencies; extending it to high frequencies is improper, as one immediately faces a divergence. The standard quantization procedure associates quanta of energy $\hbar\omega$ to modes of frequency ω. To proceed with the calculations, we set an artificial cut-off $\omega \leq \omega_D$ - as in Debye approximation - where ω_D satisfies

$$\int_{\omega_c}^{\omega_D} \rho(\omega) d\omega = 1.$$

Computing ω_D is straightforward:

$$\begin{aligned} 1 &= \int_{\omega_c}^{\omega_D} d\omega\ \rho(\omega) = \frac{z(z-1)^{-1/4}}{2\pi(z-2)^2\left(\frac{k}{m}\right)^{3/2}} \int_{\omega_c}^{\omega_D} d\omega\ \omega\sqrt{\omega^2-\omega_c^2} \\ &= \frac{z(z-1)^{-1/4}}{2\pi(z-2)^2\left(\frac{k}{m}\right)^{3/2}} \times \frac{1}{2}\frac{\left(\omega^2-\omega_c^2\right)^{3/2}}{\frac{3}{2}}; \end{aligned}$$

as a consequence

$$\omega_D^2 = \omega_c^2 + \frac{m^2}{k^2}\left[\frac{6\pi(z-2)^2}{z(z-1)^{1/4}}\right]^{2/3} . \tag{3.5.2}$$

The expected energy can then be obtained by averaging on the Bose-Einstein distribution corresponding to the density of states $\rho(\omega)$:

$$E(t) = \int_{\omega_c}^{\omega_D} d\omega\ \hbar\omega \frac{\rho(\omega)}{\exp\left(\frac{\hbar\omega}{kT}-1\right)}. \tag{3.5.3}$$

The low temperature limit can be calculated easily: as $T \to 0$, the integral is dominated by the exponential term, and

$$\begin{aligned} E(T) &\sim \int_{\omega_c}^{\omega_c+kT/\hbar} d\omega\ \hbar\omega\rho(\omega)\exp\left(-\frac{\hbar\omega}{kT}\right) \sim \frac{z(z-1)^{-1/4}}{2\pi(z-2)^2\left(\frac{k}{m}\right)^{3/2}}\left(\frac{kT}{\hbar}\right)\hbar\omega_c\rho(\omega_c) \times \\ &\times \exp\left(-\frac{\hbar\omega}{kT}\right) = \frac{z(z-1)^{-1/4}}{2\pi(z-2)^2\left(\frac{k}{m}\right)^{3/2}}\left(\frac{kT}{\hbar}\right)\hbar\omega_c^2\sqrt{2\omega_c\frac{kT}{\hbar}} \\ &= \frac{z(z-1)^{-1/4}}{\sqrt{2}\pi(z-2)^2\left(\frac{k}{m}\right)^{3/2}}\left(\frac{kT}{\hbar}\right)^{3/2}\hbar\omega_c^{5/2}\exp\left(-\frac{\hbar\omega_c}{kT}\right). \end{aligned} \tag{3.5.4}$$

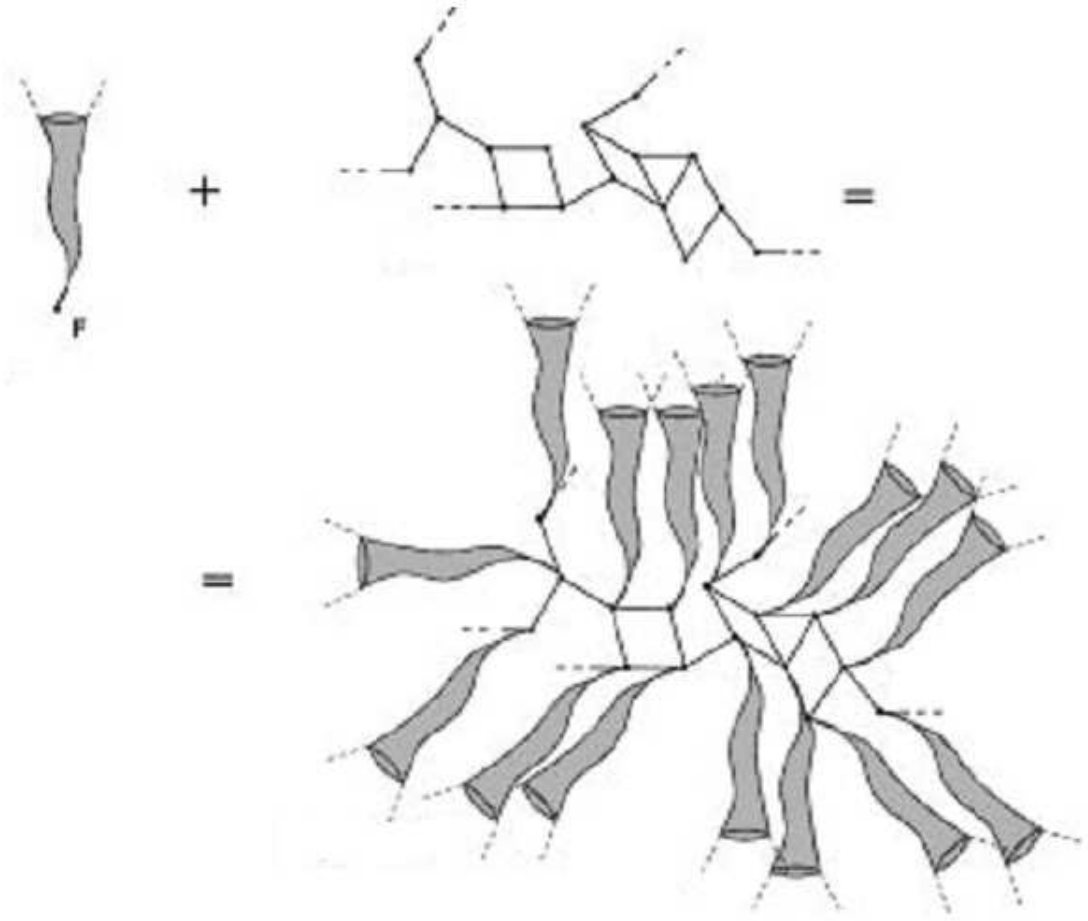

The specific heat at low temperature is readily obtained by taking the derivative of the previous equation:

$$C(T) = \frac{\partial E}{\partial T} \sim \frac{z(z-1)^{-1/4}}{\sqrt{2}\pi(z-2)^2\left(\frac{k}{m}\right)^{3/2}} \left(\frac{k\hbar}{T}\right)^{1/2} \omega_c^{7/2} \exp\left(-\frac{\hbar\omega_c}{kT}\right). \tag{3.5.5}$$

Because of the gap in the spectrum, in the $T \to 0$ limit that quantum statistics play no meaningful role, as they give the same results as the Boltzmann statistics $\exp\left(-\frac{\hbar\omega_c}{kT}\right)$.

3.6 Bundled Structures

A wide class of structures exhibiting controllable properties, as studied by Cassi and Regina [13], are the **bundled graphs**. Bundled graphs are constructed as follows: on each point of a base graph $\mathcal{B}$, a copy of a so-called fibre graph $\mathcal{F}$ is attached; the only contact point between the fibre and the base is a point f, which is the same for all fibres.

Bundled graphs are good models for the geometry and dynamics of polymers and other inhomogeneous systems. The attentive study of the transport properties of bundled graphs, which we are going to sketch in this section, highlights a very rich phenomenology, including anomalous diffusion and unusual distribution for the probability of return.

The rigorous treatment of RWs on bundled graphs is possible as they can be separated into two independent RWs, on the base and on the fibres: out of t steps, let $t_{\mathcal{B}}$ be the steps taken on the base. Between a step on the base and the next, the walker will perform a RW on $\mathcal{F}$, starting from returning to f, with a probability of death in f which is $z_{\mathcal{B}i}/(z_{\mathcal{B}i} + z_{\mathcal{F}f})$; suppose now that all the vertices on the base have the same coordination number, so that the probability of return for i on the base is

$$\begin{aligned} P_{ii}(t) &= \sum_{t_{\mathcal{B}}=0}^{\infty} \sum_{t_1=0}^{\infty} \cdots \sum_{t_{\mathcal{B}+1}=0}^{\infty} P_{ii}^{\mathcal{B}}(t_{\mathcal{B}}) \left(\frac{z_{\mathcal{B}}}{z_{\mathcal{B}} + z_{\mathcal{F}f}} \right)^{t_{\mathcal{B}}} \\ &\times P_d^{\mathcal{F}}(t_1) \dots P_d^{\mathcal{F}}(t_{t_{\mathcal{B}}+1}) \delta \left(t - t_{\mathcal{B}} - \sum_i t_i \right). \end{aligned} \tag{3.6.1}$$

The factor

$$\left(\frac{z_{\mathcal{B}}}{z_{\mathcal{B}} + z_{\mathcal{F}f}} \right)^{t_{\mathcal{B}}}$$

is the weight of the steps on the base, $P_{ii}^{\mathcal{B}}(t)$ is the probability of return on $\mathcal{B}$ considered as a stand-alone graph, and $P_d^{\mathcal{F}}(t)$ is the probability of return to f on $\mathcal{F}$, with a trap of weight $z_{\mathcal{B}}/(z_{\mathcal{B}} + z_{\mathcal{F}f})$ positioned in f.

Passing to generating functions yields straightforwardly the following expression

$$\tilde{P}_{ii}(\lambda) = \tilde{P}_d^{\mathcal{F}}(\lambda) \tilde{P}^{\mathcal{B}} \left(\frac{z_{\mathcal{B}} \, \lambda \, \tilde{P}_d^{\mathcal{F}}(\lambda)}{z_{\mathcal{B}} + z_{\mathcal{F}f}} \right). \tag{3.6.2}$$

Spectral Dimension

The asymptotic expansion of the probability of return gives the spectral dimension of the graph as (see Eq.(2.7.1))

$$P_{ii}(t) \sim t^{-\tilde{d}/2}.$$

Using Tauberian theorems, Eq.(3.6.2) entails

$$\tilde{d} = \begin{cases} \tilde{d}_{\mathcal{F}} & d_{\mathcal{F}} \geq 2 \\ 4 - \tilde{d}_{\mathcal{F}} & d_{\mathcal{F}} \leq 2, \tilde{d}_{\mathcal{B}} \geq 4 \\ \tilde{d}_{\mathcal{F}} + \tilde{d}_{\mathcal{B}} - \frac{\tilde{d}_{\mathcal{F}} \tilde{d}_{\mathcal{B}}}{2} & \tilde{d}_{\mathcal{F}} \leq 2, \tilde{d}_{\mathcal{B}} \leq 4 \end{cases}. \tag{3.6.3}$$

Logarithmic Dimension

A sophisticated expansion of $P_{ii}(t)$ can be introduced as

$$P_{ii}(t) \sim \prod_{i=0}^{\infty} \left[{}^{l}\log(t)\right]^{\beta(i)}, \tag{3.6.4}$$

where $\beta(i)$ is called **logarithmic dimension**, while ${}^{l}\log x$ is defined by

$${}^{l}\log x = \log\left({}^{l-1}\log x\right),$$

with ${}^{0}\log x = x$ and $\beta(i) = -\tilde{d}/2$.

Using Tauberian theorems, it is possible to state explicitly the dependence of $\beta(i)$ on the spectral dimensions of $\mathcal{F}$ and $\mathcal{B}$; when $\tilde{d}_{\mathcal{B}} < 4$ and $\tilde{d}_{\mathcal{F}} < 2$ the following holds:

$$\beta(i) = \begin{cases} -1 & 0 < i < m, \\ \left(1 - \frac{\tilde{d}_{\mathcal{B}}}{2}\right)\left[\beta_{\mathcal{F}}(m_{\mathcal{F}}) + I\left(\frac{\tilde{d}_{\mathcal{F}}}{2}\right)\right] - I\left(\frac{\tilde{d}_{\mathcal{F}}}{2}\right) & i = m = m_{\mathcal{F}} \\ \left(1 - \frac{\tilde{d}_{\mathcal{B}}}{2}\right)\beta_{\mathcal{F}}(i) + \theta(i - m_{\mathcal{F}} - m_{\mathcal{B}})\beta_{\mathcal{B}}(i - m_{\mathcal{F}}) + & \\ +\delta(i - m_{\mathcal{F}} - m_{\mathcal{B}})I\left(\frac{\tilde{d}}{2}\right) - \delta(l - m)I\left(\frac{\tilde{d}}{2}\right) & \end{cases}, \tag{3.6.5}$$

where

- $I(x) = 1$ for integer x, 0 otherwise;
- $m = \min\{i \geq 0 \; s.t. \; \beta(i) \neq -1\} = m_{\mathcal{F}} + \delta(\tilde{d}_{\mathcal{B}} - 2)m_{\mathcal{B}}$.

When $\tilde{f}_{\mathcal{F}} > 2$, $\beta(i) = \beta_{\mathcal{F}}(i)$ for all i.
When $\tilde{d}_{\mathcal{F}} < 2$ and $\tilde{d}_{\mathcal{B}} > 4$, the probability of return for the bundled graph can be obtained from the expression of the same quantity on the fibre alone, replacing each $\beta_{\mathcal{F}}(i)$ with

$$\begin{cases} \beta(i) = -\beta_{\mathcal{F}}(i) - 2\delta(l - m_{\mathcal{F}})I\left(\frac{\tilde{d}_{\mathcal{F}}}{2}\right) & i \geq m_{\mathcal{F}} \\ \beta(i) = \beta_{\mathcal{F}}(i) & 0 < i < m_{\mathcal{F}} \end{cases}.$$

The case of $\tilde{d}_{\mathcal{F}} < 2$ and $\tilde{d}_{\mathcal{B}} = 4$ is the same as the case $\tilde{d}_{\mathcal{F}} < 2$ and $\tilde{d}_{\mathcal{B}} > 4$ when $m_{\mathcal{B}} < -1$, and it is the same as $\tilde{d}_{\mathcal{F}} < 2$ and $\tilde{d}_{\mathcal{B}} < 4$ when $m_{\mathcal{B}} > -1$.
The case of $\tilde{d}_{\mathcal{F}} = 2$ is to be treated as $\tilde{d}_{\mathcal{F}} < 2$ if $\mathcal{F}$ is recursive, and as the case $\tilde{d}_{\mathcal{F}} > 2$ if $\mathcal{F}$ is transient.

Exactly the same procedure can be applied to the asymptotic behaviour of the average distance on the base: when the fibre is recurrent ($\tilde{d}_{\mathcal{F}} \leq 2$), and on the base considered as a separate graph

$$\langle x^2 \rangle_{\mathcal{B}} \sim \prod_{l=0}^{\infty} \left[{}^{l}\log t\right]^{\gamma_{\mathcal{B}}(l)}$$

holds, the projection of the diffusion on the base for the whole bundled graph satisfies the following:

$$\langle x^2 \rangle(t) \sim \prod_{l=0}^{\infty} \left[{}^{l} \log t \right]^{\gamma(l)}, \tag{3.6.6}$$

where

$$\gamma(i) = \begin{cases} \gamma_{\mathcal{B}}(0) \left(1 - \frac{\tilde{d}_{\mathcal{F}}}{2}\right) & i = 0 \\ 0 & 0 < i < m_{\mathcal{F}} \\ \gamma_{\mathcal{B}}(0) \left[\beta_{\mathcal{F}}(i) + I\left(\frac{\tilde{d}_{\mathcal{F}}}{2}\right)\right] & i = m_{\mathcal{F}} > 0 \\ \gamma_{\mathcal{B}}(0)\beta_{\mathcal{F}}(i) + \gamma_{\mathcal{B}}(i - m_{\mathcal{F}}) & i > m_{\mathcal{F}} \end{cases}. \tag{3.6.7}$$

One can now analyse some particular cases.

Comb Lattice. The comb lattice is obtained by using both as base and as fiber the infinite line. From Eq.(3.6.3), $\tilde{d} = 3/2$. From the properties of the probability of return on the infinite line

- $\beta_{\mathcal{B}}(0) = -1/2$, while $\beta_{\mathcal{B}}(i) = 0$ for $i > 0$;
- $m_{\mathcal{B}} = 1$;
- $\gamma_{\mathcal{B}}(0) = 1$, while $\gamma_{\mathcal{B}}(i) = 0$ for $i \neq 0$.

This entails $\beta(i = 0) = -1/4$, $\beta(i) = 0$ for $i > 0$, $\gamma(0) = 1/2$, $\gamma(i) = 0$ for $i > 0$, and

$$P_{ii}(t) \sim t^{-1/4},$$
$$\langle x^2 \rangle(t) \sim t^{1/2}.$$

Brush Lattice. The brush lattice is obtained by using an infinite square lattice as the base and the infinite line as fibre. Since $\tilde{d}_{\mathcal{B}} = 2$ and $\tilde{d}_{\mathcal{F}} = 1$, $\tilde{d} = 2$. The fundamental quantities for the base, where $P^{\mathcal{B}}_{ii}(t) \sim t^{-1}$ and $\langle x^2 \rangle_{\mathcal{B}} \sim t$, are

- $\beta_{\mathcal{B}}(0) = -1$, $\beta_{\mathcal{B}}(i) = 0$ for all $i > 0$;
- $\gamma_{\mathcal{B}}(0) = 1$, $\gamma_{\mathcal{B}})(i) = 0$ for all $i > 0$;
- $m_{\mathcal{B}} = 1$.

As a consequence $\beta(0) = 1$, $\beta(i) = 0$ for all $i > 0$, and

$$P_{ii} \sim t^{-1};$$

on the other hand $\gamma(0) = -1/2$, $\gamma(i) = 0$ for all $i > 0$, which entails

$$\langle x^2 \rangle(t) \sim t^{1/2},$$

while considering the displacement on the whole graph $\langle r^2 \rangle(t) \sim t^{-3/2}$.

4

Three Particles on a Line

In this chapter we are going to present several results on some collective properties of three independent random walkers on an infinite line. The whole chapter is a revised version of a manuscript submitted to Physical Review E [1]. In particular, we have calculated the probability that minimum and maximum distances among the walkers are in a given range, and we have also derived the asymptotic behaviour of the probability that the three particles first meet at time t, for large times.

We have performed the calculation in the graph of the inter-particle distances, which displays several advantages: it reduces the problem to a 2-d lattice, which is a quite classical trick when dealing with multiple random walkers, it has a simple and intuitive geometric form, it discards the useless details concerning the absolute position of the particles while retaining all the meaningful inter-particle relations, and it allows for a straightforward introduction of inter-particle attraction or repulsion.

For large times, the asymptotic behaviour of the probability distributions of maximum and minimum mutual distances d, which are strictly non-linear functions, displays to first order a diffusion-like scaling as d^2/t, when d is large. At higher orders, this scaling breaks down and for intermediate distances a richer behaviour is revealed.

We have also studied two different models for vicious interacting walkers, which we have been able to map onto the model for independent walkers; the aforementioned results thus hold in these cases as well.

The chapter is organized as follows: first, we define the system under study and introduce the inter-particle distance graph; next we compute the exact $t \to \infty$ asymptotic form of the probability $P(\vec{x}, t)$ of finding the walkers at a point $\vec{x}$ in the distance graph, and then infer the behaviour of the first-return probabilities. In the following sections we first compute the probability that the minimum and maximum distances between pairs of adjacent particles are smaller than some d, then focus on the probability that the walkers are no closer than d_{inf} and no farther than d_{sup}. We then study two models for vicious random walkers, and finally analyse our results.

4.1 The Distance Graph for Three Particles on a Line

We now take three independent walkers on the same lattice, leaving from i at time 0: the probability $P_{1D}^{(3)}(t)$ for all of them to meet at a time t is

$$P_{1D}^{(3)}(t) = \sum_j \left(P_{ij}^{lin}(t)\right)^3 .$$

A good choice of coordinates to tackle this problem is the following: let x be the distance between the leftmost walker and the central one, and let y be the distance between the rightmost walker and the central one. A straightforward analysis of the transition probabilities gives the following results:

- if the position at time $(t-1)$ is $(0,0)$:

$$p\left((0,0) \to (0,0)\right) = \frac{1}{4},$$
$$p\left((0,0) \to (0,2)\right) = p\left((0,0) \to (2,0)\right) = \frac{3}{8};$$

- if the position at time $(t-1)$ is $(x,0)$ or $(0,y)$:

$$p\left((x,0) \to (x,0)\right) = p\left((x,0) \to (x-2,2)\right) = p\left((x,0) \to (x,2)\right) = \frac{1}{4},$$
$$p\left((x,0) \to (x+2,0)\right) = p\left((x,0) \to (x-2,0)\right) = \frac{1}{8},$$

  and

$$p\left((0,y) \to (0,y)\right) = p\left((0,y) \to (2,y-2)\right) = p\left((0,y) \to (2,y)\right) = \frac{1}{4},$$
$$p\left((0,y) \to (0,y+2)\right) = p\left((0,y) \to (0,y-2)\right) = \frac{1}{8};$$

- if the position at time $(t-1)$ is (x,y):

$$p\left((x,y) \to (x,y)\right) = \frac{1}{4},$$
$$p\left((x,y) \to (x+2,y)\right) = p\left((x,y) \to (x-2,y)\right) = \frac{1}{8},$$
$$p\left((x,y) \to (x,y+2)\right) = p\left((x,y) \to (x,y-2)\right) = \frac{1}{8},$$
$$p\left((x,y) \to (x+2,y-2)\right) = p\left((x,y) \to (x-2,y+2)\right) = \frac{1}{8}.$$

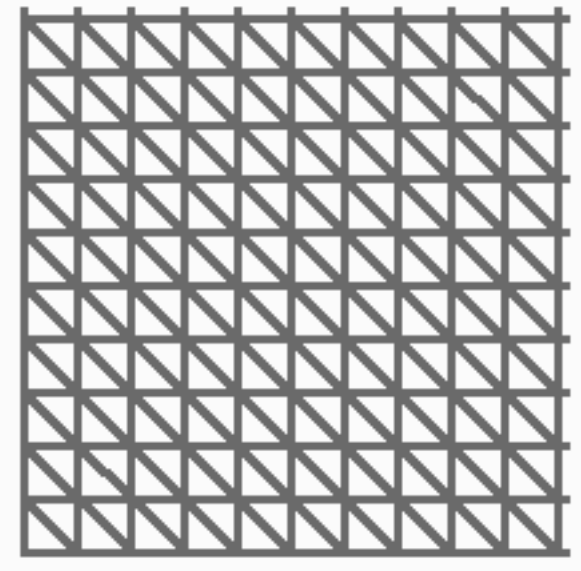

Figure 4.1: The distance graph for the random walk of three particles on a line is a 2-d lattice with diagonals.

The end result is that $P_{1D}^{(3)}(t)$ corresponds to the probability of return to the origin, for a simple random walk with waiting probability $\frac{1}{4}$, on a 2d structure with diagonals, as depicted in Fig.4.1, or equivalently on a slice of a triangular lattice, as in Fig.4.2. On both structures each step corresponds to a change of two for the reciprocal distances of the particles. Since the graph we have now obtained is inhomogeneous, a natural way to tackle it is by transforming it into a full triangular lattice (Fig.4.3). This feat is accomplished by noting that, at $(0,0)$, the probability of departing from the origin - which is 6/8 - correspond to a choice of one among the 6 axes; on the axes of Fig.4.2, on the other hand, the probability 1/4 of departing from the current axis correspond to the choice between

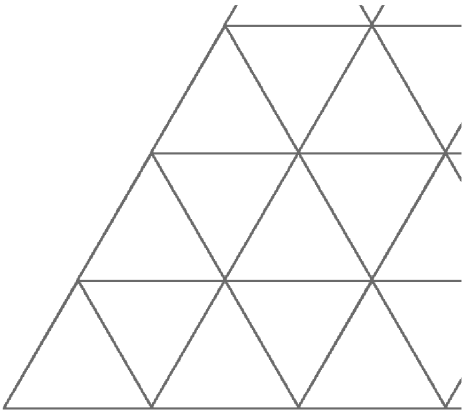

Figure 4.2: The 2-d lattice with diagonals is equivalent to a triangular lattice.

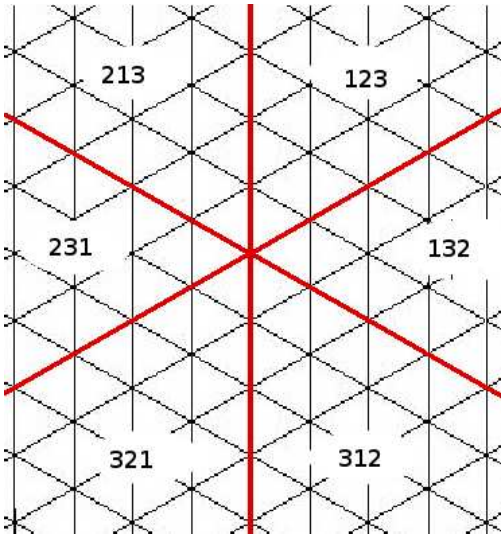

Figure 4.3: The full triangular lattice. Each slice corresponds to an ordering of the three particles, as indicated in the picture; crossing an axis corresponds to swapping two particles.

two adjacent slices in the full triangular lattice. A cogent interpretation of the full triangular lattice is obtained by noting that each of the 6 slices correspond to the possible orderings of the walkers on a 1-D lattice, and that each crossing of an axis implies a change in this order (see Fig.4.3).

The graphs in Fig.4.1, Fig.4.2 and Fig.4.3 can all be defined as **distance graphs** of the multiple random walk we are considering. It is just for computational simplicity that we will stick from now on to the latter.

This reduction to a 2-d problem is a quite classical trick, but it should be stressed that it isn't guaranteed to succeed for multiple random walks in inhomogeneous graphs, as it can prove impossible to construct a distance graph; in such cases, interesting phenomena regarding the probability of meeting can arise [18].

The full triangular lattice is a homogeneous graph, and in every point the transition probabilities are $\frac{1}{8}$ for each of the 6 first neighbours, with probability $\frac{1}{4}$ of not moving at all.

The return probabilities for this lattice can be computed via a straightforward Fourier transform:

$$P(\vec{x},t) = \frac{9}{16\pi^2}\int d^2\vec{K} e^{i\frac{3}{2}\sum_j K_j n_j}\left[\frac{1}{4}\left(1+\cos\left(\frac{3}{2}K_1\right)+\cos\left(\frac{3}{2}K_2\right)+\cos\left(\frac{3}{2}K_3\right)\right)\right]^t,$$

where $k_1+k_2+k_3=0$, $\vec{x}=\sum_j n_j\vec{e}_j$ is a site on the full triangular lattice and $\vec{e}_j$ is one of the three first-neighbour vectors

$$\begin{aligned}\vec{e}_1 &= (1,0)\\ \vec{e}_2 &= \left(\frac{1}{2},\frac{\sqrt{3}}{2}\right).\end{aligned}$$

The asymptotic behaviour of the function can be obtained exactly as $t \to \infty$ by the steepest descent method: the maximum value of the expression

$$\frac{1}{4}\left[1+\cos\left(\frac{3}{2}K_1\right)+\cos\left(\frac{3}{2}K_2\right)+\cos\left(\frac{3}{2}K_3\right)\right]$$

is obtained for $K_1 = K_2 = 0$. The integral is then well approximated by

$$\frac{9}{16\pi^2}\int d^2\vec{K}e^{i\frac{3}{2}\sum_j K_j n_j}e^{-\frac{9}{16}t\left[K_1^2+K_2^2+K_1K_2\right]}.$$

The Gaussian integral is straightforwardly solved by the following change of variables:

$$\begin{array}{l} l_1 = K_1 + K_2 \\ l_2 = K_1 - K_2 \end{array},$$

which yields

$$\begin{aligned} P(\vec{x},t) &\sim \frac{9}{32\pi^2}\int d^2\vec{l}\exp\left\{i\left[\frac{l_1+l_2}{2}(n_1-n_3)+\frac{l_1-l_2}{2}(n_2-n_3)\right]-\frac{9}{64}t\left(3l_1^2+l_2^2\right)\right\} \\ &= \frac{2}{\sqrt{3}\pi}\frac{1}{t}\exp\left\{-\frac{4}{3}\frac{\vec{x}^2}{t}\right\}, \end{aligned} \tag{4.1.1}$$

where $\vec{x}^2 = n_1^2 + n_2^2 + n_1 n_2$, and is valid for every point on the lattice as $t \to \infty$.

Taking into account the fact that each step in the distance graph corresponds to a distance 2 in the original lattice, the following holds:

$$P_{line}(x,y,t) = \begin{cases} 6P\left(\frac{x}{2}\vec{e}_1+\frac{y}{2}\vec{e}_2,t\right) & \{x,y\neq 0\} \\ 3P\left(\frac{x}{2}\vec{e}_1+\frac{y}{2}\vec{e}_2,t\right) & \{x=0,y\neq 0\}\cup\{x\neq 0,y=0\} \\ P\left(\vec{0},t\right) & \{x=0,y=0\} \end{cases}. \tag{4.1.2}$$

4.2 Normalization of the Asymptotic Probability

The probability in Eq.4.1.1 is asymptotically exact as $t \to \infty$, and the normalization provided is the correct one for the exact initial formula. It proves however useful to compute in an approximate way the normalization factor, as a way to test both the saddle point method and the technique we will use later to compute various probability functions. Without further ado, the result is once again Eq.4.1.1, as we now proceed to prove.

We look for N in the following equation:

$$1 = \sum_{\vec{x}} P(\vec{x},t) = \frac{N}{t}\sum_{\vec{x}}\exp\left\{-\frac{4}{3}\frac{\vec{x}^2}{t}\right\}.$$

We now restrict our attention to one of the 6 slices, which is described by the base vectors $\vec{e}_1$ and $\vec{e}_2$. The sum over the lattice can be written as follows:

$$\sum_{\vec{x}} = 6 \sum_{slice} -6 \sum_{axis} -5P\left(\vec{0}, t\right),$$

where the second and third term are necessary as the axes and the origin are considered multiple times in the first term. As a first step, we can evaluate the weight of these terms:

$$\sum_{axis} P\left(\vec{x}, t\right) = \frac{N}{t} \sum_{i=0}^{\infty} e^{-\frac{4}{3}\frac{\vec{x}^2}{t}}$$

satisfies

$$\sum_{axis} P\left(\vec{x}, t\right) > \frac{N}{t} \int_0^{\infty} dx\, e^{-\frac{4}{3}\frac{x^2}{t}} = \frac{N}{t}\frac{1}{2}\sqrt{\frac{3\pi t}{4}} = \frac{N}{4}\sqrt{\frac{3\pi}{t}}$$

and

$$\sum_{axis} P\left(\vec{x}, t\right) < \frac{N}{t}\left[1 + \int_1^{\infty} dx\, e^{-\frac{4}{3}\frac{(x-1)^2}{t}}\right] = \left[\frac{N}{t} + \frac{N}{4}\sqrt{\frac{3\pi}{t}}\right]$$

so that

$$\sum_{axis} P\left(\vec{x}, t\right) = \frac{N}{4}\sqrt{\frac{3\pi}{t}} + O(t^{-1}) = O(t^{-\frac{1}{2}}),$$

and

$$6 \sum_{axis} P\left(\vec{x}, t\right) + 5P\left(\vec{0}, t\right) = O(t^{-\frac{1}{2}}).$$

The next step consists in computing the sum over each slice of the exponential. This sum is best performed using the variables

$$\left\{ \begin{array}{l} l = n_1 + n_2 \\ m = n_1 - n_2 \end{array} \right. ;$$

In this base the exponential reads

$$\exp\left\{-\frac{4\left(\frac{3}{4}l^2 + \frac{1}{4}m^2\right)}{3t}\right\} = \exp\left\{-\frac{l^2}{t} - \frac{m^2}{3t}\right\}.$$

The sum over the points of the slice, $\sum_{n_1}\sum_{n_2}$, is converted into the following sum:

$$\sum_{l=0,1,\ldots} \quad \sum_{m=-l,-l+2,\ldots,l-2,l}^{l} ;$$

the sum can now be split into two terms, for even and odd l,

$$\left\{ \begin{array}{l} \sum_{\vec{x}} P\left(\vec{x}, t\right) = S + T \\ S = \sum_{l=0,2,\ldots} e^{-\frac{l^2}{t}} \sum_{m=-l,-l+2,\ldots,l} e^{-\frac{m^2}{3t}} \\ T = \sum_{l=1,3,\ldots} e^{-\frac{l^2}{t}} \sum_{m=-l,-l+2,\ldots,l} e^{-\frac{m^2}{3t}}. \end{array} \right.$$

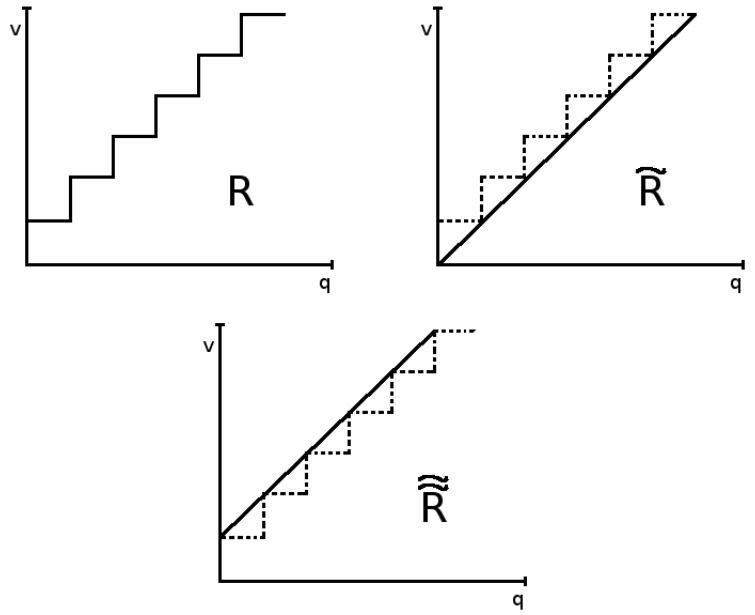

Figure 4.4:

Using as sum indices $q = \frac{l}{2}$ and $v = \frac{m}{2}$, S becomes

$$S = 2 \sum_{q=0,1,\ldots} e^{-\frac{4q^2}{t}} \sum_{v=0,1,\ldots,q} e^{-\frac{4v^2}{3t}} - \sum_{q=0,1,\ldots} e^{-\frac{4q^2}{t}};$$

as we have already seen, the second term is $O(t^{\frac{1}{2}})$, so we'll drop it and focus on the double sum, which has now to be bound as we did earlier. It is easily seen that

$$\sum_{q=0,1,\ldots} e^{-\frac{4q^2}{t}} \sum_{v=0,1,\ldots,q} e^{-\frac{4q^2}{3t}} > \int_{\tilde{R}} dq\, dv\, \exp\left\{-\frac{4q^2}{t} - \frac{4v^2}{3t}\right\}$$
$$= \frac{\sqrt{3}t}{4} \int_0^{\infty} R\, dR \int_0^{\frac{\pi}{6}} d\phi\, e^{-R^2} = \frac{\pi}{16\sqrt{3}} t,$$

where the regions R and $\tilde{R}$ are as in Fig.4.4.

As to the other bound

$$\sum_{q=0,1,\ldots} e^{-\frac{4q^2}{t}} \sum_{v=0,1,\ldots,q} e^{-\frac{4v^2}{3t}} = \sum_q e^{-\frac{4q^2}{t}} + \sum_{q=1}^{\infty}\sum_{v=1}^{\infty} \exp\left[-\frac{4q^2}{t} - \frac{4v^2}{3t}\right]$$

$$< \left[1 + O\left(\sqrt{t}\right)\right] + \sum_{q=0}^{\infty}\sum_{v=0}^{q} \exp\left[-\frac{4(q+1)^2}{t} - \frac{4(v+1)^2}{3t}\right]$$

$$< \int_{\tilde{R}} dq\, dv\ \exp\left[-\frac{32(q+1)^2}{27t} - \frac{32(v+1)^2}{27t}\right] + O(t^{\frac{1}{2}})$$

$$= \frac{\sqrt{3}t}{4}\int_0^{\infty} dr\ R\int_0^{\frac{\pi}{6}} d\phi\ e^{-R^2} + O(t^{\frac{1}{2}}) = \frac{\pi}{16\sqrt{3}}t + O(t^{\frac{1}{2}}),$$

which together with the previous result implies

$$S = \ 2\frac{\pi}{16\sqrt{3}}t + O(t^{\frac{1}{2}}) = \frac{\pi}{8\sqrt{3}}t + O(t^{\frac{1}{2}}).$$

The computation of T is perfectly analogous, with some complications in the division of the integration regions into subregions. In the end it results that, as above,

$$T = \ \frac{\pi}{8\sqrt{3}}t + O(t^{\frac{1}{2}}),$$

and

$$1 = 6N\left[\frac{\pi}{8\sqrt{3}}t + \frac{\pi}{8\sqrt{3}}t + O(t^{\frac{1}{2}})\right],$$

$$N = \frac{2}{\sqrt{3}\pi} + O(t^{-\frac{1}{2}}).$$

The normalized form of the probability is then proved to be as in Eq.4.1.1.

4.3 First Return Probability

It is also easy to give an estimate for the asymptotic probability $F(\vec{0}, t)$ of first return to the origin: the generating functions satisfy

$$\tilde{F}\left(\vec{0}, \lambda\right) = 1 - \frac{1}{\tilde{P}\left(\vec{0}, \lambda\right)}.$$

From Eq.4.1.1,

$$\tilde{P}\left(\vec{0}, \lambda\right) = \sum_t \lambda^t P\left(\vec{0}, t\right) \sim \frac{2}{\sqrt{3}\pi}\log(1-\lambda),$$

as $\lambda \sim 1$, so

$$\tilde{F}\left(\vec{0}, \lambda\right) \sim 1 - \frac{\sqrt{3}\pi}{2}\frac{1}{\log(1-\lambda)}.$$

Standard asymptotic series analysis yields

$$F\left(\vec{0},t\right)\sim\frac{1}{t\left(\log t\right)^{2}}$$

as $t\to+\infty$.

4.4 Euclidean Distance from the Origin

While not physically meaningful for the three-particles problem, the probability that a random walker on the triangular lattice is inside a circle of radius ρ in the 2-d plane will be useful later. By definition

$$Q_{\rho}(t)=\sum_{\{\vec{x}:\,|\vec{x}|<\rho^{2}\}}P\left(\vec{x},t\right).$$

The calculation is a straightforward generalization of the steps taken earlier: the regions $\tilde{R}$ and $\tilde{\tilde{R}}$ are now of finite radii, respectively ρ and $\rho+\sqrt{2}$. As to the details, for S the following holds:

$$\frac{\sqrt{3}\pi t}{2}S>\frac{3\sqrt{3}}{2}t\frac{\pi}{3}\int_{0}^{\frac{2\rho}{\sqrt{3t}}}dR\,Re^{-R^{2}}+O(t^{\frac{1}{2}})=\frac{\sqrt{3}\pi t}{4}\left[1-e^{-\frac{4\rho^{2}}{3t}}\right]+O(t^{\frac{1}{2}}),$$

$$\frac{\sqrt{3}\pi t}{2}S<\frac{3\sqrt{3}}{2}t\frac{\pi}{3}\int_{0}^{\frac{2(\rho+\sqrt{2})}{\sqrt{3t}}}dR\,Re^{-R^{2}}+O(t^{\frac{1}{2}})=\frac{\sqrt{3}\pi t}{4}\left[1-e^{-\frac{4(\rho+\sqrt{2})^{2}}{3t}}\right]+O(t^{\frac{1}{2}}).$$

Let now

$$E(\rho)=\frac{\sqrt{3}\pi t}{4}e^{-\frac{4\rho^{2}}{3t}}\left(1-e^{-\frac{8}{3t}\left(\sqrt{2}\,\rho+1\right)}\right).$$

As we'll be mostly interested in the case $1\ll\rho\ll t$, we can write

$$E(\rho)=\frac{2\sqrt{2}\pi\rho}{\sqrt{3}}e^{-\frac{4\rho^{2}}{3t}},$$

and

$$\frac{\sqrt{3}\pi t}{2}S=\frac{\sqrt{3}\pi t}{4}\left[1-e^{-\frac{4\rho^{2}}{3t}}\left(1+O\left(\frac{\rho}{t}\right)\right)\right].$$

The same procedure holds for T. The contribution of the points on the edges of each slice is $O(t^{-\frac{1}{2}})$, and it can be dropped as long as $\rho\gg1$; one then obtains

$$Q_{\rho}(t)=1-e^{-\frac{4\rho^{2}}{3t}}\left(1+O(\rho/t)\right). \tag{4.4.1}$$

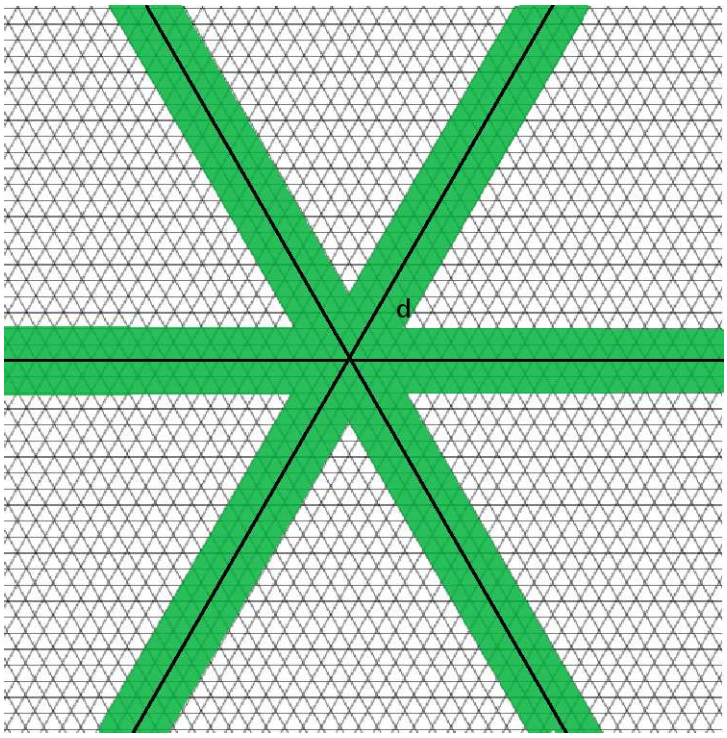

Figure 4.5: The shaded area is R_d, the region of summation for $P\left(d_{min} < d, t\right)$.

4.5 Minimum Distance Between Particles

We have previously defined x and y as the distance between the central particle and - respectively - the left-most particle and the right-most one. What are the chances that, at some time t, the minimum between x and y, $d_{min} = \min\{x, y\}$, is lower than some given value $2d$? This type of quantity can be of interest, e.g., when investigating chemical kinetics, as reactions happen at a limited range.

In the complete triangular lattice, d_{min} is the distance to the nearest of the three axes, so the probability that $d_{min}(t) < d$ is

$$P\left(d_{min} < 2d, t\right) = \sum_{\vec{x} \in R_d} P\left(\vec{x}, t\right),$$

where R_d comprises the lattice points in a region similar to the one shaded in Fig.4.5.

The region R_d can be divided into two main subregions: a circle of radius $\sqrt{3}d$ and 6 identical infinite beams, each collinear to one of the three main axes. The weight of the circle is given by $Q_{\sqrt{3}d}(t)$, while the contribution of the infinite beams is to be computed now.

We make now two approximations: as a starter, we divide one beam into two pieces, one comprising all the points at distance greater than $\sqrt{3}d$, the other one the remaining points. The contribution of the latter is $\approx e^{-\frac{4d^2}{t}} O(t^{-1})$, and in

hindsight we can safely ignore it. The former piece gives the main contribution, both to the beam and the $P(d_{min} < 2d, t)$: we approximate it in the rather crude way, which can be justified for $1 \ll d \ll t^{1/2}$, of considering the distance fixed and equal to R^2 for all the lattice points orthogonal to a given point on the axis.

A procedure analogous to the one employed earlier yields, for $1 \ll d \ll t^{1/2}$,

$$\begin{aligned} P\left(d_{min} < 2d, t\right) &= 1 - e^{-4d^2/t} + \frac{6d}{\sqrt{\pi t}}\left[1 - \mathrm{Erf}\left(\frac{2d}{\sqrt{t}}\right)\right]\left(1 + O(d^{-1})\right) \\ &\quad 1 - e^{-4y^2} + \frac{6y}{\sqrt{\pi}}\left[1 - \mathrm{Erf}\left(2y\right)\right]\left(1 + O(d^{-1})\right) \\ &= \frac{6d}{\sqrt{\pi t}}\left(1 + O(d^{-1})\right) - \frac{4(6-\pi)d^2}{\pi t}\left(1 + O(d^{-1})\right) + O\left(\frac{d^2}{t}\right)^{3/2} \\ &= \frac{6y}{\sqrt{\pi}}\left(1 + O(d^{-1})\right) - \frac{4(6-\pi)y^2}{\pi}\left(1 + O(d^{-1})\right) + O\left(y^3\right) \end{aligned} \quad (4.5.1)$$

where we have set $y = \sqrt{d^2/t}$; it is worthwhile to explicitly note that the leading terms of the probability are a function of d^2/t, which thus describes the time evolution of a fixed probability surface. This regular diffusion-like behaviour, unlike in the two-particle case, is not trivial: even though the probability of meeting at a given point is led, for long times, by a Gaussian propagator, the minimum distance is a strictly non-linear function of the positions of the particles, so that *a priori* it is hazardous to guess this behaviour. Furthermore, the diffusion-like behaviour is not guaranteed to hold at higher orders because of the $O(d^{-1})$ error which one introduces when approximating the sums with integrals.

4.6 Maximum Distance Between Particles

Another quantity of interest is the probability that at any given moment the maximum distance between two adjacent particles is lower than $2d$: the set of points satisfying $d_{Max} < 2d$ corresponds to the shaded area R in Fig.4.6:

$$P\left(d_{Max} < 2d, t\right) = \sum_{\vec{x} \in R} P\left(\vec{x}, t\right).$$

A quantity like this can be of interest, e.g., when investigating the robustness of a dynamic network of wireless devices, whose nodes can move randomly in space [19].

Instead of computing sums, we compute integrals, as we did in the previous sections: by doing so we introduce errors which are $O(d^{-1})$, so that we can safely ignore them as long as $1 \ll d \ll t$; we now divide R into two regions, the circle of radius d, C_d, and $R \setminus C_d$, and write

$$P\left(d_{Max} < 2d, t\right) = Q_d(t) + \sum_{\vec{x} \in R \setminus C_d} P\left(\vec{x}, t\right).$$

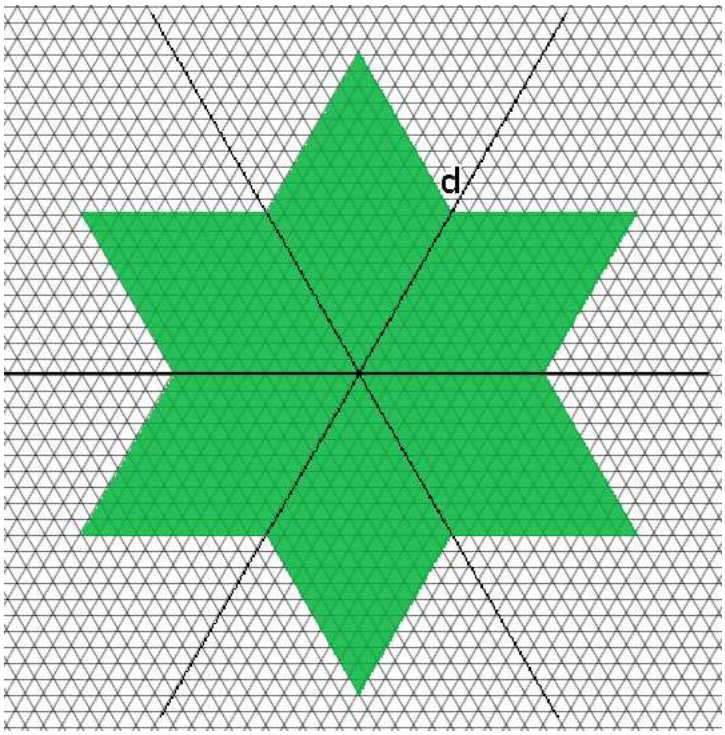

Figure 4.6: The shaded area is R, the region of summation for $P\left(d_{Max} < 2d, t\right)$.

The second piece can be written by substituting

$$\begin{cases} l = \frac{n_1+n_2}{2} \\ m = \frac{n_1-n_2}{2} \end{cases},$$

and approximated with an integral over the slices as follows:

$$\sum_{\vec{x}\in R\setminus C_d} P\left(\vec{x}, t\right) = \left(\frac{1}{2\pi}\right) 12 \int_{2d/\sqrt{3t}}^{2d/\sqrt{t}} d\bar{q}\, \frac{\pi}{3} \left(\frac{\frac{2d}{\sqrt{t}} - \bar{q}}{\sqrt{3}-1}\right) e^{-\bar{q}^2} \left(1 + O(d^{-1})\right).$$

The result can be stated in an analytic, if somewhat unclear, formula as follows:

$$P\left(d_{Max} < 2d, t\right) = 1 + \left\{ -\frac{3+\sqrt{3}}{2} e^{-\frac{4d^2}{3t}} + \frac{\sqrt{3}+1}{2} e^{-\frac{4d^2}{t}} \right.$$

$$\left. + \left(\sqrt{3}+1\right)\sqrt{\pi}\frac{d}{\sqrt{t}} \left[\mathrm{Erf}\left(\frac{2d}{\sqrt{t}}\right) - \mathrm{Erf}\left(\frac{2d}{\sqrt{3t}}\right) \right] \right\} \left(1 + O(d^{-1})\right). \qquad (4.6.1)$$

A straightforward computation leads, in the same limits as before, $1 \ll d \ll t^{1/2}$, to

$$P\left(d_{Max} < 2d\right) = \frac{4}{\sqrt{3}}\frac{d^2}{t}\left(1 + O(d^{-1})\right) - \frac{8}{27}\left(3 + 4\sqrt{3} + O(d^{-1})\right)\left(\frac{d^2}{t}\right)^2$$

$$+ \frac{32}{405}\left(12 + 13\sqrt{3} + O(d^{-1})\right)\left(\frac{d^2}{t}\right)^3 + O\left[\frac{d^2}{t}\right]^4.$$

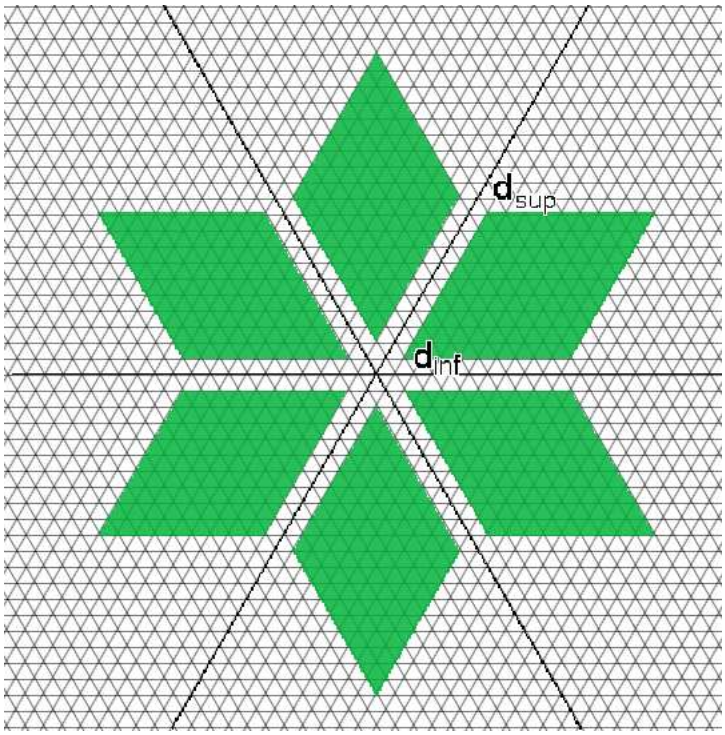

Figure 4.7: The region of summation for $P(d_{min} > 2d_{inf}, d_{Max} < 2d_{sup}, t)$ is the shaded area.

4.7 Particles With Bounded Maximum and Minimum Distance

To complete the picture, we next compute the probability that the pairs of adjacent particles are not closer than $2d_{inf}$, and not farther apart than $2d_{sup}$:

$$P(d_{min} > 2d_{inf}, d_{Max} < 2d_{sup}, t) = \sum_{R_m} P(\vec{x}, t),$$

where R_m is the shaded region in Fig.4.7. This quantity is of interest in reactions involving a catalyst, e.g. in a cell, as it is known [20] that an optimal distance exists at which the reaction is favoured.

As in the previous section, we approximate the sum with an integral, and obtain

$$P(d_{min} > 2d_{inf}, d_{Max} < 2d_{sup}, t) = \frac{12}{\sqrt{3}\pi}\left(1 + O(d_{inf}^{-1})\right)\left\{\int_{2d_{inf}/\sqrt{t}}^{(d_{inf}+d_{sup})/\sqrt{t}} dq \left(q - \frac{2d_{inf}}{\sqrt{t}}\right)e^{-q^2} + \int_{(d_{inf}+d_{sup})/\sqrt{t}}^{2d_{sup}/\sqrt{t}}\left(\frac{2d_{sup}}{\sqrt{t}} - q\right)e^{-q^2}\right\}$$
$$= 6\left(1 + O(d_{inf}^{-1})\right)\left[\frac{e^{-\frac{4d_{inf}^2}{t}} + e^{-\frac{4d_{sup}^2}{t}} - 2e^{-\frac{\left(d_{inf}+d_{sup}\right)^2}{t}}}{\sqrt{3}\pi} + \frac{2\left(\mathrm{Erf}\left[\frac{2d_{inf}}{\sqrt{t}}\right]d_{inf} + \mathrm{Erf}\left[\frac{2d_{sup}}{\sqrt{t}}\right]d_{sup} - \mathrm{Erf}\left[\frac{d_{inf}+d_{sup}}{\sqrt{t}}\right](d_{inf}+d_{sup})\right)}{\sqrt{3\pi t}}\right]. \tag{4.7.1}$$

This exact result is quite cumbersome, but one can extract the leading terms in the expansion under the conditions $1 \ll d_{inf} < d_{sup} \ll t^{1/2}$:

$$P(d_{min} > 2d_{inf}, d_{Max} < 2d_{sup}, t) = \frac{12\left(d_{\mathrm{inf}}^2 - 2d_{\mathrm{inf}}d_{\mathrm{sup}} + d_{\mathrm{sup}}^2\right)}{\sqrt{3}\pi t}\left(1 + O(d_{inf}^{-1})\right) + -6\frac{7d_{\mathrm{inf}}^4 - 4d_{\mathrm{inf}}^3 d_{\mathrm{sup}} - 6d_{\mathrm{inf}}^2 d_{\mathrm{sup}}^2 - 4d_{\mathrm{inf}}d_{\mathrm{sup}}^3 + 7d_{\mathrm{sup}}^4}{3\sqrt{3}\pi t^2}\left(1 + O(d_{inf}^{-1})\right).$$

As soon as we set $d_{sup} = kd_{inf}$, the asymptotic diffusion-like behaviour becomes apparent:

$$P(d_{min} > 2d_{inf}, d_{Max} < 2d_{sup}, t) = \frac{12}{\sqrt{3}\pi t}(k-1)^2 d_{\mathrm{inf}}^2\left(1 + O(d_{inf}^{-1})\right).$$

4.8 Interacting Multiple Random Walks

It is indeed possible to extend the previous results to two different types of interacting multiple random walks.

First consider a random walk, on an infinite line, for three particles which can stay on the same vertex but never change their ordering. Let x be the distance between the left-most particle and the central one, and let y be the distance between the central particle and the right-most one. The motion of the particles can be easily represented on the slice in Fig.4.2. As long as x and y are both greater than zero (everywhere outside the axes and the origin), the most straightforward choice for the transition rates is the same as in the case of non-interacting particles. When $x = 0$ or $y = 0$, instead, the probability distribution for the outcoming configurations are arbitrary, depending on what physical sense we give to the encounters among particles.

For the probability of transition on the axes (excluding the origin), we decide that when two particles try to cross one another they bounce back. This immediately entails the same probability of transition as in the non-interacting case, and we can once again describe the problem in a graph like the one in Fig.4.3. The difference is that each triangular slice is a mirror copy of the adjacent ones, while in the first case each slice carries a specific ordering of the particles. The probability $P^{nc}(\vec{x},t)$ of finding the three non-crossing particles at given distances $(2x,2y)$ is then obtained by summing the probability for non-interacting particles over all the corresponding points:

$$P^{nc}(\vec{x},t)=\begin{cases}6P(\vec{x},t) & x,y>0\\ 3P(\vec{x},t) & x=0,y>0\\ 3P(\vec{x},t) & x>0,y=0\\ P(\vec{x},t) & x=y=0\end{cases}. \tag{4.8.1}$$

The other quantities, which are already summed over equivalent points, are the same as in the non-interacting case.

A slightly more complex case is when the three walkers are solid and can neither sit on the same vertex nor cross each other. In this case the motion can be described on the interior of the slice in Fig.4.2, i.e. on sites of the form

$$\vec{x}=\frac{x}{2}\vec{e}_1+\frac{y}{2}\vec{e}_2,$$

with $x,y\geq 2$, which correspond to distances (x,y). Whenever $x,y>2$, the probability of transition are the same as in the non interacting case. When two particles are adjacent ($x=2$ or $y=2$, but not both), our choice about bouncing yields the following probabilities of transition:

$$\begin{aligned}&p\left((2,y)\to(2,y)\right)=\frac{1}{4},\\ &p\left((2,y)\to(2,y-2)\right)=p\left((2,y)\to(2,y+2)\right)=\frac{1}{8},\\ &p\left((2,y)\to(4,y-2)\right)=p\left((2,y)\to(4,y)\right)=\frac{1}{4}.\end{aligned}$$

When the particles are all adjacent ($x=y=2$), the probabilities are as follows:

$$\begin{aligned}&p\left((2,2)\to(2,2)\right)=\frac{1}{4},\\ &p\left((2,2)\to(2,4)\right)=p\left((2,2)\to(4,2)\right)=\frac{3}{8}.\end{aligned}$$

If we now send (x,y) to $(x-2,y-2)$, we can immediately recognize that all these probability are the same as in the case of non-crossing particles. Thus for solid random walkers the probability function $P^{srw}(\vec{x},t)$ satisfies

$$P^{srw}(\vec{x},t)=P^{nc}(\vec{x}-\vec{e}_1-\vec{e}_2),t), \tag{4.8.2}$$

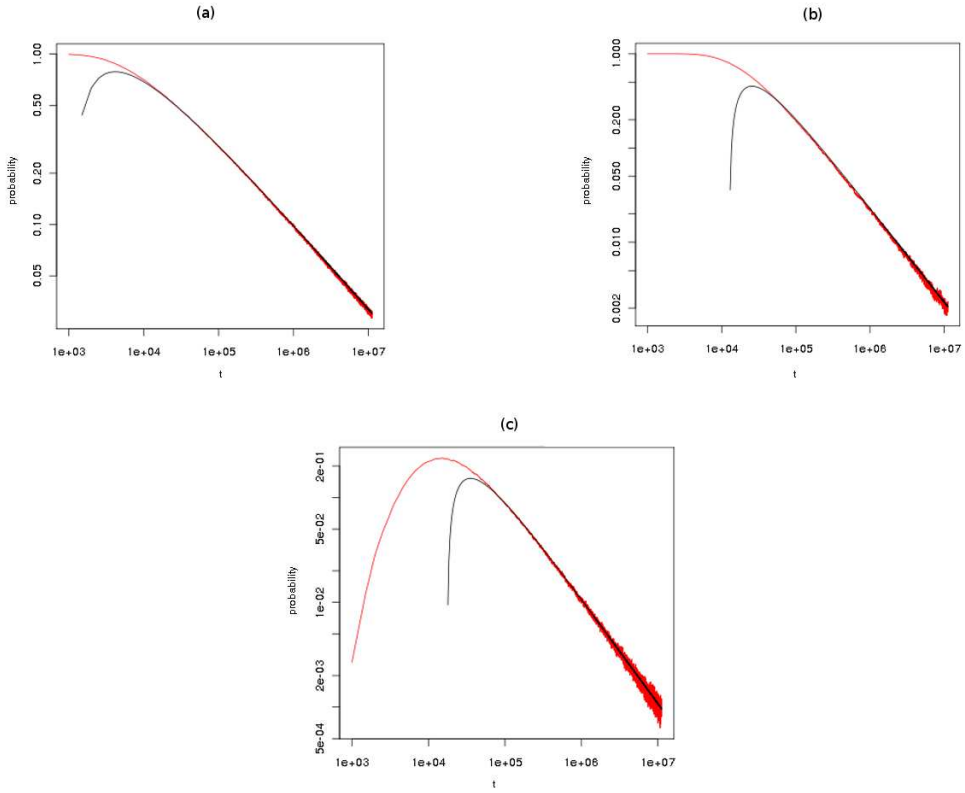

Figure 4.8: In all figures, the black lines show the asymptotic behaviour, while red lines are the results of simulations for $d_{inf} = 30$, $d_{sup} = 100$. (a) $P(d_{min} < 2d_{inf}, t)$ is plotted together with the first two terms of Eq.4.5.1. (b) $P(d_{Max} < 2d_{sup}, t)$ and (c) $P(d_{inf} < 2d_{min}, d_{Max} < 2d_{sup}, t)$ are also plotted together with the second order behaviour.

and analogously for the other quantities we have computed.

While the choice we have made for the transition probability of adjacent particles can be justified, from an intuitive point of view, by calling up independence of the Brownian motion of different particles and momentum conservation in collisions, it should be stressed that it is nevertheless an arbitrary position, and different choices will yield different results.

4.9 Simulation Results and Discussion

To verify that the asymptotic behaviour is a good approximation at large finite times, we performed several simulations after obtaining the analytical results. Leaving aside the technical details, we ran multiple random walks both on the line and the distance graph, so as to verify each step. The results were comforting, and we have summarised them in Fig.4.8. The asymptotic behaviour sets in,

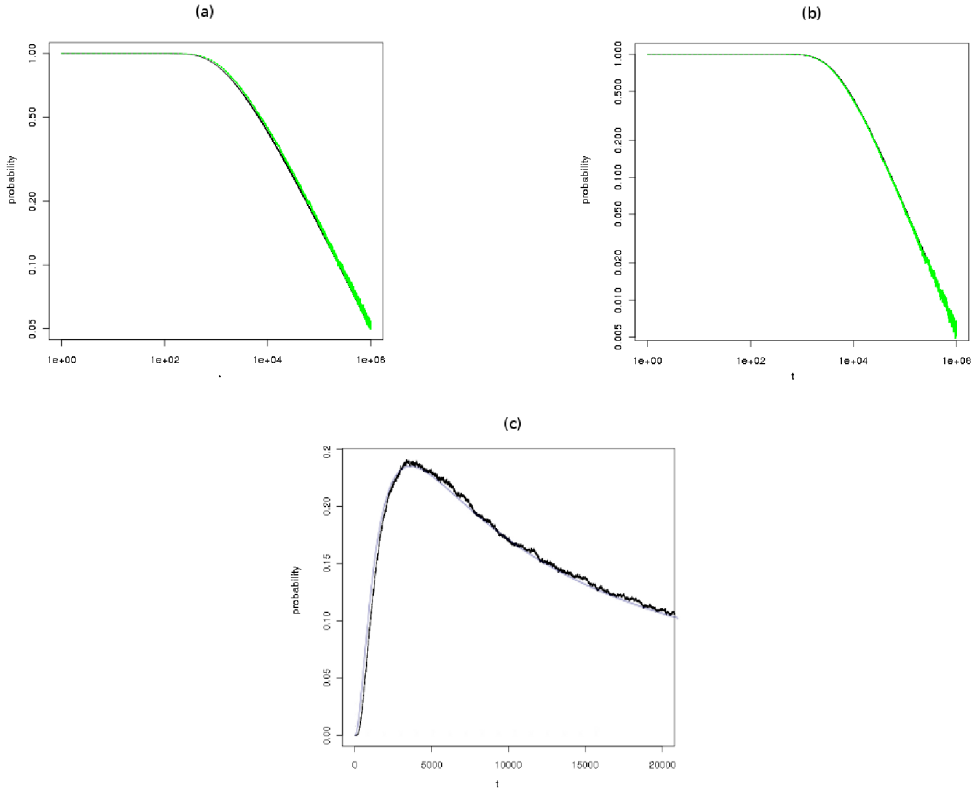

Figure 4.9: (a) The simulation results for $P(d_{min} < 2d_{inf}, t)$ are plotted with the exact formula from Eq.4.5.1. (b) $P(d_{Max} < 2d_{inf}, t)$ is plotted with Eq.4.6.1. (c) The expression for $P(d_{inf} < 2d_{min}, d_{Max} < 2d_{sup}, t)$ from Eq.(4.7.1) is plotted at intermediate times together with simulation results. Other choices for d_{inf} and d_{sup} give similar results

as expected, when either $\sqrt{d^2/t}$ or d^2/t becomes sufficiently small; what is quite interesting is that, even at intermediate times, the exact results obtained via the steepest descent method agree well with the simulations.

In this chapter we explored an area which up to now has been just grazed by research; we have been able to compute the leading terms of several probability functions, all related to collective properties of the random walks of three particles, namely the minimum and maximum distances among particles. For large times t and large distances d, our results highlight that such probability distributions display a diffusion-like scaling as d^2/t, although they regard non-linear functions of mutual distances. This regularity, which is hinted at by the Gaussian shape of the probability of meeting, but is nevertheless non-trivial because of the non-linearity of the minimum and maximum distances, breaks down for intermediate distances, where a richer behaviour is revealed as the integral approximation of the sum over lattice sites no longer holds.

4.10 Further Developments

Two possible directions for further research are: the extension to 4 and more particles of the present calculations; the study of structures that don't admit a distance graph.

When considering n independent particles on a line, with coordinates $x_1, \ldots, x_n$, the corresponding distance graphs become ever more complex, but they should prove analytically manageable. An initial consideration is the following proposition.

Proposition. The 2^n possible choices for the motion of the particles map onto $(2^n - 2)$ different movements in the space of distances, whose coordinates are $d_i = x_{i+1} - x_i$ for $i = 1, \ldots, (n-1)$.

> While it is evident that the distances will remain untouched when the all the particles move either to the left or to the right, it is not so obvious that all the other choices for the x_i lead to independent outcomes; to prove that it is indeed the case, one can proceed by induction: take all the 2^n configurations for n particles, and add a further particle; only the two configurations where all the particles move left or all the particles move right will yield no change in the distance coordinates; since for the n particles all the non zero $(2^n - 2)$ configurations yield different shifts by virtue of the inductive hypothesis, all the $(2^{n+1}-2)$ non zero configurations obtained by adding the $(n+1)$-th particle are strictly different. Since for $n = 2$ the inductive hypothesis is true, it holds for every n.

As the distance graphs, from 4 particles onwards, become quite difficult to visualize, finding a translational invariant lattice as for the case $n = 3$ is a geometrical challenge in itself. Once a method for calculation will have been established for

arbitrary n, however, interesting quantities, along the lines of the ones computed in this chapter, will become available even in the large n limit, with a big improvement on the application side (e.g. for mobile wireless networks).

About multiple random walks on structures that do not allow a distance graph not much can be said in general, since the pretty properties of translational invariance are lost: one can thus expect queer behaviour to happen for several observables, in particular for multiple random walks. Among the simplest observables one can study are the properties of collision of two particles: let

$$\mathcal{P}_{ij}(t)$$

be the probability that two particles, starting from i, meet in j at time t, and let

$$\mathcal{F}_{ij}(t)$$

be the probability that the first encounter of the particles happen at time t in j. Since two particles can have already met before meeting at j, the following holds:

$$\mathcal{P}_{ij}(t) = \sum_{\tau} \sum_{k} \mathcal{F}_{ik}(\tau)\mathcal{P}_{kj}(t-\tau) + \delta_{ij}\delta_{0t}.$$

Summing over t and j, the previous equation becomes

$$\mathcal{P}_i = \sum_{k} \sum_{\tau} \mathcal{F}_{ik}(\tau)\mathcal{P}_k + 1,$$

where $\mathcal{P}_i = \sum_t \sum_k \mathcal{P}_{ik}(t)$; if, as on homogeneous lattices, $\mathcal{P}_i$ doesn't depend on i, and the graph is recurrent, which entails $\mathcal{P}_i = \infty$, it immediately follows that

$$\sum_{\tau} \sum_{k} \mathcal{F}_{ik}(\tau) = 1,$$

that is the same as saying that the two particles are bound to meet, sooner or later. On the other hand, when $\mathcal{P}_i$ does depend on i, even on recurrent lattices it is possible that two particles never meet. The apparent incompatibility between an infinite average number of encounters and a finite probability of never meeting can be easily interpreted: the infinite expected number of encounters ($\mathcal{P}_i = \infty$) may be due to a small number of random walks which clash infinitely often, while a great number of other pairs of walkers never manage to meet. This kind of phenomenon is currently under study.

5 Ising Model: Fundamentals

5.1 Introduction

The Ising model is a rough approximation to the equilibrium statistical mechanics of a magnet, in which every atom is portrayed as having spin 1/2, and interacts with its first neighbours only. While the Ising model can correctly describe a single domain in a ferromagnet, its renown is largely due to the widespread use that researchers in the most diverse fields make of it and its many generalizations.

The historical importance of the Ising model consists in its being the first model proved to display a phase transition in the thermodynamic limit. The story goes along this line: in 1920 Wilhelm Lenz gave his student Ernst Ising the task of calculating some observables out of a classical approximation to the quantum Heisenberg problem, on a one-dimensional infinite lattice; this classical approximation was subsequently called the *Ising model*.

The system was proven to have no phase transition, and in its 1925 paper [21] Ising wrongly induced that the model would have no phase transition in higher dimensions too; the mistake he incurred was to underestimate the geometry of the system, which is of paramount importance for the mechanics of phase transition.

The error was quickly acknowledged, and Rudolf Peierls proved in 1936 [22] that the two-dimensional Ising model presented a spontaneous magnetization: he was able to show that at low enough temperature the fluctuations of the system are unable to perturb a magnetized state. Its technique was later refined by Griffiths [23], and originated several lines of research investigating higher dimensional lattices, as in the works by Dobrushin [24], Isakov [25], Pirogov-Sinai [26], or Lebowitz and Mazel [27]. The Ising model was then proved to display a phase transition on all regular lattice of dimension at least two.

As we have seen in the case of random walks, regular lattices do not tell the whole story, and peculiar phenomena can appear when leaving the assuring grounds of translational invariance. The next category of graphs which was studied in depth are fractals, where the self-similarity of the structures allowed to outline

a comprising picture [28]: the factor determining whether the graphs undergo a phase transition appears to be its minimum order of ramification, which is linked to how well the structure is connected at long range.

More general graphs [29–33] have become increasingly popular in the last twenty years: the main difference with the previous cases is that the metric structure of the embedding space ceases to play an essential role, as in its most general form a graph is a topological structure which is not necessarily embeddable in a finite dimensional Euclidean space. The absence of translational invariance and scale invariance makes general graphs very difficult to study, as *ad hoc* techniques must be employed that usually admit no straightforward generalization.

5.2 The Ising Model

Let $\mathcal{G} = (\mathcal{P}, \mathcal{L})$ be an arbitrary graph, with $\#\mathcal{P} = N$, and let $\sigma_i = \pm 1$ be a spin variable for each vertex $i \in \mathcal{P}$. We define the **Ising Hamiltonian** $\mathcal{H}$ on a graph as

$$\mathcal{H} = -\sum_{(i,j)\in\mathcal{P}\times\mathcal{P}} J_{ij}\sigma_i\sigma_j - \sum_{i\in\mathcal{P}} \sigma_i h_i. \tag{5.2.1}$$

The couplings J_{ij} are symmetric, so that $J_{ij} = J_{ji}$, and, since we are defining the Hamiltonian on the graph $\mathcal{G}$, $J_{ij} > 0$ iff $(i,j) \in \mathcal{L}$. Analogously we could give total freedom of choice for the couplings, and then define the graph $\mathcal{G}$ as the pair made of the collection of vertices and the set

$$\mathcal{L} = \{(i,j) | J_{ij} > 0\}.$$

What matters here is that there is consistency between the non-zero couplings and the edges of the graph. The parameter h_i is an external field, and it is usually set to a constant value for all the vertices.

Depending on the characteristics of the couplings J_{ij}, one usually differentiates two main cases:

- $J_{ij} \geq 0$ for all $i \in \mathcal{P}$: ferromagnetic Ising model,
- $J_{ij} \leq 0$ for all $i \in \mathcal{P}$: antiferromagnetic Ising model.

A **configuration** of the system is obtained by specifying the value of each spin σ_i in $\mathcal{P}$, and the equilibrium statistical mechanics of the Ising model, at inverse temperature $\beta = 1/kT$, is obtained by associating a Boltzmann weight to each configuration:

$$P(\{\sigma_i\}) = \mathcal{Z}^{-1} e^{-\beta\mathcal{H}\{\sigma_i\}}, \tag{5.2.2}$$

where the normalization factor is the partition function

$$\mathcal{Z} = \sum_{\{\sigma_i\}} e^{-\beta\mathcal{H}\{\sigma_i\}}. \tag{5.2.3}$$

With these definitions, one can compute the thermodynamic average value of any observable $\mathcal{O}\{\sigma_i\}$ as

$$\langle \mathcal{O} \rangle = \mathcal{Z}^{-1} \sum_{\{\sigma_i\}} \mathcal{O}\{\sigma_i\} e^{-\beta \mathcal{H}\{\sigma_i\}} \tag{5.2.4}$$

The usual statistical mechanics relations between thermodynamic quantities and the partition function hold:

- specific Helmholtz free energy $F = -\frac{kT}{N} \log \mathcal{Z}$,
- specific internal energy $\langle E \rangle = -\frac{1}{N} \frac{\partial \log \mathcal{Z}}{\partial \beta}$,
- specific heat
$$C = \frac{\partial \langle E \rangle}{\partial T} = \frac{k\beta^2}{N} \mathrm{Var}(E) = \frac{k\beta^2}{N} \frac{\partial^2 \log \mathcal{Z}}{\partial \beta^2},$$
- average spin magnetization
$$\langle \sigma \rangle = \frac{1}{N} \sum_{i \in \mathcal{P}} \langle \sigma_i \rangle = -\frac{1}{N} \frac{\partial \log \mathcal{Z}}{\partial h}.$$

As long as the graph is finite, $\mathcal{Z}$ is a finite sum of analytic functions, and is thus analytic itself: no phase transition is then possible, and all the derivatives are well defined.

5.3 Infinite Graphs

When the graph is infinite, on the other hand, $\mathcal{Z}$ is ill-defined, and to obtain a meaningful quantity one has to compute the energy density $\langle E \rangle$ choosing an appropriate sequence of growing graphs. The most versatile way of accomplishing this objective is by employing Van Hove spheres (see Sec.1.2), while on lattices more regular structures can be employed [23]. In two fundamental papers of 1952, Lee and Yang [34, 35] prove the following

Theorem. In a regular d-dimensional lattice $\mathcal{V}$, take a sequence of growing sublattices $\mathcal{V}_N$ such that

$$\lim_{N \to \infty} \mathcal{V}_N = \mathcal{V},$$

and whose surfaces $\partial \mathcal{V}_N$ don't increase faster than $(\#\mathcal{V}_N)^{(d-1)/d}$. Then the thermodynamic limit

$$F = \lim_{N \to \infty} \frac{kT}{\#\mathcal{V}_N} \log \mathcal{Z}_{\mathcal{V}_N}$$

exists and is independent of the shape of the sublattices. Moreover, F is a continuous and monotonically decreasing function of the magnetic field h and the couplings J_{ij}.

Far more interesting is a second result, which states a sufficient condition for the analyticity of the free energy: since $F = kT/N \log \mathcal{Z}_N$, its singularities are determined by the zeros of the partition function. In particular, considering $\beta = 1/kT$ as a complex variable, for all finite N the roots of $\mathcal{Z}_N$ will lie outside the real line, which is the same as saying that there is no singularity of F_N as the temperature varies. If the same holds in the limit $N \to \infty$, then no phase transition will be present, as the following theorem states.

Theorem. Let $y_{\{\sigma_i\}}(\beta, J_{lm}, h_n) = e^{-\beta \mathcal{H}\{\sigma_i\}}$. If in the complex plane of variable $y_{\{\sigma_i\}}$ a region R exists, which covers a segment of the real positive axis, such that for all N no zeros of $\mathcal{Z}_N$ fall in R, then everywhere in R the quantities

$$\lim_{N\to\infty} \frac{1}{N} \frac{\partial^k \log \mathcal{Z}_N}{\partial \left(\log y_{\{\sigma_i\}}\right)^k}$$

exist and approach limits analytic in $y_{\{\sigma_i\}}$. Moreover, limiting procedure and derivatives commute.

Thus, in order to find possible singularities of the Ising model, or more in general of the free energy for a statistical model, one can study the distribution of the roots of the partition function. It is noteworthy that the roots, in the continuous limit, are ordered along lines which reflect to some extent the symmetries of the system [35–39]

A less general but powerful result [40], derived from the theorems by Lee and Yang, concerns the ferromagnetic Ising model ($J_{ij} \geq 0$):

Theorem. Let $z_i = \exp -2\beta h_i$. If $|z_i| \geq 1$, which means $h_i \geq 0$ (it can be always satisfied as long as all the external fields have the same orientation), then the zeros of $\mathcal{Z}$ satisfy

$$|z_1| = |z_2| = \cdots = |z_{\#\mathcal{V}_N}| = 1 \tag{5.3.1}$$

The previous theorem implies that phase transition, for the Ising model, can occur at finite temperature only if all the magnetic fields are turned off, as otherwise the free energy is an analytic function of β even as $N \to \infty$.

The expression of observables as derivatives of $\log \mathcal{Z}$ is of course useless when the partition function is not analytic. However, the quantities are well defined for $h_i \equiv h \neq 0$, as the free energy is analytic by virtue of the previous theorem; the two limits $h \to 0^+$ and $h \to 0^-$ can however yield different results, and indeed they do in several cases. As a first example, on a 2-dimensional infinite square lattice, at low temperatures,

$$\lim_{h\to 0^+} \langle \sigma \rangle > 0,$$

$$\lim_{h\to 0^-} \langle \sigma \rangle = -\lim_{h\to 0^+} \langle \sigma \rangle < 0.$$

More in general one can easily see that, since the transformation

$$\begin{cases} \sigma_i \to -\sigma_i \\ h \to -h \end{cases}$$

leaves unchanged $\exp(-\beta\mathcal{H}\{\sigma_i\})$, the following holds:

$$\lim_{h\to 0^+} \langle \sigma_{i_1}\sigma_{i_2}\ldots\sigma_{i_k}\rangle = (-)^k \lim_{h\to 0^-} \langle \sigma_{i_1}\sigma_{i_2}\ldots\sigma_{i_k}\rangle. \tag{5.3.2}$$

5.4 Correlation Functions

The spin-spin correlation functions $\langle\sigma_i\sigma_j\rangle$ are important observables, and thus deserve a particular attention. In a series of papers dating back to $1966-1967$ [41–43], Griffiths derived several fundamental results on general graphs, which constitute both the founding stone of a prolific area of research [44–47] and a powerful tool for investigators.

A first observation is that $\langle\sigma_i\sigma_j\rangle$ can be obtained as a derivative of $\mathcal{Z}$:

$$\begin{aligned} \langle\sigma_i\sigma_j\rangle &= \mathcal{Z}^{-1}\sum_{\{\sigma_i\}} \sigma_i\sigma_j \exp\left\{-\beta\left[-\sum J_{lm}\sigma_l\sigma_m - \sum h_l\sigma_l\right]\right\} \\ &= \frac{1}{\beta^2}\frac{\partial^2 \log\mathcal{Z}}{\partial h_i \partial h_j}. \end{aligned} \tag{5.4.1}$$

Theorem. **Griffiths' Inequalities**: for $J_{ij} \geq 0$, and under the condition that

- either $h_i \equiv h > 0$,
- or $h_i \equiv h = 0$ and $\sigma_j = +1$ for $j \in U$ for some set U,
- or $h_i \equiv 0$ and no spins are kept fixed,

the following is verified:

$$\langle\sigma_i\sigma_j\rangle \geq 0 \text{ for all } i,j \tag{5.4.2}$$

$$\beta^{-1}\frac{\partial\langle\sigma_i\sigma_j\rangle}{\partial J_{km}} = \langle\sigma_i\sigma_j\sigma_k\sigma_m\rangle - \langle\sigma_i\sigma_j\rangle\langle\sigma_k\sigma_m\rangle \geq 0 \text{ for all } i,j,k,m \tag{5.4.3}$$

$$\langle\sigma_i\sigma_k\rangle \geq \langle\sigma_i\sigma_j\rangle\langle\sigma_j\sigma_k\rangle \text{ for all } i,j,k \tag{5.4.4}$$

$$\langle\sigma_i\rangle \geq 0 \text{ for all } i \tag{5.4.5}$$

$$\langle\sigma_i\sigma_j\rangle \geq \langle\sigma_i\rangle\langle\sigma_j\rangle \text{ for all } i,j. \tag{5.4.6}$$

If the sign of the external magnetic field or of the fixed spins is reversed, the two latter inequalities are reversed, according to Eq.(5.3.2).

5.5 Magnetization

The **mean spin value** $\langle \sigma_i \rangle$ is in general different at every vertex i.

For the case of **finite** systems, if no external field nor boundary condition is set, the rule

$$\sigma_i \mapsto -\sigma_i$$

leaves the energy unchanged, so that

$$\langle \sigma_i \rangle = -\langle \sigma_i \rangle \Rightarrow \langle \sigma_i \rangle = 0. \tag{5.5.1}$$

For infinite systems, the same results hold from a formal point of view, as

$$\lim_{N\to\infty} \langle \sigma_i \rangle_{\nu_N} = 0;$$

however, the expression bears no significance on its own: the states of opposite magnetization which cancel each other's contribution can be unable to be explored from a physical point of view, as in the case of spontaneous magnetization the thermal fluctuations of the system are not enough to overturn a magnetic ordering, once that it has been attained. The equilibrium statistical mechanics is then wrong to some extent, as the system is unable to explore all the phase space. Nevertheless, meaningful quantities can be computed: observables which are even in the fields are not zeroed by the averaging process, and can give meaningful results.

When the external field is turned on, it is indeed possible that

$$\lim_{h\to 0^+} \lim_{N\to\infty} \langle \sigma_i \rangle_{\nu_N} = +\mu > 0,$$

$$\lim_{h\to 0^-} \lim_{N\to\infty} \langle \sigma_i \rangle_{\nu_N} = -\mu < 0,$$

which is exactly what happens when a spontaneous magnetization occurs.

Likewise, when external spins are held fixed, i.e. a boundary condition is set, it's possible that

$$\lim_{N\to\infty} \langle \sigma_i \rangle_{\nu_N} = \pm\mu,$$

with $\mu \neq 0$.

The **average magnetization** of the graph is another meaningful quantity:

$$m = \frac{1}{N} \sum_{i\in\mathcal{P}} \sigma_i; \tag{5.5.2}$$

when averaged on the thermodynamic ensemble for homogeneous lattices, it is trivially equal to the $\langle \sigma_i \rangle$, while on general structures it can be zero even though all the single $\langle \sigma_i \rangle$ are strictly greater than zero.

Another interesting quantity is the **modulus of the magnetization**, $|m|$, which

can be used to extract useful information about the magnetization properties of a graph even when neither external field nor fixed spins are set, as it is a strictly positive quantity which is left untouched by spin reversal.

The same is true for the **square magnetization**

$$m^2 = \frac{1}{N^2} \sum_{i,j \in \mathcal{P}} \sigma_i \sigma_j. \tag{5.5.3}$$

Even though $|\, m| < 1$ implies $m^2 < |\, m|$, the two quantities have to be both zero or both non-zero simultaneously: the variance of $|\, m|$ is

$$\Delta |\, m| = \langle m^2 \rangle - \langle |\, m| \rangle^2 \geq 0,$$

which entails

$$\begin{cases} \langle m \rangle^2 \leq \langle |\, m| \rangle \leq \sqrt{\langle m^2 \rangle} \\ \langle |\, m| \rangle \leq \sqrt{\langle m^2 \rangle} \leq \sqrt{\langle |\, m| \rangle} \end{cases} ; \tag{5.5.4}$$

as a consequence, $\langle |\, m| \rangle \neq 0$ is equivalent to $\langle m^2 \rangle \neq 0$.

Both the average square magnetization and the average modulus of the magnetization are strictly positive at all $N < \infty$. However, as $N \to \infty$, in the absence of spontaneous magnetization they will both become zero. The easiest way to understand this process is by analysing the average square magnetization,

$$\langle m^2 \rangle = \frac{1}{N^2} \sum_{ij} \langle \sigma_i \sigma_j \rangle, \tag{5.5.5}$$

as it immediately highlights the importance of the spin-spin correlation functions: as N grows, the vast majority of all the pairs (i, j) will be separated by an arbitrary distance, so that in order for $\langle \sigma_i \sigma_j \rangle$ to remain finite, the number of pairs at fixed distance must outbalance the decreasing weight of each correlation function.

A simple (and simplistic) way of keeping this into account, which works well for homogeneous lattices, but is otherwise useless, is as follows: in homogeneous lattices the correlation functions only depend on the relative distance between the spins (in general a vector distance), and in the specific case of Euclidean lattices they just depend on the Euclidean distance (for large lattices in the proximity of a phase transition). In particular, when the temperature of the system is not critical, correlation functions decay exponentially to zero, so that

$$\langle m^2 \rangle = \frac{1}{N^2} \sum_{ij} \langle \sigma_i \sigma_j \rangle \sim \frac{N}{N^2} \to 0.$$

At the critical temperature, correlation functions are power-like; even in this case, $\langle m^2 \rangle$ fails to be non zero in the thermodynamic limit: let

$$\langle \sigma_i \sigma_j \rangle \sim d_{ij}^{-\alpha},$$

and write the number of vertices at Euclidean distance at most R from a point as

$$N(R) \sim R^{d_{\text{frac}}};$$

the number of points at distance about R is then approximately $R^{d_{\text{frac}}-1}$, and

$$\langle m^2 \rangle \sim \frac{1}{R^{d_{\text{frac}}}} \sum_{\rho}^{R} R^{d_{\text{frac}}-1} R^{-\alpha} \sim R^{-\alpha},$$

which tends to zero in the thermodynamic limit. The only case in which one achieves a non-zero average square magnetization is then when the correlation functions tend to a finite non-zero constant, as we will prove in the following section.

5.6 A Consideration on the Magnetization of the Ising Model

In the thermodynamic limit, $\langle m^2 \rangle$ can become zero even though it is a strictly positive quantity for every finite graph. What exactly is the connection between this phenomenon and the characteristics of the correlation functions? To answer this question choose a graph $\mathcal{G} = (\mathcal{P}, \mathcal{L})$ and consider the measure μ of a set as defined in Sec.1.3.

Proposition. The existence, in the thermodynamic limit, of a non-zero measure set of correlation functions, such that all its correlation functions are greater than some $\epsilon > 0$, is a necessary and sufficient condition for $\langle m^2 \rangle$ to be greater than zero.

If in the thermodynamic limit a subset $A \subset \mathcal{P} \times \mathcal{P}$ of measure $\mu(A) = \alpha > 0$ exists such that $\forall_{(i,j)\in A} \ \langle \sigma_i \sigma_j \rangle \ \geq \epsilon > 0$, then

$$\langle m^2 \rangle \ = \lim_{N\to\infty} \sum_{(i,j)\in\mathcal{P}\times\mathcal{P}} \frac{\langle \sigma_i \sigma_j \rangle}{N^2} \geq \epsilon\alpha > 0.$$

If there is no such subset, then for any given ϵ and for any $A \subset \mathcal{P} \times \mathcal{P}$, a set $B \subset A$ exists which has measure $\mu(B) = \mu(A)$ and that satisfies $\langle \sigma_i \sigma_j \rangle < \epsilon$ for all $(i, j) \in \mathcal{P} \times \mathcal{P}$. This is true in particular for $A = \mathcal{P} \times \mathcal{P}$, and for any ϵ

$$\langle m^2 \rangle \ = \lim_{N\to\infty} \sum_{(i,j)\in\mathcal{P}\times\mathcal{P}} \frac{\langle \sigma_i \sigma_j \rangle}{N^2} \leq \epsilon,$$

so $\langle m^2 \rangle = 0$.

5.7 The Ising Model on an Infinite Line

The simplest exactly solvable lattice is the infinite line, which allows one to introduce the transfer matrix formalism. What is particularly noteworthy is that it is possible to find a full solution in the presence of an external field.

As anticipated, no phase transition is possible on the line: let all the couplings be equal to J, let the external field be homogeneous ($h_i \equiv h$), and define the **transfer matrix** P as having elements

$$\langle \sigma_i | \, P | \, \sigma_j \rangle = \exp \left\{ \beta \left[J \sigma_i \sigma_j + h \left(\sigma_i + \sigma_j \right) / 2 \right] \right\}, \tag{5.7.1}$$

or

$$P = \begin{pmatrix} e^{\beta(J+h)} & e^{-\beta J} \\ e^{-\beta J} & e^{\beta(J-h)} \end{pmatrix}.$$

Because of the sum over configurations, the partition function $\mathcal{Z}$ becomes a trace:

$$\begin{aligned} \mathcal{Z} &= \sum_{\sigma_1} \cdots \sum_{\sigma_N} \langle \sigma_1 | \, P | \, \sigma_2 \rangle \ldots \langle \sigma_{N-1} | \, P | \, \sigma_N \rangle \\ &= \sum_{\sigma_1} \langle \sigma_1 | \, P^N | \, \sigma_1 \rangle \\ &= \mathrm{Tr} \left(P^N \right). \end{aligned} \tag{5.7.2}$$

Since $\mathrm{Tr} \left(P^N \right) = \lambda_1^N + \lambda_2^N$, where λ_i are the eigenvalues of P, one first calculates them, then turns to the limit for large N, which selects the greatest between the eigenvalues:

$$\lambda_\pm = e^{\beta J} \left[\cosh \beta h \pm \sqrt{\sinh^2 \beta h + e^{-4\beta J}} \right];$$

since λ_+ is the greatest eigenvalue,

$$\mathcal{Z} = \mathrm{Tr} \left(P^N \right) \sim \lambda_+^N, \tag{5.7.3}$$

and the free energy becomes

$$F = \lim_{N \to \infty} -\frac{kT}{N} \log \mathcal{Z}_{\mathcal{V}_N} = -J - kT \log \left[\cosh \beta h + \sqrt{\sinh^2 \beta h + e^{-4\beta J}} \right]. \tag{5.7.4}$$

It is obvious now that the only singularity point for the free energy at real T and h is at $T = 0$, so we can conclude that no phase transition occurs.

Computing the other observables is now straightforward; in particular

$$\langle m \rangle = \frac{\partial F}{\partial h} = -kT \frac{\sinh \beta h + \frac{\sinh \beta h \cosh \beta h}{\sqrt{\sinh^2 \beta h + e^{-4\beta J}}}}{\cosh \beta h + \sqrt{\sinh^2 \beta h + e^{-4\beta J}}}.$$

In the limit $h \to 0^{\pm}$, $\langle m \rangle = 0$, so no spontaneous magnetization occurs at any non-zero temperature, as anticipated by the analyticity in T of the free energy.

It is noteworthy that computing F_N in the reverse order, first taking the limit $h \to 0$ and then $N \to \infty$, would have produced the same result: this property fails just when a phase transition occurs, as then the order in which the limits are taken decides what the final result is; in particular, the thermodynamic limit needs be taken first, as otherwise the finite size of each system $\mathcal{V}_N$ guarantees the absence of any singularity.

5.8 The Path Expansion of the Ising Model

A powerful technique for dealing with the difficulties of the Ising model on graphs is the path expansion in zero field: due to the discrete nature of the spin variables, it is possible to express the partition function as a sum over all the possible loops which are made by choosing at most once each edge.

A trick is the key to prove the result: when $h_i \equiv 0$ and no spins are held fixed, the fragment of the Boltzmann weight $\exp \beta J_{ij} \sigma_i \sigma_j$ can be written as

$$\exp \beta J_{ij} \sigma_i \sigma_j = \cosh \beta J_{ij} + \sigma_i \sigma_j \sinh \beta J_{ij}. \tag{5.8.1}$$

The partition function can then be written as

$$\begin{aligned} \mathcal{Z}_{\mathcal{V}_N} &= \sum_{\{\sigma_i\}} \prod_{i,j} \left[\cosh \beta J_{ij} + \sigma_i \sigma_j \sinh \beta J_{ij} \right] \\ &= \sum_{\{\sigma_i\}} \prod_{i,j} \cosh \beta J_{ij} \left[1 + \sigma_i \sigma_j \tanh \beta J_{ij} \right]. \end{aligned}$$

The product of all the square brackets on the right hand side is a sum of terms which display a product of spin variables: whenever any spin variable appears with an odd power, the sum over configurations of that term can be written as

$$\sum_{\sigma_l} \sigma_l^{2t+1} \sum_{\sigma_i} \sum_{\sigma_k} \cdots = + \sum_{\sigma_i} \sum_{\sigma_k} \cdots - \sum_{\sigma_i} \sum_{\sigma_k} \cdots = 0.$$

The picture described at the beginning of this paragraph now emerges: only those terms which display an even power for all the spin variables contribute to the partition function, and these terms correspond exactly to choosing edges (i.e. terms like $\sigma_l \sigma_m \sinh \beta J_{lm}$) in such a way as to make closed loops. In addition to the loops, a term equal to 1 has to be taken into account. Using the terminology of Sec.1.2, we call such loops **cycles**, and write

$$\mathcal{Z}_{\mathcal{V}_N} = \left[\prod_{(l,m)} \cosh \beta J_{lm} \right] \left[1 + \sum_{\gamma_{\text{cycle}}} \prod_{(i,j) \in \gamma} \tanh \beta J_{ij} \right]. \tag{5.8.2}$$

Exactly the same procedure yields an expression for the sum over configurations of the product $\sigma_i\sigma_j \exp\left[-\beta\mathcal{H}\{\sigma_i\}\right]$: here the sum over loops is replaced by a sum over all the paths $\gamma_{i\to j}$, created by taking at most once each edge, which lead from i to j. The direct consequence is that

$$\langle\sigma_i\sigma_j\rangle = \frac{\sum_{\gamma_{i\to j}} \prod_{(i,j)\in\gamma} \tanh\beta J_{ij}}{1+\sum_{\gamma_{\rm cycle}} \prod_{(i,j)\in\gamma} \tanh\beta J_{ij}}. \tag{5.8.3}$$

Analogous relations hold for the expectation values of arbitrary products of spin values $\langle\sigma_i\ldots\sigma_k\rangle$, where the sum at the numerator is over all the paths which have a hanging leg at each of the vertices $i,\ldots,k$.

The path expansion can immediately be applied to the 1-dimensional Ising model: since no cycle is possible, the denominator in Eq.(5.8.3) is 1, while the only possible path from i to j is a segment of length d_{ij}. Then

$$\langle\sigma_i\sigma_{i+l}\rangle = \prod_{m=i}^{i+l-1} \tanh\beta J_{m(m+1)}.$$

5.9 The Mermin-Wagner Theorem and its Extensions

One of the first general results regarding phase transitions was the Mermin-Wagner theorem [48]; even if it does not regard the Ising model, it is important enough to be recalled:

Theorem. At finite temperatures, the quantum spin-S Heisenberg model with isotropic and finite-range exchange interactions on one- or two-dimensional lattices can be neither ferromagnetic nor antiferromagnetic.

Without any pretence to analyse the details, the Mermin-Wagner theorem, along with other results both in statistical physics [49] and in quantum field theory [50], states that on regular lattices continuous symmetries cannot be broken in dimension lower than or equal to 2.

A powerful extension of the Mermin-Wagner theorem to arbitrary graphs [51] takes into account whether simple random walks on the structure are recurrent, this characteristic becoming a substitute for the dimension of the graph. It is however not applicable to the Ising model.

Theorem. The classical $O(n)$ ($n \geq 2$) and quantum Heisenberg ferromagnetic models on a graph cannot have spontaneous magnetization if simple random walks on the structure are recurrent on average (see Sec.2.7).

As a simple corollary descending from the definition of recurrence on average, graphs whose average spectral dimension $\bar{d}$ is lower than or equal to 2 have no spontaneous magnetization.

The classical example of the thesis failing when the symmetry is discrete is the Ising model itself, as on the infinite plane it shows spontaneous magnetization. This fact is traditionally explained with the impossibility for thermodynamical fluctuations to reverse big blocks of oriented spins when the possible orientations are just up and down, thus leaving the magnetized lattice in a state which cannot be overturned; on the contrary, when the symmetry is continuous adjacent spins can be at arbitrarily small angles, thus allowing whole blocks of spins to be flipped increasing the energy of the system by an infinitesimal amount.

A theorem of this family which can also be applied to the Ising model actually exists [52], and gives a sufficient condition for spontaneous magnetization:

Theorem. The family of $O(n)$ models shows spontaneous magnetization in the limit $h \to 0^{\pm}$ if the graph is transient on average.

This theorem immediately implies that regular lattices with $d \geq 3$ have spontaneous magnetization, and also allows one to decide the magnetizability of more exotic structures just by investigating their properties under a random walk. The weakness of the latter theorem is that it says nothing on a lot of important structures, including the square lattice, all the planar fractals and many more general graphs. One of the results of my work as a Ph.D. student has been to devise two theorems, which can be applied to a huge variety of graphs, stating sufficient conditions both for magnetizability and non-magnetizability of a graph. They will be discussed at length in the following two chapters.

6

A Sufficient Condition for No Spontaneous Magnetization

In this chapter, a theorem is presented which states that a very large class exists whose graphs, which we call **weakly separable**, magnetize. Together with another theorem, which the reader will find in the next chapter, it makes a powerful instrument for determining whether a given graph magnetizes.

This work has been published in Modern Physics Letters B [3].

As a first step towards the proof of our results, we are now going to state some general results about the Ising model that we'll need later.

6.1 Combination of Two Points in a Graph

We are now going to prove rigorously that increasing a given coupling J_{ij} to infinity is equivalent to joining the two points i and j: the same model can thus be studied on a new graph, where the set of points is changed to $\mathcal{P}' = \mathcal{P} \setminus \{i,j\} \cup \{k\}$, and the new couplings are defined as $J'_{km} \equiv J_{im} + J_{jm}$, or $J'_{lm} \equiv J_{lm}$ if $l, m \neq k$.

Let $\mathcal{G}_\mathcal{N}$ be a given graph and $\mathcal{H} = -\sum_{i<j} J_{ij}\sigma_i\sigma_j$ the Ising energy on $\mathcal{G}_\mathcal{N}$, with $J_{ij} \leq J_{Max} < \infty$ and correlation number $z_i \leq z_{Max} < \infty$. Now take two point α and β on $\mathcal{G}_N$, and let ${\mathcal{G}'}_N$ denote the graph obtained by coalescing the point α and β into γ, with couplings $J'_{\gamma\delta} = J_{\alpha\delta} + J_{\beta\delta}$ for every δ in ${\mathcal{G}'}_N$.
We prove in the following that the relationship

$$\lim_{J_{\alpha\beta}\to\infty} \langle\sigma_i\sigma_j\rangle_{\mathcal{G}_N}^{J_{\alpha\beta}} = \langle\sigma_i\sigma_j\rangle_{{\mathcal{G}'}_N}$$

holds uniformly in the thermodynamic limit, so that the double limit

$$\lim_{N\to\infty}\lim_{J_{\alpha\beta}\to\infty} \langle\sigma_i\sigma_j\rangle_{\mathcal{G}_N}^{J_{\alpha\beta}} = \langle\sigma_i\sigma_j\rangle_{{\mathcal{G}'}_N}$$

doesn't depend on the order of limits.

The correlation functions are

$$\langle \sigma_i \sigma_j \rangle_{\mathcal{G}_N}^{J_{\alpha\beta}} = \frac{\mathcal{Z}^{++} + \mathcal{Z}^{--} - \mathcal{Z}^{+-} - \mathcal{Z}^{-+}}{\mathcal{Z}^{++} + \mathcal{Z}^{--} + \mathcal{Z}^{+-} + \mathcal{Z}^{-+}},$$

where $\mathcal{Z}^{++}$ is the correlation function calculated at $\sigma_i = +1, \sigma_J = +1$, and analogously for $\mathcal{Z}^{--}, \mathcal{Z}^{+-}$ and $\mathcal{Z}^{-+}$. In terms of the coupling $J_{\alpha\beta}$, the correlations functions can be written as follows:

$$\mathcal{Z}^{++} = e^{+\beta J_{\alpha\beta}} \left[\mathcal{Z}_{++}^{++} + \mathcal{Z}_{--}^{++} + e^{-2\beta J_{\alpha\beta}} \left(\mathcal{Z}_{+-}^{++} + \mathcal{Z}_{-+}^{++} \right) \right],$$

with $\mathcal{Z}_{--}^{++}$ denoting the correlation functions with (σ_i, σ_j) fixed by the upper indeces, $(\sigma_\alpha, \sigma_\beta)$ by the lower ones. We now define

$$\mathcal{Z}_{conc}^{\sigma_i\sigma_j} \equiv \mathcal{Z}_{++}^{\sigma_i\sigma_j} + \mathcal{Z}_{--}^{\sigma_i\sigma_j},$$
$$\mathcal{Z}_{disc}^{\sigma_i\sigma_j} \equiv \mathcal{Z}_{+-}^{\sigma_i\sigma_j} + \mathcal{Z}_{-+}^{\sigma_i\sigma_j},$$

so as to write, exploiting the inversion symmetry of the Ising model,

$$\langle \sigma_i \sigma_j \rangle_{\mathcal{G}_N}^{J_{\alpha\beta}} = \frac{\mathcal{Z}_{conc}^{++} - \mathcal{Z}_{conc}^{+-} + e^{-2\beta J_{\alpha\beta}} \left(\mathcal{Z}_{disc}^{++} - \mathcal{Z}_{disc}^{+-} \right)}{\mathcal{Z}_{conc}^{++} + \mathcal{Z}_{conc}^{+-} + e^{-2\beta J_{\alpha\beta}} \left(\mathcal{Z}_{disc}^{++} + \mathcal{Z}_{disc}^{+-} \right)}.$$

Since both the correlation number z_l and J_{lm} are uniformly limited, the energy difference between two states, differing at most for the spin values at the two points α, β, is bounded:

$$-2 z_{Max} J_{Max} \leq \mathcal{H}_{++}^{\sigma_i\sigma_j} - \mathcal{H}_{+-}^{\sigma_i\sigma_j} \leq 2 z_{Max} J_{Max},$$
$$e^{-2\beta z_{Max} J_{Max}} \leq e^{\beta \left(\mathcal{H}_{++}^{\sigma_i\sigma_j} - \mathcal{H}_{+-}^{\sigma_i\sigma_j} \right)} \leq e^{+2\beta z_{Max} J_{Max}}.$$

Defining now

$$\begin{cases} \mathcal{Z}_{conc} \equiv \mathcal{Z}_{conc}^{++} + \mathcal{Z}_{conc}^{+-} \\ \mathcal{Z}_{disc} \equiv \mathcal{Z}_{disc}^{++} + \mathcal{Z}_{disc}^{+-} \end{cases},$$

we can write, denoting by $\sum'_{\{\sigma_k\}}$ the sum over the configurations at fixed α, β, i, j,

$$\begin{aligned}
\mathcal{Z}_{conc} &= \sum'_{\{\sigma_k\}} \left(e^{-\beta \mathcal{H}_{++}^{++}} + e^{-\beta \mathcal{H}_{--}^{++}} + e^{-\beta \mathcal{H}_{++}^{+-}} + e^{-\beta \mathcal{H}_{--}^{+-}} \right) \\
&= \sum'_{\{\sigma_k\}} \left(e^{-\beta \mathcal{H}_{+-}^{++}} e^{-\beta \left(\mathcal{H}_{++}^{++} - \mathcal{H}_{+-}^{++} \right)} + e^{-\beta \mathcal{H}_{-+}^{++}} e^{-\beta \left(\mathcal{H}_{--}^{++} - \mathcal{H}_{-+}^{++} \right)} \right. \\
&+ \left. e^{-\beta \mathcal{H}_{+-}^{+-}} e^{-\beta \left(\mathcal{H}_{++}^{+-} - \mathcal{H}_{+-}^{+-} \right)} + e^{-\beta \mathcal{H}_{-+}^{+-}} e^{-\beta \left(\mathcal{H}_{--}^{+-} - \mathcal{H}_{-+}^{+-} \right)} \right) \\
&\leq e^{+2\beta J_{Max} z_{Max}} \sum'_{\{\sigma_k\}} \left(e^{-\beta \mathcal{H}_{+-}^{++}} + e^{-\beta \mathcal{H}_{-+}^{++}} + e^{-\beta \mathcal{H}_{+-}^{+-}} + e^{-\beta \mathcal{H}_{-+}^{+-}} \right) \\
&= e^{+2\beta J_{Max} z_{Max}} \left(\mathcal{Z}_{disc} \right).
\end{aligned}$$

An analogous relation holds for every value of σ_i, σ_j and also if we exchange $\mathcal{Z}_{conc}^{\sigma_i\sigma_j}$ and $\mathcal{Z}_{disc}^{\sigma_i\sigma_j}$, so that

$$e^{-2\beta J_{Max} z_{Max}} \mathcal{Z}_{conc} \leq \mathcal{Z}_{disc} \leq e^{+2\beta J_{Max} z_{Max}} \mathcal{Z}_{conc},$$
$$e^{-2\beta J_{Max} z_{Max}} \mathcal{Z}_{disc} \leq \mathcal{Z}_{conc} \leq e^{+2\beta J_{Max} z_{Max}} \mathcal{Z}_{disc}.$$

We can therefore write

$$\mathcal{Z}_{disc} = \eta \mathcal{Z}_{conc},$$

where $\eta \in \left(e^{-2\beta J_{Max} z_{Max}}, e^{+2\beta J_{Max} z_{Max}}\right)$. The correlation function now reads

$$\langle \sigma_i \sigma_j \rangle_{\mathcal{G}_N}^{J_{\alpha\beta}} = \frac{\mathcal{Z}_{conc}^{++} - \mathcal{Z}_{conc}^{+-}}{\left(\mathcal{Z}_{conc}^{++} + \mathcal{Z}_{conc}^{+-}\right)\left(1 + \eta e^{-2\beta J_{\alpha\beta}}\right)}$$
$$+ e^{-2J_{\alpha\beta}} \frac{\mathcal{Z}_{disc}^{++} - \mathcal{Z}_{disc}^{+-}}{\left(\mathcal{Z}_{disc}^{++} + \mathcal{Z}_{disc}^{+-}\right)\left(1 + \eta^{-1} e^{-2\beta J_{\alpha\beta}}\right)}.$$

It is now possible to notice that

$$\langle \sigma_i \sigma_j \rangle_{\mathcal{G'}_N} = \frac{\mathcal{Z}_{conc}^{++} - \mathcal{Z}_{conc}^{+-}}{\mathcal{Z}_{conc}^{++} + \mathcal{Z}_{conc}^{+-}},$$

while $\frac{\mathcal{Z}_{disc}^{++} - \mathcal{Z}_{disc}^{+-}}{\mathcal{Z}_{disc}^{++} + \mathcal{Z}_{disc}^{+-}}$ is the correlation function of a graph $\mathcal{G''}_N$, equal to $\mathcal{G'}_N$ but for the couplings $J''_{\gamma\delta} = J_{\alpha\delta} - J_{\beta\delta}$. Since for any two points, whose distance d_{ij} is fixed, the correlation function is greater than $(\tanh \beta J_{min})^{d_{ij}}$, the following inequality holds:

$$\langle \sigma_i \sigma_j \rangle_{\mathcal{G'}_N} \frac{1}{1 + \eta e^{-2\beta J_{\alpha\beta}}} \leq \langle \sigma_i \sigma_j \rangle_{\mathcal{G}_N}^{J_{\alpha\beta}} \leq \langle \sigma_i \sigma_j \rangle_{\mathcal{G'}_N} \times$$
$$\times \left(\frac{1}{1 + \eta e^{-2\beta J_{\alpha\beta}}} + \frac{e^{-2\beta J_{\alpha\beta}}}{1 + \eta^{-1} e^{-2\beta J_{\alpha\beta}}} \frac{1}{(\tanh \beta J_{min})^{d_{ij}}} \right).$$

Since $\langle \sigma_i \sigma_j \rangle_{\mathcal{G'}_N}$doesn't depend on $J_{\alpha\beta}$ and $\eta \in \left(e^{-2\beta J_{Max} z_{Max}}, e^{+2\beta J_{Max} z_{Max}}\right)$, the following limit exists and is independent of the limit order:

$$\lim_{N \to +\infty} \lim_{J_{\alpha\beta} \to +\infty} \langle \sigma_i \sigma_j \rangle_{\mathcal{G}_N}^{J_{\alpha\beta}} = \langle \sigma_i \sigma_j \rangle_{\mathcal{G'}_\infty}.$$

6.2 Narrowings in Graphs and Correlation Functions

A general result by Griffiths [41] (see Eq.5.4.3) states that $\frac{\partial \langle \sigma_i \sigma_j \rangle}{\partial J_{lm}} \geq 0$; when used in conjunction with the previous result, it implies that joining points on a graph increases all the correlation functions.

Lemma. When all the possible paths between two points i and j share a common link (l, m), the correlation function satisfies

$$\langle \sigma_i \sigma_j \rangle = \langle \sigma_i \sigma_l \rangle \, \langle \sigma_m \sigma_j \rangle \tanh \beta J_{lm}. \tag{6.2.1}$$

If all the paths between i and j share a common link, the graph $\mathcal{G}$ is made up of two subgraphs, $\mathcal{G}_1$ and $\mathcal{G}_2$, connected by the single link J_{lm}. Employing the well known path expansion of the correlation functions [53] and supposing that $i \in \mathcal{G}_1$ and $j \in \mathcal{G}_2$, we can write

$$\begin{aligned}
\langle \sigma_i \sigma_j \rangle_{\mathcal{G}} &= \frac{\sum_{\gamma: i \to j}^{\mathcal{G}} \prod_{(p,q)\in\gamma} \tanh \beta J_{pq}}{1 + \sum_{\gamma_{loop}}^{\mathcal{G}} \prod_{(p,q)\in\gamma_{loop}} \tanh \beta J_{pq}} \\
&= \frac{\left(\sum_{\gamma: i \to l}^{\mathcal{G}_1} \prod_{(p,q)\in\gamma} \tanh \beta J_{pq} \right)}{\left(1 + \sum_{\gamma_{loop}}^{\mathcal{G}_1} \prod_{(p,q)\in\gamma_{loop}} \tanh \beta J_{pq} \right)} \cdot \\
&\quad \cdot \frac{\left(\sum_{\gamma: l \to j}^{\mathcal{G}_2} \prod_{(p,q)\in\gamma} \tanh \beta J_{pq} \right) \tanh \beta J_{lm}}{\left(1 + \sum_{\gamma_{loop}}^{\mathcal{G}_2} \prod_{(p,q)\in\gamma_{loop}} \tanh \beta J_{pq} \right)} \\
&= \langle \sigma_i \sigma_l \rangle_{\mathcal{G}_1} \ \langle \sigma_l \sigma_m \rangle_{\mathcal{G}_2} \ \tanh \beta J_{lm};
\end{aligned}$$

in the previous equation, the symbols $\mathcal{G}$, $\mathcal{G}_1$ and $\mathcal{G}_2$ imply that the sums are to be taken over all the paths available in the relative subgraph.

6.3 Strongly Separable Graphs

We are now going to prove our main result for a class of graph, that we call **strongly separable**, that we now define.

Definition. A graph $\mathcal{G}$ is *strongly separable* if, for any integer k, a set $C_k \subset V \times V$ with measure $\mu(C_k) = 1$ exists such that for each pair $(i, j) \in C_k$ a collection of k finite subgraph $\{\mathcal{I}_1, \ldots, \mathcal{I}_k\}$ exists, satisfying

- $i \in \mathcal{I}_1 \subset \cdots \subset \mathcal{I}_k \subset \mathcal{G}$,
- j is in $\mathcal{G} \setminus \mathcal{I}_u$ for all $u = 1, \ldots, k$,
- each $\mathcal{I}_j$ is **l-disconnectable**, that's to say it can be disconnected from $\mathcal{G} \setminus \mathcal{I}_j$ by cutting no more than l links, where l is a constant depending on the graph.

The basic idea behind this definition can be traced down to the Peierls argument: when a very large set is l-disconnectable, flipping all the spins inside it costs a small amount of energy; when this is true everywhere on a graph, reducing the magnetization of any given infinite configuration is possible spending a finite energy.

In practice, we can most easily verify this definition in a Sierpinski gasket: for each pair (i, j), it is possible to choose the sets $\mathcal{I}_l$, $l = 1, \ldots, k$, as follows: $\mathcal{I}_l$ is obtained by $\mathcal{I}_{l-1}$ adding a set of triangles such that the number of links is 8 or less; this can always be accomplished, provided that the $d_{ij} > 2^{k+1}$. Since the set

$$B_k = \left\{(i, j) \in \mathcal{P} \times \mathcal{P} : d_{ij} > 2^k\right\}$$

has measure 1, the Sierpinski gasket is strongly separable.

Another example of non trivial *strong separability* are those bundled graphs in which the base is a line and each fibre has a finite extension (see Fig.6.1); in this case, letting $d_{ij}^{(b)}$ be the distance on the base,

$$B_k = \left\{(i, j) \in \mathcal{P} \times \mathcal{P} : d_{ij}^{(b)} \geq k\right\}$$

is appropriate: for each pair $(i, j) \in B_k$, it is sufficient to let $\mathcal{I}_1$ be the fibre that i belongs to, then construct $\mathcal{I}_l$ by adding to $\mathcal{I}_{l-1}$ the two fibres adjacent to it. The sets $\mathcal{I}_l$ are 2-disconnectable and thus the graph is strongly separable.

To perform a quick check of whether a given graph is strongly separable, it suffices to verify that, for each point i, an arbitrary sequence of growing l-disconnectable subgraphs, all including i, can be constructed. The key factor here is that the size of the growing subgraphs doesn't grow arbitrarily fast for arbitrary points, as in that case the measure of B_k may be less than 1.

An example of graph which isn't strongly separable is the 2-d lattice, as in the best case the number of links to be cut to separate any subgraph grow linearly with its radius.

6.4 Strongly Separable Graphs Do Not Magnetize

We are now to prove the following result:

Theorem. On any *strongly separable* graph, at any $T > 0$, $\langle M^2 \rangle = 0$ in the thermodynamic limits.

Proof. We are going to prove that all correlation functions tend to zero as the distance between the spins tends to infinity: for all k and for all the pairs $(i, j) \in C_k$, take a sequence of subgraphs $\{\{i\}, \mathcal{I}_1, \ldots, \mathcal{I}_k\}$, each including the previous, each l-disconnectable and each satisfying $j \in \mathcal{G} \setminus \mathcal{I}_u$ for $u = 1, \ldots, k$. Notice that this can be done by virtue of the hypothesis.

For each $\mathcal{I}_j$, $j = 1, \ldots, k$, first join all the points of the vertex boundary $\partial\mathcal{I}_j$, then all the points of the vertex boundary $\partial(\mathcal{G} \setminus \mathcal{I}_j)$, by sending the couplings between the points belonging to the vertex boundaries to infinity: since $J_{lm} \leq J_{Max}$, the resulting graph $\mathcal{G}'$ will have no coupling greater than lJ_{Max}.

Since $\mathcal{G}'$ is a graph made up of a sequence of subgraphs connected by just one link, by iterating k times the relation (6.2.1) we obtain

$$\langle \sigma_i \sigma_p \rangle_{\mathcal{G}} \;\leq\; \langle \sigma_i \sigma_p \rangle_{\mathcal{G}'} \;\leq\; \left[\tanh\left(\beta l J_{Max}\right)\right]^k . \tag{6.4.1}$$

Therefore all the correlation functions in C_k tend to zero as the distance between points goes to infinity and, by virtue of **Proposition I**, $\langle M^2 \rangle = 0$ in the thermodynamic limit.

□

One main merit of the previous theorem is that its hypothesis, while being easily inspectable, gives profound information about the behaviour of the model.

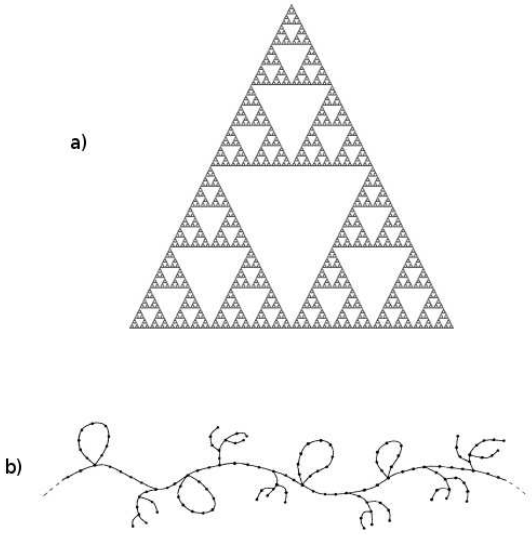

Figure 6.1: Examples of *strongly separable* graphs: **(a)** the Sierpinski gasket **(b)** a bundled graph with finite fibres.

Some immediate applications are in order: the *strongly separable* graph condition is verified for many well known graphs, e.g. the linear chain, the ladder graph, all the bundled graphs having a linear base and finite fibres (see Fig. 6.1): in each of these cases the lack of spontaneous magnetization is consistent with the results from scientific literature. The exactly decimable fractals, as the aforementioned Sierpinski gasket, are also *strongly separable*.

On the other hand, the failure to verify the **strong separability** condition is by no means sufficient to imply spontaneous magnetization: as an example, the comb lattice [54, 55] doesn't magnetize at finite temperature, even though it doesn't verify the hypothesis of the previous theorem. To be able to treat such cases, we have to introduce a broader class of graphs.

6.5 Weakly Separable Graphs

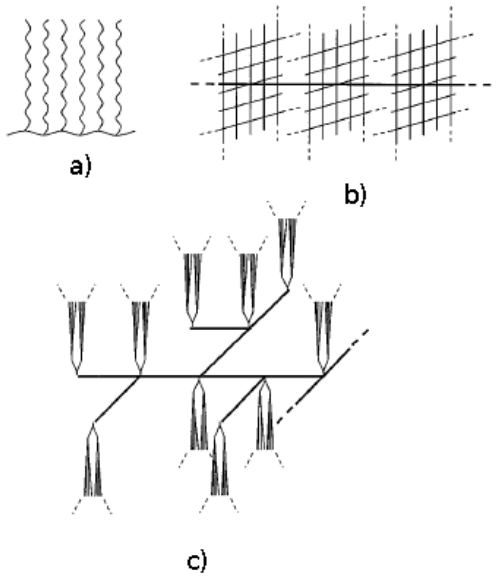

Figure 6.2: Example of weakly separable graphs: **(a)** a comb-like lattice **(b)** the infinite planes kebab **(c)** a bundled structure with infinite fibres.

Recalling the definition of bond boundary found in Sec.1.2, we can define the class of weakly separable graphs.

Definition. A graph is **weakly separable** when for all integer $k > 0$ it is possible to find an infinite set $B_k \subset \mathcal{P} \times \mathcal{P}$ such that

- $\mu(B_k) = 1$;
- for all $(i, j) \in B_k$, i and j are separated by at least k distinct bond boundaries, each of them made of no more than $l(k)$ links, where $\lim_{k\to\infty} \frac{l(k)}{\log k} = 0$.

As an example, we prove that the kebab lattice is weakly separable. The kebab lattice is a bundled graph which has an infinite line as base and infinite planes as fibres (see Fig.6.2b). Let $d_{ij}^{(b)}$ be the distance between the projections on the base of the vertices i and j, and for each k define

$$C_k = \left\{(i, j) : d_{ij}^{(b)} > k\right\}.$$

For each $(i,j) \in C_k$, one can find at least k bond boundaries - made of exactly one link of the basis - separating the two vertices. Since k is finite, the set of pairs in $\mathcal{P} \times \mathcal{P} \setminus C_k$ has zero measure: for any given i, the number of pairs (i,j) not in C_k grows with the square of the radius of the Van Hove sphere, while the total number of pairs contained in the sphere grows with its cube, so that

$$\mu\left(\mathcal{P} \times \mathcal{P} \setminus C_k\right) \propto \lim_{r\to\infty} \frac{r^4}{r^6} = 0.$$

6.6 Weakly Separable Graphs Do Not Magnetize

With the definition of weakly separable graph, it is easy to extend the first theorem.

Theorem. For all $T > 0$, a *weakly separable* graph satisfies $\langle M^2 \rangle = 0$ in the thermodynamic limit.

Proof. Since the graph is weakly separable, for any $\epsilon' > 0$ a constant k' exists such that $\frac{l(k)}{\log k} < \epsilon'$ for all $k \geq k'$. Joining the vertices at each bond boundary as in the previous theorem, it can be proved that $\langle M^2 \rangle$ satisfies

$$\langle M^2 \rangle \leq \left[\tanh\left(\beta J_{Max} l(k)\right)\right]^k$$

for all $k \geq k'$. If $\lim_{k\to\infty} l(k)$ is finite, the same reasoning as in the strongly separable case is valid, and the theorem holds. On the other hand, when $\lim_{k\to\infty} l(k) = \infty$, for k large enough the expansion

$$\tanh A = \exp\left(-2e^{-2A}\right) + O\left(e^{-4A}\right)$$

can be used, and the following holds:

$$\begin{aligned} \langle M^2 \rangle &\leq \exp\left(-2ke^{-\beta J_{Max} l(k)}\right) \leq \exp\left(-2ke^{-\beta J_{Max}(\epsilon' \log k)}\right) \\ &= \exp\left(-2k^{1-\beta J_{Max}\epsilon'^2}\right). \end{aligned}$$

For a given ϵ' small enough, $\alpha = 1 - \beta J_{Max} l(k) > 0$; as a consequence, for all $\epsilon'' > 0$ a k'' exists such that

$$\exp\left(-2k^{\alpha}\right) < \epsilon'',$$

so for all $k \geq \sup\{k', k''\}$

$$\langle M^2 \rangle \leq \epsilon'',$$

which proves the thesis.

The latter version of our theorem is a big improvement, as the weakly separable class includes all the tree-like graphs, as well as many types of graphs with infinite

fibres that are each magnetizable, but fail to do so in a coherent manner when put together (see Fig. 6.2).

The clearest example here is the kebab of infinite planes [13]: in such a system an infinite quantity of states exist which have zero magnetization and an energy only finitely different from the ground state, even in the thermodynamic limit (these low energy states can be obtained from the ground state e.g. by flipping the spins on all the planes on the right of a given link).

The statistics of this multitude of states determines the zero magnetization of the system: while in the presence of a small external field all the planes would magnetize coherently, in zero field the lack of correlation among planes doesn't allow for a non-zero average orientation. This is a perfect example of how different definitions of spontaneous magnetization give different results on general graphs, as we discussed in an earlier chapter.

In general, all the bundled graphs having a *weakly separable* base and infinite size fibres, none of which of a finite measure, are as a whole *weakly separable*, and as such do not magnetize.

As expected, the theorem hypothesis is falsified on d-dimensional regular and crystal lattices (where the minimum number of links to separate a subgraph of size N scales as $N^{\frac{d-1}{d}}$), on the Sierpinski carpet [56] and on all the structures we were able to check that exhibit spontaneous magnetization, yielding a sound check of its validity.

6.7 Summing Things Up

The procedure we have followed to prove the theorems can be intuitively understood as follows: the fact that the spins must communicate by crossing a small number of passages makes it impossible to propagate a small effect to a great distance, and hence no long range order, and thus magnetization, is allowed.

As far as our knowledge goes, all the graphs that display spontaneous magnetization are not *weakly separable*, suggesting that it may be not only a sufficient condition for the absence of magnetizability, but a necessary one too. Actually some comments are in order that make this conclusion a little far fetched: on the one hand, while locally it is quite easy to find a graph displaying a growing $l(k)$ (e.g. growing ladders or wedge graphs [2, 57]), it is unclear whether a graph with such characteristics everywhere exists; further research on this subject is needed. On the other hand, looser conditions over the growth of bond boundaries with k may as well imply an absence of magnetization.

7

A Sufficient Condition for Spontaneous Magnetization

We will now prove a theorem complementary to the one presented in the previous chapter, which gives a sufficient condition for the magnetization of a graph to be strictly greater than zero in the thermodynamic limit. This work has been published on Physical Review E [2].

7.1 Open and Closed Borders in a Graph

In order to state the theorem we first need to extend the definition of boundaries given in Sec.1.1.

Definition. Given a connected graph $\mathcal{G} = (\mathcal{P}, \mathcal{L})$, we can define a **border** $\mathcal{B}$ as a set of bonds that separates exactly two connected subgraphs. It means that two sets $\mathcal{P}_1, \mathcal{P}_2 \subset \mathcal{P}$ exist such that

- $\mathcal{P}_1 \cap \mathcal{P}_2 = \emptyset$ and $\mathcal{P}_1 \cup \mathcal{P}_2 = \mathcal{P}$,
- any path on $\mathcal{G}$ from a point of $\mathcal{P}_1$ to a point of $\mathcal{P}_2$ must contain at least one bond of $\mathcal{B}$,
- a path exists between any two points in $\mathcal{P}_i$ $(i = 1, 2)$ that doesn't contain any bond of $\mathcal{B}$.

It is noteworthy that the union of two disjoint borders is not a border itself under this definition, as it divides the graph into three subgraphs. This is a feature we'll later need to avoid overcounting different configurations.

The intuitive idea of open and closed border is actually an artifact created by our visualizing regular lattices as immersed in a finite dimensional real space: the seeming adjacency of the vertices creates a contour of the graph, which we use to define closed and open borders. The fact is that this contour is heavily dependent

on what particular immersion we employ, and ceases to exist when we consider the graph for itself. The border in itself has no geometry whatsoever, since it is just a collection of links, and even the notion of "continuous" border, without further specifications, makes no sense from a graph-theoretic point of view: in a general graph, a border is just a collection of links that splits it into two parts. We now define open and closed borders with respect to an external set of points, as it will be useful later.

Definition. Given a border $\mathcal{B}$ and a set of points $\mathcal{E} \subset \mathcal{P}$, we say that $\mathcal{B}$ is **closed** with respect to the *external points set* $\mathcal{E}$ if either $\mathcal{P}_1 \cap \mathcal{E} = \emptyset$ or $\mathcal{P}_2 \cap \mathcal{E} = \emptyset$, otherwise $\mathcal{B}$ is **open**.

For any finite subgraph $\mathcal{G}_N$ of a given graph $\mathcal{G}$, we choose the natural set of external points $\mathcal{E}$:

$$\mathcal{E} \equiv \{i \in \mathcal{G}_N : (i,j) \in \mathcal{L} \;\; for \;\; some \;\; j \in \mathcal{G} \setminus \mathcal{G}_N\}\,.$$

Now, given a border $\mathcal{B}_i$ that divides $\mathcal{G}_N$ into two subgraphs A_i and C_i, we define A_i as

- *internal* if
  - $\mathcal{B}_i$ is closed and $A_i \cap \mathcal{E} = \emptyset$, or
  - $\mathcal{B}_i$ is open and A_i contains fewer elements than C_i, or
  - $\mathcal{B}_i$ is open, A_i has the same size as C_i and the points in A_i linked to $\mathcal{B}_i$ have negative spin;
- *external* if
  - $\mathcal{B}_i$ is closed and $A_i \cap \mathcal{E} \neq \emptyset$, or
  - $\mathcal{B}_i$ is open and A_i has more elements than C_i, or
  - $\mathcal{B}_i$ is open, A_i has the same size as C_i and the points in A_i linked to $\mathcal{B}_i$ have positive spin.

The reason why we need to select a finite subgraph $\mathcal{G}_N$ is that we need to be able to count the number of spins in the graph for the previous definitions to make sense.

7.2 Equivalence Between Sets of Borders and Spin Configurations

Our next step is to prove that we can substitute the sum over configurations of the graph with a sum over possible *border classes*, that we now define.

Definition. A **border class** is a class $C = \{C^i\}$ of border sets $C^i = \left\{B_1^i, B_2^i, \ldots, B_{N_i}^i\right\}$, where $i = 1, \ldots, N_C$, such that

- $B_u^i \cap B_v^i = \emptyset$ for all $i = 1, \ldots, N_C$ and $u, v = 1, \ldots, N_i$,
- $\cup^{l=1,\ldots,N_i} B_l^i = \cup^{m=1,\ldots,N_j} B_m^j$ for all $i, j = 1, \ldots, N_C$.

Theorem. To any given border class corresponds one and only one configuration of spins on $\mathcal{P}$, once we set the value of a single spin.

Proof. To prove that, for any border class and a given spin $p \in \mathcal{P}$, we can construct a single spin configuration, we first choose an arbitrary representative $C^i = \{B_1^i, \ldots, B_N^i\}$ of C and set all the spins to the value of p, then for each $B_k^i \in C^i$ we flip all the spins of the subgraph which doesn't contain p. The result is independent of the order in which we choose the B_k^i, since each spins changes sign once for every border that separates it from the fixed spin p, and is independent of the specific i.
To prove that for any given spin configuration we can create a single border class, we proceed as follows: let $R^\pm$ be the sets of all plus (minus) spins,

$$R^\pm \equiv \{i \in \mathcal{G} : \sigma_i = \pm 1\};$$

We now choose the subsets $R_i^\pm$ of $R^\pm$, so that each $R_i^\pm$ is connected, while for all $i \neq j$ $R_i^\pm$ and $R_j^\pm$ are disconnected; moreover we require that

$$R^\pm \equiv R_1^\pm \cup R_2^\pm \cup \cdots \cup R_S^\pm,$$
$$R_i^\pm \cap R_j^\pm = \emptyset \quad \forall_{i \neq j}.$$

We are selecting individual clusters of homogeneous spins, so satisfying the above requisites is always possible. Setting now

$$\partial R_i^\pm \equiv \left\{(a, b) \in \mathcal{L} : a \in R_i^\pm, b \notin R_i^\pm\right\},$$

the sets $B^\pm \equiv \partial R_1^\pm \cup \cdots \cup \partial R_S^\pm$ are a collection of links each defined unambiguously, and furthermore $B^+ \equiv B^-$. It may happen that for some i the subgraph $\mathcal{G} \setminus R_i^\pm$ is made of two disconnected subgraphs (e.g. when a ring of plus spins is surrounded by minus spins); as a consequence $\partial R_i^\pm$ is not a border according to our definition. In that case it is possible to split $\partial R_i^\pm$ into subsets, so that each of them divides $\mathcal{G}$ into two connected subgraphs. After dealing in this way with all the $R_i^\pm$, we are left with a collection of well-defined borders ∂T_j^+, with $j = 1, \ldots, U_+$, and ∂T_k^-, with $k = 1, \ldots, U_-$ where $U_+, U_- > S$. It is still possible that some of the borders T_i^+, while defining exactly the same zones, have no correspondent in T_i^- but, since they nevertheless verify $B^+ \equiv B^-$, they belong to the same border class, completing the proof.

The main consequence of this result is that we can substitute a sum over border classes for a sum over configurations whenever needed, and we can infer from the structure of the borders some limiting properties for the spins distributions, as we'll see soon. It is worthwhile to explicitly notice that, when we pass from a sum over configurations to one over borders, and not border classes, we overcount some borders, as there are more than one representative of each border class: this is not going to be a problem in the use we'll make of this result.

7.3 Generalized Peierls-Griffiths' Theorem

We can divide the set of all configurations on $\mathcal{G}_N$ into two classes:

- all the negative spins are internal to some border (class $\mathcal{N}$),
- at least a negative spin exists that is external to all borders (class $\mathcal{P}$).

The second case implies that every positive spin lies inside some border, since it must lie on the opposite side of the negative spin which is always external.

We now restrict our attention to the configurations belonging to the first class, denoting by a subscript $\mathcal{N}$ the quantities that pertain to it; we can obtain a good estimate of the number of negative spins, $\langle N_- \rangle_{\mathcal{N}}$, as follows: the sign of a spin p is negative if it is contained inside an odd number of borders, positive otherwise; we obtain a very naive, yet effective, approximation if we consider any spin contained inside at least one border as negative: letting I^p be 1 if p is inside at least a border, 0 otherwise, we can write

$$\langle N_- \rangle_{\mathcal{N}} \leq \sum_{p \in \mathcal{G}} \langle I^p \rangle.$$

We are now to give a reasonable estimate of $\langle I^p \rangle$: take all the configurations $\mathcal{C}$ with at least one border containing p, call b_{min} the length of the shortest border in $\mathcal{C}$ containing p and let k be the number of borders containing p, so as to write

$$\langle I^p \rangle = \mathcal{Z}^{-1} \sum_{\mathcal{C}|_{p\ inside}} e^{-\beta \mathcal{H}} = \mathcal{Z}^{-1} \sum_{b_{min} \geq 1} \sum_{k \geq 1} \sum_{\mathcal{C}|^{b_{min}}_{k\ borders}} e^{-\beta \mathcal{H}}.$$

Now fix b_{min} and consider the configurations containing k borders: if we remove the shortest border from such a configuration $\mathcal{C}$, we obtain a new configuration $\mathcal{C}'$ with $(k-1)$ borders containing p, each of them at least b_{min} long. $\mathcal{C}'$ will be present in the partition function $\mathcal{Z}$, but different configurations with k borders $\mathcal{C}$ may give the same $\mathcal{C}'$; defining now $\mu^p(b)$ as the number of possible borders of b links containing p, the degeneration induced by removing the shortest border is not greater than $\mu^p(b_{min})$. The energy of a configuration $\mathcal{C}$ and the corresponding Boltzmann factor obey

$$\begin{aligned} E_{\mathcal{C}} &\geq E_{\mathcal{C}'} + 2\beta J_{min} b_{min}, \\ e^{-\beta \mathcal{H}_{\mathcal{C}}} &\leq e^{-\mathcal{H}_{\mathcal{C}'}} e^{-2\beta J_{min} b_{min}}; \end{aligned}$$

if we now limit the sum in the partition functions to those configurations obtained by removing a border from the numerator, we can write

$$\mathcal{Z}^{-1} \sum_{k \geq 1} \sum_{\mathcal{C}|_{k\ borders}} e^{-\beta \mathcal{H}} \leq \mu^p(b_{min})\ e^{-2\beta J_{min} b_{min}}.$$

In this way the average number of minus spins is bounded by a function depending only on the number of borders encircling a given spin:

$$\langle N_- \rangle_{\mathcal{N}} \ \leq \sum_{p \in \mathcal{G}} \sum_{b_{min}} \mu^p(b_{min})\ e^{-2\beta J_{min} b_{min}};$$

this result states that, no matter what the maximum number of spins you can isolate inside a border is, as long as $\mu^p(b)$ grows at most exponentially the value of $\langle N_- \rangle_{\mathcal{N}}$ can be limited at low enough temperatures. An analogous result holds for configurations of class $\mathcal{P}$ when exchanging the roles of positive and negative spins:

$$\langle N_+ \rangle_{\mathcal{P}} \ \leq \sum_{p \in \mathcal{G}} \sum_{b_{min}} \mu^p(b_{min})\ e^{-2\beta J_{min} b_{min}}.$$

Let now $\mu(b)) = \sup_p \mu^p(b)$. We can now prove the following theorem:

Theorem. If on an infinite graph $\mu(b) \leq A^b$, definitely for $b \geq \bar{b}$ and for some for some $A > 0$, then the graph exhibits spontaneous magnetization at large enough β (low enough temperatures).

Proof. The average modulus of magnetization is $|M| = N^{-1}(N_+ - N_-)$; writing the Boltzmann factor for a configuration $\mathcal{C}$ as $P_{\mathcal{C}} = \mathcal{Z}^{-1} e^{-\beta \mathcal{H}(\mathcal{C})}$, we can write the following:

$$\begin{aligned}
\langle |M| \rangle \ &= \sum_{\mathcal{C} \in \mathcal{P} \cup \mathcal{N}} |M_{\mathcal{C}}|\ P_{\mathcal{C}} \ = \sum_{\mathcal{C} \in (\mathcal{P} \cup \mathcal{N})^+} M_{\mathcal{C}}\ P_{\mathcal{C}} - \sum_{\mathcal{C} \in (\mathcal{P} \cup \mathcal{N})^-} M_{\mathcal{C}}\ P_{\mathcal{C}} \\
&= \left(\sum_{\mathcal{C} \in \mathcal{N}^+} M_{\mathcal{C}} P_{\mathcal{C}} - \sum_{\mathcal{C} \in \mathcal{N}^-} M_{\mathcal{C}} P_{\mathcal{C}} \right) + \left(\sum_{\mathcal{C} \in \mathcal{P}^+} M_{\mathcal{C}} P_{\mathcal{C}} - \sum_{\mathcal{C} \in \mathcal{P}^-} M_{\mathcal{C}} P_{\mathcal{C}} \right) \\
&= \left(\sum_{\mathcal{C} \in \mathcal{N}} M_{\mathcal{C}} P_{\mathcal{C}} - \sum_{\mathcal{C} \in \mathcal{P}} M_{\mathcal{C}} P_{\mathcal{C}} \right) + 2 \left(\sum_{\mathcal{C} \in \mathcal{P}^+} M_{\mathcal{C}} P_{\mathcal{C}} - \sum_{\mathcal{C} \in \mathcal{N}^-} M_{\mathcal{C}} P_{\mathcal{C}} \right) \\
&\geq \left(\sum_{\mathcal{C} \in \mathcal{N}} M_{\mathcal{C}} P_{\mathcal{C}} - \sum_{\mathcal{C} \in \mathcal{P}} M_{\mathcal{C}} P_{\mathcal{C}} \right) = 1 - \frac{2}{N} \left(\sum_{\mathcal{C} \in \mathcal{N}} (N_-)_{\mathcal{C}} P_{\mathcal{C}} + \sum_{\mathcal{C} \in \mathcal{P}} (N_+)_{\mathcal{C}} P_{\mathcal{C}} \right) \\
&\geq 1 - \frac{4}{N} \sum_{p \in V} \sum_{b_{min}} \mu^p(b_{min})\ e^{-2\beta J_{min} b_{min}} \\
&\geq 1 - 4 e^{-2\beta J_{min}} \sum_{b \geq 1} \mu(b_{min})\, e^{-2\beta (b-1) J_{min}},
\end{aligned}$$

When the sum on the last line converges, the equation tells us that, for large enough β (low temperatures), $\langle |M| \rangle$ is greater than a positive constant, so that spontaneous magnetization on an infinite graph is achieved, while in general $\langle |M| \rangle$ is finite for every N, but can tend to zero as $N \to \infty$.

7.4 Isoperimetric Dimension and Bounding $\mu(b)$

The main problem in employing the previous theorem is determining bounds on $\mu(b)$. The simplest case in which the hypothesis does not hold is a situation in which for some finite b the number of borders surrounding a given point is infinite. As a sound check of the validity of the theorem, all the *weakly separable* [3] graphs, which do not magnetize, belong to this category.

To further our understanding of the result, we need to present a new parameter. Given a subgraph $A \subset \mathcal{G}$, we define its external boundary ∂A as the set of points in $\mathcal{G} \setminus A$ that have a bond to a point in A; denoting the number of vertices in A as $|A|$ we now present the **isoperimetric dimension** d_{iso} as the minimum d such that $\partial A \geq C \cdot |A|^{\frac{d-1}{d}}$. The largest set of points encompassable with b links is thus smaller than $b^{\frac{d_{iso}}{d_{iso}-1}}$; since these points are connected, $b^{\frac{d_{iso}}{d_{iso}-1}}$ is also the maximum radius of a set including i with a border b, so the set of reachable points, $V(b) \subset \mathcal{P}$, has a cardinality $|V(b)| \leq b^{\frac{d_{iso} d_{frac}}{d_{iso}-1}}$.

Given a point p and for each border $\mathcal{B}$, consider $\bar{\mathcal{B}}$, the collection of vertices contributing to $\mathcal{B}$ which are on the inside of $\mathcal{B}$ with respect to p. As the two are in one to one relation once p is chosen, counting the borders is the same as counting the vertex borders.

As a consequence of the previous paragraphs, the following holds:

Proposition. In a graph with isoperimetric dimension $d_{iso} > 1$, the number of possible borders surrounding p is bounded by

$$\mu^p(b) \leq \sum_q^{|V(b)|} N_q(b) \leq b^{\frac{d_{iso} d_{frac}}{d_{iso}-1}} \cdot N_{Sup}(b),$$

where the sum is over the points q which can be enclosed in a border of size b, $N_q(b)$ is the maximum number of vertex borders of length b, containing p, which can be created starting from the point q, and $N_{Sup}(b) = \sup_{q \in V(b)} N^p(b)$.

A border is *connected* if the corresponding vertex border is a connected set. We will need the following proposition regarding $N^p(b)$ to obtain a general result.

Proposition. The number of connected vertex borders starting from a given point p grows at most exponentially with b: $N^p(b) \leq const \cdot C^b$.

Proof. A **tree** is a graph that has no loops. From each connected subgraph A we can draw a number of different spanning trees, i.e. trees having the same set of points $\mathcal{P}$ as the original A. For any spanning tree we can construct a path visiting all its vertices in no less than $b-1$ steps, and in no more than $2 z_{Max} b$ steps. While the former statement is obvious, we now prove the latter using the following algorithm: starting from i, choose link and cross it; at each vertex on the path, choose a link not yet crossed; if there is no free link, step back through the link from which the path first arrived at the vertex. With this algorithm, each link

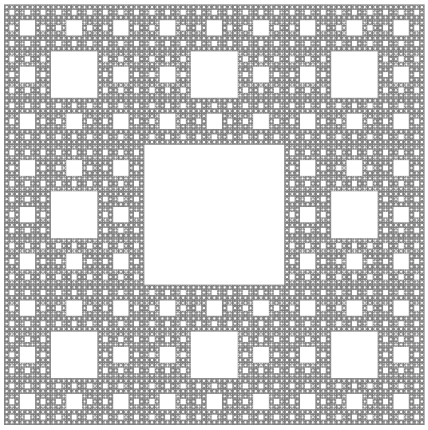

Figure 7.1: The Sierpinski carpet allows for disconnected borders, but they can be connected with no more with $l \cdot b$ links, so the number of possible borders grows no faster than an exponential with b, and the graph magnetizes.

is crossed no more than twice, so the path is of no more than $2z_{Max}b$; furthermore, all the links are crossed, so, since the boundary is connected, all the points are visited. As a consequence, all the spanning trees of b points starting from a vertex i can be constructed as paths of $b-1, b, \ldots, 2z_{Max}b$ steps. Since each step can be chosen among at most z_{Max} links, the total number of possible spanning trees, starting from i and made of b vertices, is less than

$$z_{Max}^{b-1} + z_{Max}^{b} + \cdots + z_{Max}^{2z_{Max}b} = \frac{z_{Max}^{2z_{Max}b+1} - z_{Max}^{b-1}}{z_{Max} - 1},$$

and the thesis follows:

$$N^p(b) \leq const \cdot C^b.$$

When a vertex border is made of more disconnected parts, $\mu(b)$ grows exponentially if, for all borders, it's possible to connect all the parts using no more than $l \cdot b$ vertices, where l is a constant of the graph: in fact in this case to each border of length b corresponds one connected vertex border of length between b and $b \cdot l$, so that

$$N(b) \leq C^b + C^{b+1} + \cdots + C^{l \cdot b} = \frac{C^{l \cdot b+1} - C^b}{C - 1}.$$

Noting that $d_{iso} > 1$ implies that there is no border length b for which $\mu^p(b)$ is infinite, the previous results can be combined to form the following theorem.

Theorem. For all graphs with isoperimetric dimension $d_{iso} > 1$ and vertex borders which are connectable with no more than $l \cdot b$ vertices, a finite critical $\beta_c < \infty$ exists such that for all $\beta > \beta_c$ spontaneous magnetization is achieved.

7.5 Applications

To the latter category belong the regular lattices in $d \geq 2$ dimensions and crystals with any kind of elementary cells; we explicitly note that for an Euclidean lattice in $d = 2$ dimensions we recover the result by Griffiths [23]. In addition, each vertex border can be connected with no more than $l \cdot b$ vertices in the Sierpinski carpet too, which therefore magnetizes, in accord with the existing literature [56] (see Fig.7.1).

Consider now the ladders of infinitely growing height (see Fig.7.2): they are structures described, at any offset n on the semi-infinite base line, by a non-decreasing integer function $h(n)$; as long as the isoperimetric dimension of the ladder is strictly greater than one ($h(n) \geq A_0 n^\alpha + B_0$, for $\alpha > 0$, $A_0 > 0$ and $B_0 > 0$) the previous arguments apply, so the ladder magnetizes; on the other hand, when $d_{iso} = 1$ a little more work is required: the total number $V(b)$ of vertices which can be included in at least one border of length b can not grow faster than the number of points on the left of the rightmost border of length b; the latter is at at offset $n(b) = \max\{n' | b = h^{-1}(n')\}$, so that $V(b)$ satisfies $V(b) \sim \sum_{i=1}^{n(b)} h(i)$ for large b; when

$$B_0 + A_0 \log i \leq h(i) \leq B_1 + A_1 i^\alpha$$

for some $A_0, A_1 > 0$, $B_0, B_1 \geq 0$ and $\alpha \geq 1$, the volume satisfies

$$V(b) \leq \int_1^{e^{b/A_0}} di \ (B_1 + A_1 i^\alpha) \sim \frac{b}{A_0} \frac{A_1}{2\,(\alpha+1)} \, e^{2(\alpha+1)b/A_0},$$

and since the borders are all connected $\mu(b)$ is exponential and the graph magnetizes. When instead $\lim_{n\to\infty} \frac{h(n)}{\log n} = 0$, for all $\epsilon > 0$ and n large enough $h(n) \leq \epsilon \log n$ holds; as a consequence,

$$V(b) \geq \int_0^{\frac{b}{\epsilon}} di \ h(i) \ > \int_0^{\frac{b}{\epsilon}} di = e^{\frac{b}{\epsilon}}$$

holds for all $\epsilon > 0$; in this case the sum $\sum_b \mu(b) e^{-2\beta(b-1)J_{min}}$ diverges for all temperatures, so the hypotheses of our theorem are not fulfilled. These results are in agreement with a result by Chayes and Chayes [57] about more general structures called d-wedges, where it is proved that $h(n) \geq \log n$ is both a sufficient and a necessary condition for spontaneous magnetization.

7.6 Discussion

To give a more intuitive interpretation of the theorem we proved, we can proceed as follows: if the number of borders grows less than exponentially, we can argue that all of these borders will contain a number of spins increasing slowly with the

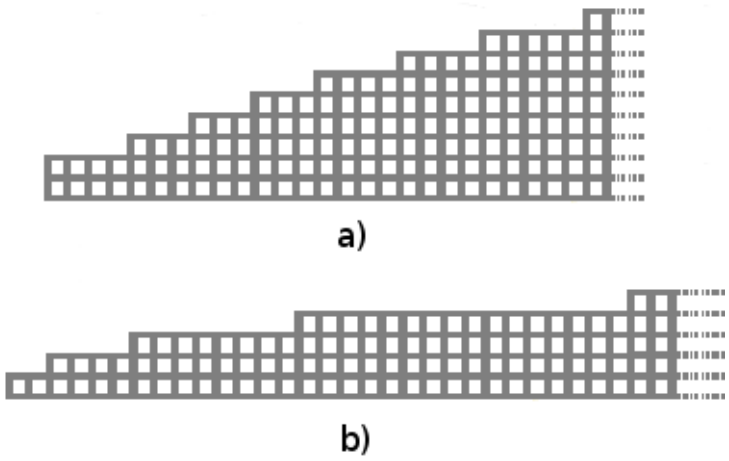

Figure 7.2: Two examples of growing ladder graphs: in (a) all the borders are connected (remember that, following the definition we use here, a border divides a graph into exactly two subgraphs, each *connected*), and as a consequence the graph will magnetize. In (b) too the borders are connected, and even if the growth in width of the ladder is very slow (logarithmic) the same result holds.

length of the border; as a consequence, the formation of large clusters of spins in a magnetized graph will be energetically unfavoured, so that the latter will result a stable state. On the other hand, if $\mu^i(b)$ grows very fast with b, we expect that some of the borders will be far from the vertex i, so that more and more vertices will be enclosed in short (low b) borders; this in turn means that large clusters of spins can be flipped spending a small amount of energy, so that a magnetized graph may be unstable with regard to thermal fluctuations.

The condition of our theorem is a strong one, in that it investigates a global property of the graph. For this reason it can not be a necessary condition for achieving spontaneous magnetization: if a graph has a part, which has zero measure in the thermodynamic limit, for which the number of boundaries $\mu^p(b)$ is greater than any exponential (e.g. a semi-infinite line connected to a point on a plane), the hypothesis of the theorem is false but the graph as a whole can still magnetize.

An important, yet straightforward, observation is that whenever a subgraph of non zero measure exists that is magnetizable, all the graph is magnetizable: in fact all the correlation functions, as computed on the subgraph, are smaller than or equal to the corresponding ones in the complete graph; when, on the other hand, the graph is formed by a collection of zero measure, weakly connected, magnetizable subgraphs (e.g. an infinite collection of parallel planes, each connected via a single link to the next one), there is no guarantee that $\langle |M| \rangle > 0$.

7.7 No Man's Land

Our result about the Ising model on graphs is a further step towards a full comprehension of the mechanism of phase transitions on general networks: together with the sufficient condition for the lack of spontaneous magnetization analysed in the previous chapter, it allows to ascertain the magnetizability of a large number of structures with a minimal amount of computation.

There is, however, a gap between the hypotheses for the theorem found here and the class of weakly separable graphs, as defined in the previous chapter: to explore it, one must carefully construct graphs for which either $\mu(b)$ grows faster than an exponential, or the weakly separable hypothesis is only slightly invalid.

Since such queer architectures do not belong with graphs portraying physical structures, their importance outside the mathematical realm is quite limited, and thus I haven't further investigated them.

8

Definitions of Magnetization: Some Considerations

The definition of magnetization we have used in the previous chapters involved free boundary conditions for the graph and no external magnetic field. There are however other possibilities, widely used in the scientific literature, that are not guaranteed to yield the same results. In this chapter we are going to analyse the relations among different definitions, extending some results from a paper by Martin-Löf [58] and highlighting some cases deserving attention.

8.1 Some Facts About Correlation Functions

Kelly and Sherman [44] generalized the Griffiths' inequalities to arbitrary products of spin variables: letting

$$\sigma_A = \prod_{i \in A} \sigma_i,$$

under the condition that $J_{ij} \geq 0$, positive or null external field, positive or null boundary conditions, the following relations hold:

$$\begin{cases} \langle \sigma_R \rangle \geq 0 & \text{for all } R \subset \mathcal{P} \\ \langle \sigma_R \sigma_S \rangle - \langle \sigma_R \rangle \langle \sigma_S \rangle \geq 0 & \text{for all } R, S \subset \mathcal{P} \end{cases} . \tag{8.1.1}$$

In order to easily discuss the different definitions of magnetization, we introduce the following notation for spin correlation functions [58]:

$$\langle \sigma_A \rangle_{h, \mathcal{G}_N, b}$$

is a correlation function as computed on a (finite) graph $\mathcal{G}_N$, under an external magnetic field h and with boundary conditions chosen in the set $\{+, -, n\}$, where n stands for no boundary conditions. It is understood that one considers the finite graphs $\mathcal{G}_N$ as subgraphs of the infinite graph

$$\mathcal{G} = \lim_{N \to \infty} \mathcal{G}_N,$$

and that the boundary is defined as in Sec.1.1.

As noticed by Griffiths, having a positive fixed magnetic field $h_i \equiv h$ is the same as considering all the spins in the graph to be attached to a fictitious vertex $\sigma_0 = +1$ with coupling $J_{0i} \equiv h$; thus, by virtue of

$$\frac{\partial \langle \sigma_R \rangle}{\partial J_{lm}} = \langle \sigma_R \sigma_l \sigma_m \rangle - \langle \sigma_R \rangle \langle \sigma_l \sigma_m \rangle \geq 0,$$

adding a positive magnetic field can only increase the correlation functions, and hence the magnetization:

$$\langle \sigma_i \sigma_j \rangle_{0,\mathcal{G}_N,b} \leq \langle \sigma_i \sigma_j \rangle_{h,\mathcal{G}_N,b}. \tag{8.1.2}$$

Since also the boundary conditions can be treated as simple couplings between a fixed spin and a free one, it is also true that

$$\langle \sigma_i \sigma_j \rangle_{0,\mathcal{G}_N,n} \leq \langle \sigma_i \sigma_j \rangle_{h,\mathcal{G}_N,b}.$$

The inequality must thus hold in the thermodynamic limit,

$$\langle \sigma_i \sigma_j \rangle_{h,b} = \lim_{N \to \infty} \langle \sigma_i \sigma_j \rangle_{h,\mathcal{G}_N,b},$$

so that

$$\langle \sigma_i \sigma_j \rangle_{0,n} \leq \langle \sigma_i \sigma_j \rangle_{h,b}. \tag{8.1.3}$$

8.2 Correlation Functions and Magnetization

In several papers about the Ising model, the spontaneous magnetization is computed as a local quantity as

$$m_i^* = \lim_{h \to 0^+} \langle \sigma_i \rangle_{h,b}, \tag{8.2.1}$$

where the zero field limit is taken *after* the thermodynamic limit, and the dependence on the boundary is fictitious, provided that the ratio of surface to volume of the graph goes to zero in the thermodynamic limit, i.e.:

$$\frac{\#\partial \mathcal{G}_N}{\#\mathcal{G}_N} \longrightarrow 0, \text{ as } N \to \infty.$$

The proof that the dependence on the boundary condition is irrelevant follows.

Proof. Divide the energy of the system in two parts, one accounting for the external field and the inter-spin interactions, the other for the boundary:

$$\mathcal{H} = \mathcal{H}^0 + \mathcal{H}^b;$$

the Boltzmann weight for a configuration $\{\sigma_i\}$ can thus be written as

$$\rho_B\{\sigma_i\} = e^{-\beta\mathcal{H}^0\{\sigma_i\}-\beta\mathcal{H}^b\{\sigma_i\}},$$

and it is easy to give an estimate on the contribution the partition functions receives from the boundary conditions: for a finite graph $\mathcal{G}_N$,

$$-4\beta J_{Max}\#\partial\mathcal{G}_N \leq \mathcal{H}^0\{\sigma_i\} \leq 4\beta J_{Max}\#\partial\mathcal{G}_N,$$

and

$$e^{-4\beta J_{Max}\#\partial\mathcal{G}_N}\mathcal{Z}^0 \leq \mathcal{Z} \leq e^{4\beta J_{Max}\#\partial\mathcal{G}_N}\mathcal{Z}^0,$$

where we let $\mathcal{Z}^0$ denote the contribution to the partition function of $\mathcal{H}^0$.

Most importantly, the free energy density of the model can now be bounded:

$$F_N^0 - 4\beta J_{Max}\frac{\#\partial\mathcal{G}_N}{\#\mathcal{G}_N} \leq F_N \leq F_N^0 + 4\beta J_{Max}\frac{\#\partial\mathcal{G}_N}{\#\mathcal{G}_N},$$

and as $N \to \infty$ both the free energies converge uniformly, for $\beta \in (0, B)$ (for any finite B), to the same function, provided that the ratio of surface to volume of the graph tends to zero.

If we are considering the case with $h \neq 0$, we also know that the free energy is an analytic function (see Sec.5.3), and thus all the spin correlation functions can be computed as its derivatives, so that m_p^* is the same whatever the boundary condition.

□

One can also inquire about the global magnetization of the structure by averaging over all the vertices; in homogeneous graphs it is obvious that the average magnetization is just m_p^*, while more in general the quantity

$$\lim_{h\to 0^+}\langle m\rangle_h = \lim_{h\to 0^+}\lim_{N\to\infty}\frac{1}{\#\mathcal{G}_N}\sum_i\langle\sigma_i\rangle_{h,\mathcal{G}_N,b}$$

can have a rude behaviour, as it can be zero even if all the local magnetizations are not.

It can be easier to cope with the square magnetization m^2: since

$$\langle m^2\rangle_h - \langle m\rangle_h^2 = \text{Var } m \geq 0,$$

$\langle m^2\rangle_h \neq 0$ if $\langle m\rangle_h \neq 0$.

For $\langle m^2\rangle_h$ the observations of Sec.5.6 holds in full generality, so one needs only study the long-distance correlation functions to know how it behaves.

8.3 Hierarchies of Correlation Functions

In Eq.8.1.2 we have seen a first example of inequality, which immediately entails that

$$\langle m^2\rangle_{0,n} = \lim_{N\to\infty} \frac{1}{N} \sum_{i,j\in\mathcal{P}} \langle \sigma_i\sigma_j\rangle_{0,\mathcal{G}_N,n} \leq \langle m^2\rangle_{h,b}.$$

Other powerful relations between different magnetizations can be inferred with some trickery.

Theorem. An important relation tells us that, under positive boundary conditions, the vanishing field limit and the thermodynamic limit can be exchanged:

$$\lim_{h\to 0^+} \lim_{N\to\infty} \langle\sigma_R\rangle_{h,\mathcal{G}_N,+} = \lim_{N\to\infty} \lim_{h\to 0^+} \langle\sigma_R\rangle_{h,\mathcal{G}_N,+}. \tag{8.3.1}$$

Proof. In zero field (i.e. performing first the vanishing field limit) the magnetization

$$\lim_{N\to\infty} \langle\sigma_R\rangle_{0,\mathcal{G}_N,+}$$

exists, since $\langle\sigma_R\rangle_{0,\mathcal{G}_N,+}$ is positive, bounded by 1 and grows with N, as adding links to the system increases the couplings. The same holds for the thermodynamic limit in non zero field,

$$\lim_{N\to\infty} \langle\sigma_R\rangle_{h,\mathcal{G}_N,+},$$

and its $h \to 0^+$ limit, which can be obtained as a decreasing sequence bounded from below by zero.

Now to the inequalities at finite N: first we prove that, for all $h > 0$ and for all N large enough, so that $\mathcal{G}_N$ contains all the spins σ_A,

$$\langle\sigma_R\rangle_{h,\mathcal{G}_{N'},+} \leq \langle\sigma_R\rangle_{h,\mathcal{G}_N,+}$$

whenever $N' \geq N$; this counter-intuitive inequality is entirely due to the positive boundary conditions, and it is straightforwardly proven by noting that one can reconstruct the boundary conditions for $\mathcal{G}_N$ just by coupling all the spins in $\mathcal{G}'_N \setminus \mathcal{G}_N$ to a fixed positive spin with infinite intensity; since this means increasing coupling constants from 0 to infinity, the correlation functions can't but increase, whence the inequality (see Fig.8.1).

The latter inequality also holds in the $N \to \infty$ limit:

$$\langle\sigma_R\rangle_{h,+} = \lim_{N\to\infty} \langle\sigma_R\rangle_{h,\mathcal{G}_N,+} \leq \langle\sigma_R\rangle_{h,\mathcal{G}_N,+} \tag{8.3.2}$$

for all $N < \infty$.

On the other hand, decreasing the external field is the same as decreasing the coupling of all spins to fixed positive spin, and thus

$$\langle\sigma_R\rangle_{h',+} \leq \langle\sigma_R\rangle_{h,+}$$

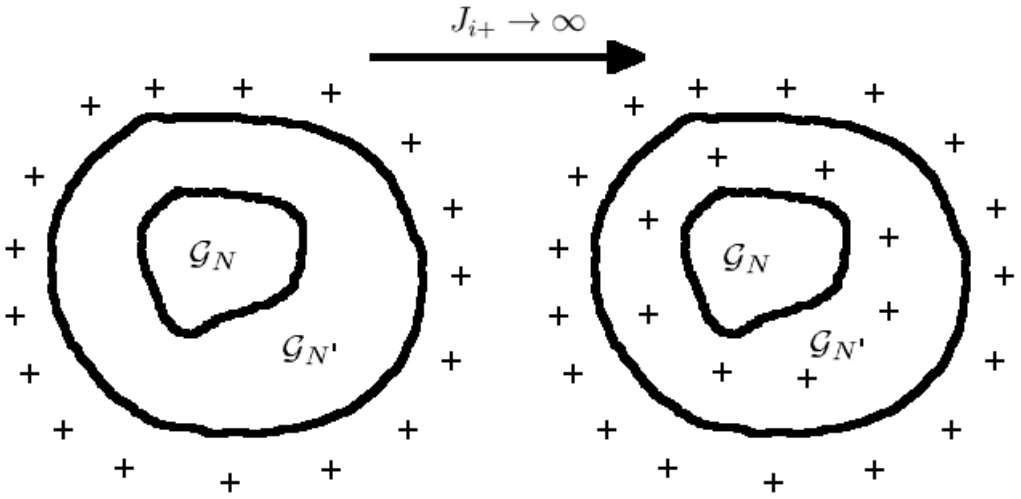

Figure 8.1: One can reconstruct the + boundary conditions of a contained subgraph by taking the limit $J_{i+} \to \infty$ for each $i \in \mathcal{G}_{N'} \setminus \mathcal{G}_N$.

whenever $h' \leq h$; combining the inequality in Eq.8.3.2 with the former one entails

$$\lim_{h\to 0^+} \langle \sigma_R \rangle_{h,+} \leq \lim_{h\to 0^+} \langle \sigma_R \rangle_{h,\mathcal{G}_N,+} = \langle \sigma_R \rangle_{0,\mathcal{G}_N,+}.$$

Since this is true for all $N < \infty$, it must also hold in the limit $N \to \infty$, so that

$$\lim_{h\to 0^+} \langle \sigma_R \rangle_{h,+} \leq \lim_{N\to\infty} \langle \sigma_R \rangle_{0,\mathcal{G}_N,+}. \tag{8.3.3}$$

Now we set off to prove the inverse inequality: for a given N

$$\langle \sigma_R \rangle_{h,\mathcal{G}_N,+} \geq \langle \sigma_R \rangle_{h',\mathcal{G}_N,+}$$

if $h \geq h'$. When $h' \to 0^+$ the last inequality becomes

$$\langle \sigma_R \rangle_{h,\mathcal{G}_N,+} \geq \langle \sigma_R \rangle_{0,\mathcal{G}_N,+}.$$

Taking now the thermodynamic limit

$$\langle \sigma_R \rangle_{h,+} = \lim_{N\to\infty} \langle \sigma_R \rangle_{h,\mathcal{G}_N,+} \geq \lim_{N\to\infty} \langle \sigma_R \rangle_{0,\mathcal{G}_N,+};$$

finally, taking the limit $h \to 0$ entails

$$\lim_{h\to 0^+} \langle \sigma_R \rangle_{h,+} \geq \lim_{N\to\infty} \langle \sigma_R \rangle_{0,\mathcal{G}_N,+}, \tag{8.3.4}$$

and the thesis follows from Eq.8.3.3 and Eq.8.3.4.

□

We now write the theorem just proved as

$$\langle\sigma_R\rangle_{0^+,+} = \langle\sigma_R\rangle_{0,+};$$

with this notation it is easier to state other relations. By virtue of symmetry, it is evident that

$$\langle\sigma_R\rangle_{0^-,-} = (-)^{\#R}\langle\sigma_R\rangle_{0^+,+}.$$

It is still not clear whether the equation

$$\langle\sigma_R\rangle_{0^+,-} = (-)^{\#R}\langle\sigma_R\rangle_{0^+,+}$$

holds. As a matter of fact it does as long as the ratio of surface and volume of the graph tends to zero in the thermodynamic limit, as one can prove with the same considerations about free energy that we employed in Sec.8.2.

We can sum up the results obtained up to this point as follows:

$$\langle\sigma_R\rangle_{0,n} \leq \begin{array}{c}\langle\sigma_R\rangle_{0,+}\\ \|\\ (-)^{\#R}\langle\sigma_R\rangle_{0,-}\end{array} = \begin{array}{c}\langle\sigma_R\rangle_{0^+,b}\\ \|\\ (-)^{\#R}\langle\sigma_R\rangle_{0^-,b}\end{array} \tag{8.3.5}$$

for all graphs such that

$$\lim_{N\to\infty} \frac{\#\partial\mathcal{G}_N}{\#\mathcal{G}_N} = 0.$$

8.4 Average Magnetizations

When we deal with the average magnetization,

$$\langle m\rangle_{h,\mathcal{G}_N,b},$$

instead of the single spin, or with the average square magnetization,

$$\langle m^2\rangle_{h,\mathcal{G}_N,b},$$

which are the two most common realizations of the averages

$$\frac{1}{(\mathcal{P}_N)^{\#R}} \sum_{R\in\mathcal{P}_N^{\#R}} \langle\sigma_R\rangle_{h,\mathcal{G}_N,b}$$

for a graph $\mathcal{G}_N = (\mathcal{P}_N, \mathcal{L}_N)$, several problems can arise.

The first decision one has to make is the way the thermodynamic limit is approached: it is possible either to take the graph as an infinite entity, and compute

$$\langle m_R\rangle_{h,b}^{inf} = \lim_{N\to\infty} \sum_{R\in S_N\subset\mathcal{P}^{\#R}} \frac{1}{\#S_N}\langle\sigma_R\rangle_{h,b},$$

where the correlation functions are relative to the infinite graph, or to calculate the average magnetization on each finite subgraph, and then send its size to infinity, i.e.

$$\langle m_R\rangle_{h,b} = \lim_{N\to\infty} \sum_{R\in\mathcal{P}_N^{\#R}} \frac{1}{(\#\mathcal{P}_N)^{\#R}}\langle\sigma_R\rangle_{h,\mathcal{G}_N,b}.$$

The two definitions can actually lead to different results - the latter being lower than or equal to the former - as in the case of the Bethe lattice discussed below. Usually the latter way of proceeding will be the best choice in a physical context, as real structures are all finite, while from a mathematical point of view both possibilities are viable.

The other point one has to draw attention to is that the pretty relation

$$\langle\sigma_R\rangle_{0^+,+} = \langle\sigma_R\rangle_{0,+}$$

doesn't extend naturally to the averaged quantities. Nevertheless, the symmetry relations hold good, and also in this case the boundary conditions do not matter as long as an external field is present and the ratio of surface to volume of the graph tends to zero. Thus, when

$$\lim_{N\to\infty} \frac{\#\partial\mathcal{G}_N}{\#\mathcal{G}_N} = 0,$$

one can summarize the valid relations as follows:

$$\langle m_R\rangle_{0,n} \leq \begin{array}{c} \langle m_R\rangle_{0,+} \\ \| \\ (-)^{\#R}\langle m_R\rangle_{0,-} \\ \nparallel \\ \langle m_R\rangle_{0^+,n} \\ \| \\ (-)^{\#R}\langle m_R\rangle_{0^-,n} \end{array} \quad \leq \quad \begin{array}{ccc} \langle m_R\rangle_{0^+,+} & = & \langle m_R\rangle_{0^+,-} \\ \| & & \| \\ (-)^{\#R}\langle m_R\rangle_{0^-,+} & = & (-)^{\#R}\langle m_R\rangle_{0^-,-} \end{array} \quad . \tag{8.4.1}$$

The same holds for $\langle m_R\rangle_{h,b}^{inf}$.

We will now treat in some detail two limiting cases that have drawn our attention:

- the zero field, no boundary conditions square magnetization yields a different result than the other cases;
- the ratio of surface to volume doesn't approach 0 in the thermodynamic limit.

8.5 Linear Bundled Graphs

All the bundled graphs [12,13,59] (see Sec.3.6) with linear base whose fibres, taken as independent graphs, can magnetize, have a schizophrenic behaviour: they display spontaneous magnetization if and only if boundary conditions or a vanishing external field are set, as we now proceed to prove.

To have a working example at hand, consider the kebab of infinite planes of Fig.6.2b, even though any other magnetizable fibre will do: under a positive external field, cut all the links between different planes, thus reducing $\langle m \rangle$, and then consider the resulting graph as a trivial juxtaposition of independent infinite planes; under a critical temperature T_c, all the magnetizations of the single planes are positive, and equal, in the $h \to 0^+$ limit; thus the magnetization of the whole graph will be positive.

When the external field is strictly null and no boundary condition is set, however, the theorem of Sec.6.6 applies, and no square magnetization $\langle m^2 \rangle$ appears. Under the frame we adopted in the previous paragraph, each infinite plane (or fibre) can have a non zero magnetization; however, since each of them can be randomly positive or negative, the total is zero.

From a statistical point of view, when no boundary conditions are set one is essentially averaging over all the possible realizations of broken symmetry of the system.

The Case for Two Fibres

This is also true when considering a pair of attached magnetizable fibres, e.g. two infinite planes linked by a single edge: as long as you have an external field or fixed boundary conditions, the total square magnetization is the same as in the single plane case; on the other hand, when no conditions are set the lack of correlation between the two parts of the system has a powerful impact.

In a sketchy way, we can write the square magnetization as

$$\langle m^2 \rangle = \lim_{N\to\infty} \frac{1}{N^2} \sum_{ij} \langle \sigma_i \sigma_j \rangle = \lim_{N\to\infty} \frac{1}{N^2} \left(\sum_{i,j\in S_1} + \sum_{i,j\in S_2} + 2 \sum_{i\in S_1, j\in S_2} \right) \langle \sigma_i \sigma_j \rangle;$$

letting S_1 and S_2 denote the two infinite planes, J_{link} the coupling of the link between S_1 and S_2, and

$$l = \lim_{d_{ij}\to\infty} \langle \sigma_i \sigma_j \rangle \text{ for } i,j \in S_1 \text{ or } i,j \in S_2,$$

by virtue of the Lemma in Sec.6.2, we can write, under no boundary condition,

$$\lim_{d_{ij}\to\infty} \langle \sigma_i \sigma_j \rangle = l^2 \tanh \beta J_{link} \text{ for } i \in S_1 \text{ and } j \in S_2.$$

It follows that the total magnetization is strongly reduced because of the scarce connectivity between the two halves of the graph:

$$\langle m^2\rangle = \lim_{N\to\infty}\frac{1}{N^2}\left(l\frac{N^2}{4}+l\frac{N^2}{4}+2l^2\frac{N^2}{4}\tanh\beta J_{link}\right)=\frac{l}{2}\left(1+l\tanh\beta J_{link}\right).$$

A Matter of Correlation

A similar calculation for a bundled graph shows that the $\langle m^2\rangle = 0$ without resorting to the theorem of Sec.6.6. In the same spirit as previously, one can write, for N fibres of $V(N)$ vertices each,

$$\lim_{d_{ij}\to\infty}\langle\sigma_i\sigma_j\rangle = t^d l^2,$$

if i and j belong to fibres which are separated by d links on the basis, l is the limit to which the correlation functions tend to on the same fibre, and $t=\tanh\beta J_{link}$. Letting S denote any given fibre, the square magnetization can be written as

$$\langle m^2\rangle = \lim_{N\to\infty}\frac{1}{N^2V^2(N)}\left(N\sum_{i,j\in S}\langle\sigma_i\sigma_j\rangle+2(N-1)tl^2\sum_{i,j\in S}\langle\sigma_i\sigma_j\rangle+\dots\right.$$

$$\left.+2t^{N-1}l^2\sum_{i,j\in S}\langle\sigma_i\sigma_j\rangle\right)=\lim_{N\to\infty}\frac{1}{N^2V^2(N)}\left(NV^2(N)l+2(N-1)V^2(N)l^2t\right.$$

$$\left.+2(N-2)V^2(N)l^2t^2+\dots+2V^2(N)l^2t^{N-1}\right). \quad (8.5.1)$$

One can first consider the degenerate case $J_{link}\to\infty$, which means that all the points on the base of the bundled graph are actually only one point, to which infinite graphs are attached; then $t=1$ and

$$\langle m^2\rangle = \lim_{N\to\infty}\frac{1}{N^2V^2(N)}\left(NV^2(N)l+2V^2(N)\frac{N(N-1)}{2}\,l^2\right)=l^2,$$

so that even in this extreme case the magnetization is strongly reduced.

Whenever we're dealing with a true bundled graph, $t<1$, we can bound the magnetization as follows:

$$\langle m^2\rangle \le \lim_{N\to\infty}\frac{1}{N^2V^2(N)}\left(NV^2(N)l+2NV^2(N)l^2t\frac{1-t^{N-1}}{1-t}\right)$$

$$\sim\frac{2l^2t}{(1-t)}\lim_{N\to\infty}\frac{1-t^{N-1}}{N}=0,$$

so no spontaneous magnetization is achieved, independently of the actual value of t.

It is worthwhile to specify that, when boundary conditions are set, this calculation is not correct because the Lemma of Sec.6.2 is no longer valid.

8.6 Cayley Trees

The other extremal case happens when the ratio of surface to volume of the graph doesn't tend to zero in the thermodynamic limit: the Bethe lattice (see Sec.3.4) of coordination number z is the typical case, as

$$\lim_{N\to\infty} \frac{\#\partial\mathcal{G}_N}{\#\mathcal{G}_N} = \frac{z-2}{z-1}.$$

Because of this property and of its peculiar topology, the Bethe lattice displays a rich phenomenology, which has been widely studied in literature [60–62] and which we now review.

A first point to note is that almost all the things can behave awkwardly do in fact so on the Bethe lattice, namely

- the local magnetization is different from the global one,
- different results are obtained for different ways of reaching the thermodynamic limit,
- almost none of the relations in Sec.8.3 holds.

To be definite, consider the usual Ising energy

$$\mathcal{H}\{\sigma_i\} = -\sum_{ij} J_{ij}\sigma_i\sigma_j - h\sum_i \sigma_i,$$

where $J_{ij} = JA_{ij}$ and A_{ij} is the adjacency matrix of the Bethe Lattice.

Fixed Boundary Conditions

When boundary conditions are set, $\langle m\rangle > 0$, whatever the temperature, also in the thermodynamic limit: to quickly and effectively see this, take an n-th generation Bethe Lattice (i.e. one that grows branches up to a chemical distance N from a root spin) and remove all the links of the graphs but those which connect the $z(z-1)^{N-1}$ spins of the outer shell to the boundary (see Fig.8.2). In this way the magnetization $\langle m\rangle$ can only have decreased; with a bit of algebra, it is easy to prove that

$$\langle m\rangle \longrightarrow \frac{z-2}{z-1}\tanh\beta J(z-1)$$

for $N\to\infty$. This result is quite trivial, as setting boundary conditions implies a very powerful bias (of the order $\exp\beta J(z-1)$) on all the spins which lay near $\partial\mathcal{G}_N$: since they are a meaningful part of the total - in fact they account for a fraction $(z-2)/(z-1)$ in the thermodynamic limit - the magnetization is trivially non zero.

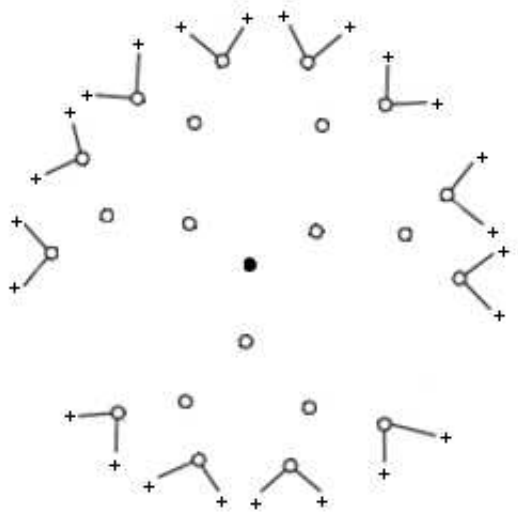

Figure 8.2: The outer shell of a $z = 3$ Bethe lattice.

External Magnetic Field

Things are more complex when a magnetic field is applied to the system, as $\langle m \rangle$ depends on the thermodynamic limit is reached. As a starter, one can see [60] that the root spin σ_0 has a finite limit,

$$\langle \sigma_0 \rangle = \lim_{h \to 0^+} \lim_{N \to \infty} \langle \sigma_0 \rangle_{h, \mathcal{G}_N, n} > 0,$$

when $T < T_c$, for

$$T_c = \frac{J}{(z-1) \log\left(\frac{z}{z-2}\right)}.$$

What happens when one computes $\langle m \rangle$ now depends on how we approach the thermodynamic limit.

If we compute

$$\lim_{h \to \infty} \lim_{N \to \infty} \langle m \rangle_{h, \mathcal{G}_N, n},$$

the result is zero at all finite temperatures [60]. The reason for this is that, while many spins near the root of the lattice have indeed positive magnetization, the totality of the spins near the border approach smoothly zero as $h \to 0^+$, and in the thermodynamic limit the former spins have no weight, so the graph doesn't magnetize.

This way of computing the magnetization makes sense in particular for practical realization of the lattice, which are not new to science (see e.g. Kopelman et a. [63]).

While no physical realization of the actually infinite Bethe lattice is possible, one

can nevertheless study it [62]: in this case the magnetization of each spin is finite under T_c, and thus one trivially obtains

$$\langle m \rangle = \langle \sigma_0 \rangle.$$

Only the Void

When no external conditions are set, the theorems we proved in the previous chapters apply to the system, and it is indeed very easy to prove that no magnetization is achieved: in particular, the Cayley tree is a weakly separable graph, so the theorem of Sec.6.6 applies and

$$\lim_{N\to\infty} \langle m^2 \rangle_{0,\mathcal{G}_N,n} = 0.$$

Without resorting to the theorem, one can simply employ the observation of Sec.5.6: since the Bethe lattice is a tree, the correlation function for two spins at chemical distance d is just

$$(\tanh \beta J)^d,$$

which tends to zero as $d \to \infty$; since all the correlation functions tend exponentially to zero, no magnetization is achieved.

Although the calculation of $\langle m^2 \rangle$ for the growing, but finite, Bethe lattice has not been undertaken, the picture of the phenomenology is nevertheless satisfying, and we will not delve deeper in that direction.

8.7 Conclusions

In this chapter we have discussed at length about the different types of definitions of magnetization, the connections which can be drawn among them, and finally we examined some graphs in order to exemplify our findings.

The variety of behaviours of the Ising model which is found in the jungle of the possible graphs have been well portrayed, even though one cannot state that it is in all aspects complete. We have no example, for definiteness, of a graph which displays no magnetization in the $h \to 0$ limit, $\langle m \rangle_{0^+} = 0$, while retaining a long range order, $\langle m^2 \rangle_{0^+} > 0$. It may prove the case, however, that such structures (if they indeed exist) are pathological cases of queer architecture; further inquiry is needed in this direction.

Ringraziamenti

- You are drunk Sir Winston, you are disgustingly drunk.
- Yes, Mrs. Braddock, I am drunk. But you, Mrs. Braddock are ugly, and disgustingly fat. But, tomorrow morning, I, Winston Churchill, will be sober.

Winston Churchill (1874-1965)

Lode alla causa di, e soluzione a, tutti i problemi.

All science is either physics or stamp collecting.

Ernest Rutherford (1871-1937)

Al quantitativo - e digitale - spirito di tolleranza.

Wie? Ist der Mensch nur ein Fehlgriff Gottes?
Oder Gott nur ein Fehlgriff des Menschen?

Friedrich Nietzsche (1844-1900)

Alla meravigliosa sorprendevolezza del mondo, perché, nonostante tutta la scienza faticosamente coltivata dell'uomo, ci sono fantasie che superano ogni verità.

In Italy for thirty years under the Borgias they had warfare, terror, murder and bloodshed but they produced Michelangelo, Leonardo da Vinci and the Renaissance. In Switzerland, they had brotherly love; they had five hundred years of democracy and peace and what did they produce? The cuckoo clock.

Orson Welles (1915-1985)

A patriot must always be ready to defend his country against his government.

Edward Abbey (1927-1989)

Al pietoso stato in cui sprofonda vieppiù la nostra umile Italia, che rende senz'altro quelli attuali tempi interessanti.

Si hoc legere scis nimium eruditionis habes.

Anonimo

Un bon mot ne prouve rien.

François-Marie Arouet detto Voltaire (1694-1778)

A Davide Cassi, per la pazienza, l'umanità e la scienza.

Le secret d'ennuyer est celui de tout dire.

François-Marie Arouet detto Voltaire (1694-1778)

Di rito e dovere i ringraziamenti al dott. A. Camobreco per aver portato un tocco di finezza in un mondo *Barbaro & Bestiale* (cit).

Bibliography

[1] R. Campari and D. Cassi, "Statistics of Reciprocal Distances for Random Walks of Three Particles in One Dimension", *Phys. Rev. E*.

[2] R. Campari and D. Cassi, "Generalization of the Peierls-Griffiths theorem for the Ising model on graphs", *Phys. Rev. E*, 81 (2010), 2, p. 021108.

[3] R. Campari and D. Cassi, "Absence of Spontaneous Magnetization for the Ising Model on Weakly Separable Graphs", *Mod. Phys. Lett. B*, (2011).

[4] R. Burioni, D. Cassi, and A. Vezzani, "Random walks and physical models on infinite graphs: an introduction", in V. A. Kaimanovich (editor), *Random Walks and Geometry*, pp. 35–71, Berlin, de Gruyter, 2001.

[5] F. Harary and N. A. S. Institute, *Graph theory and theoretical physics*, Academic P., London, New York, 1967.

[6] A. Einstein, "Über die von der molekularkinetischen Theorie der Wärme geforderte Bewegung von in ruhenden Flüssigkeiten suspendierten Teilchen.", *Ann. Phys-Berlin*, 17 (1905), pp. 549–560.

[7] M. Smoluchowsky, "Zur kinetischen Theorie der Brownschen Molekularbewegung und der Suspensionen", *Ann. Phys-Berlin*, 21 (1906), pp. 756–780.

[8] E. W. Montroll and G. H. Weiss, "Random walks on lattices. II", *J. Math. Phys.*, 6 (1965), 2, pp. 167–181.

[9] H. S. Wilf, *Generatingfunctionology*, 1990.

[10] P. Flajolet and R. Sedgewick, *Analytic Combinatorics*, Cambridge University Press, 2009.

[11] R. Burioni and D. Cassi, "Random walks on graphs: ideas, techniques and results", *J. Phys. A*, 38 (2005), pp. R45–R78.

[12] D. Cassi and S. Regina, "Diffusion and harmonic oscillations on bundled structures: analytical techniques and dynamical dimension splitting", *Mod. Phys. Lett. B*, 23 (1997), pp. 997–1011.

[13] D. Cassi and S. Regina, "Random walks on bundled structures", *Phys. Rev. Lett.*, 76 (1995), 16, pp. 2914–2917.

[14] R. Burioni, D. Cassi, and C. Destri, "Spectral partitions on infinite graphs", *J. Phys. A*, 33 (2000), pp. 3627–3636.

[15] D. Cassi, "Local vs Average Behavior on Inhomogeneous Structures: Recurrence on the Average and a Further Extension of Mermin-Wagner Theorem on Graphs", *Phys. Rev. Lett.*, 76 (1996), 16, pp. 2941–2944.

[16] D. Cassi, "Low-frequency vibrational spectrum and low-temperature specific heat of Bethe lattices", *Phys. Rev. B*, 45 (1992), 1, pp. 454–455.

[17] D. Cassi, "Random walks on Bethe lattices", *Europhys. Lett.*, 9 (1989), 7, pp. 627–631.

[18] R. Campari and D. Cassi, *in preparation.*

[19] M. Grossglauser and D. N. C. Tse, "Mobility increases the capacity of ad hoc wireless networks", *IEEE/ACM Trans. Netw.*, 10 (2002), 4, pp. 477–486.

[20] R. Feres, G. Yablonsky et al., "Probabilistic analysis of transport-reaction processes over catalytic particles: Theory and experimental testing", *Chem. Eng. Sci.*, 64 (2009), 3, pp. 568 – 581.

[21] E. Ising, "Beitrag zur Theorie des Ferromagnetismus", *Z. Phys.*, 31 (1925), 1, pp. 253–258.

[22] R. Peierls, "On Ising's model of ferromagnetism", *P. Camb. Philos. Soc.*, 32 (1936), p. 477.

[23] R. B. Griffiths, "Peierls Proof of Spontaneous Magnetization in a Two-Dimensional Ising Ferromagnet", *Phys. Rev.*, 136 (1964), 2A, pp. A437–A439.

[24] R. L. Dobrushin, "Existence of a phase transition in the two-dimensional and three-dimensional Ising models", *Dokl. Akad. Nauk*, 160 (1964), pp. 1046–1048.

[25] S. N. Isakov, "Nonanalytic Features of the First Order Phase Transition in the Ising Model", *Commun. Math. Phys.*, 95 (1984), p. 427.

[26] I. G. Sinai, *Theory of phase transitions : rigorous results*, Pergamon Press, New York, 1982.

[27] J. L. Lebowitz and A. E. Mazel, "Improved Peierls Argument for High-Dimensional Ising Models", *J. Stat. Phys.*, 90 (1998), pp. 1051–1059.

[28] Y. Gefen, B. B. Mandelbrot, and A. Aharony, "Critical Phenomena on Fractal Lattices", *Phys. Rev. Lett.*, 45 (1980), pp. 855–858.

[29] R. Jullien, K. Penson, and P. Pfeuty, "The Ising model in a transverse field on comb-like ramified linear structures", *J. Phys. (France) Lett.*, 40 (1979), pp. 237–240.

[30] T. Regge and R. Zecchina, "Exact solution of the Ising model on group lattices of genus $g > 1$", *J. Math. Phys.*, 37 (1996), 6, pp. 2796–2814.

[31] A. Ceresole, M. Rasetti, and R. Zecchina, "Geometry, topology, and physics of non-Abelian lattices", *Riv. Nuovo Cimento*, 21 (1998), 5, pp. 1–56.

[32] C. P. Herrero, "Ising model in small-world networks", *Phys. Rev. E*, 65 (2002), 6, p. 066110.

[33] S. N. Dorogovtsev, A. V. Goltsev, and J. F. F. Mendes, "Ising model on networks with an arbitrary distribution of connections", *Phys. Rev. E*, 66 (2002), 1, p. 016104.

[34] C. N. Yang and T. D. Lee, "Statistical Theory of Equations of State and Phase Transitions. I. Theory of Condensation", *Phys. Rev.*, 87 (1952), 3, pp. 404–409.

[35] T. D. Lee and C. N. Yang, "Statistical Theory of Equations of State and Phase Transitions. II. Lattice Gas and Ising Model", *Phys. Rev.*, 87 (1952), 3, pp. 410–419.

[36] P. J. Kortman and R. B. Griffiths, "Density of Zeros on the Lee-Yang Circle for Two Ising Ferromagnets", *Phys. Rev. Lett.*, 27 (1971), 21, pp. 1439–1442.

[37] R. Kenna and C. B. Lang, "Scaling and density of Lee-Yang zeros in the four-dimensional Ising model", *Phys. Rev. E*, 49 (1994), 6, pp. 5012–5017.

[38] R. Burioni, D. Cassi, and L. Donetti, "Lee-Yang zeros and the Ising model on the Sierpinski gasket", *J. Phys. A-Math. Gen.*, 32 (1999), 27, p. 5017.

[39] M. Biskup, C. Borgs et al., "General Theory of Lee-Yang Zeros in Models with First-Order Phase Transitions", *Phys. Rev. Lett.*, 84 (2000), 21, pp. 4794–4797.

[40] R. B. Griffiths, *Ising Model, Phase Transitions and Critical Phenomena*, vol. 1, chap. 2, Academic Press Inc (London), 1972.

[41] R. B. Griffiths, "Correlation in Ising Ferromagnets. I", *J. Math. Phys.*, 8 (1967), 3, pp. 478–483.

[42] R. B. Griffiths, "Correlation in Ising Ferromagnets. II. External Magnetic Fields", *J. Math. Phys.*, 8 (1967), 3, pp. 484–489.

[43] R. B. Griffiths, "Correlations in Ising ferromagnets. III", *Commun. Math. Phys.*, 6 (1967), pp. 121–127.

[44] D. G. Kelly and S. Sherman, "General Griffiths' Inequalities on Correlations in Ising Ferromagnets", *J. Math. Phys.*, 9 (1968), 3, pp. 466–484.

[45] J. Ginibre, "General formulation of Griffiths' inequalities", *Commun. Math. Phys.*, 16 (1970), pp. 310–328.

[46] J. L. Lebowitz, "GHS and other inequalities", *Commun. Math. Phys.*, 35 (1974), pp. 87–92.

[47] C. M. Newman, "Inequalities for Ising models and field theories which obey the Lee-Yang Theorem", *Commun. Math. Phys.*, 41 (1975), pp. 1–9.

[48] N. D. Mermin and H. Wagner, "Absence of Ferromagnetism or Antiferromagnetism in One- or Two-Dimensional Isotropic Heisenberg Models", *Phys. Rev. Lett.*, 17 (1966), 22, pp. 1133–1136.

[49] P. C. Hohenberg, "Existence of Long-Range Order in One and Two Dimensions", *Phys. Rev.*, 158 (1967), 2, pp. 383–386.

[50] S. Coleman, "There are no Goldstone bosons in two dimensions", *Commun. Math. Phys.*, 31 (1973), pp. 259–264.

[51] D. Cassi, "Phase transitions and random walks on graphs: A generalization of the Mermin-Wagner theorem to disordered lattices, fractals, and other discrete structures", *Phys. Rev. Lett.*, 68 (1992), 24, pp. 3631–3634.

[52] R. Burioni, D. Cassi, and A. Vezzani, "Inverse Mermin-Wagner theorem for classical spin models on graphs", *Phys. Rev. E*, 60 (1999), 2, pp. 1500–1502.

[53] C. Domb, *Ising Model, Phase Transitions and Critical Phenomena*, vol. 3, chap. 6, Academic Press Inc (London), 1974.

[54] D. C. Mattis, "Soluble Ising model in $2 + 1N$ dimensions and XY model in $1 + 1N$ dimensions", *Phys. Rev. B*, 20 (1979), 1, pp. 349–351.

[55] S. Havlin, "Anomalous diffusion on a random comblike structure", *Phys. Rev. A*, 36 (1987), 3, pp. 1403–1408.

[56] A. Vezzani, "Spontaneous magnetization of the Ising model on the Sierpinski carpet fractal, a rigorous result", *J. Phys. A*, 36 (2003), pp. 1593–1604.

[57] J. T. Chayes and L. Chayes, "Critical points and intermediate phases on wedges of Z^d", *J. Phys. A*, 19 (1986), pp. 3033–3048.

[58] A. Martin-Lof, "On the Spontaneous Magnetization in the Ising Model", *Commun. Math. Phys.*, 24 (1972), 4, pp. 253–259.

[59] D. Cassi and S. Regina, "Spectral dimension of branched structures: Universality in geometrical disorder", *Phys. Rev. Lett.*, 70 (1993), 11, pp. 1647–1649.

[60] T. P. Eggarter, "Cayley trees, the Ising problem, and the thermodynamic limit", *Phys. Rev. B*, 9 (1974), 7, pp. 2989–2992.

[61] E. Müller-Hartmann and J. Zittartz, "New Type of Phase Transition", *Phys. Rev. Lett.*, 33 (1974), 15, pp. 893–897.

[62] R. J. Baxter, *Exactly Solved Models in Statistical Mechanics*, Academic Press, 1982.

[63] R. Kopelman, M. Shortreed et al., "Spectroscopic Evidence for Excitonic Localization in Fractal Antenna Supermolecules", *Phys. Rev. Lett.*, 78 (1997), 7, pp. 1239–1242.